



HAL
open science

The rise and demise of deep accretionary wedges: A long-term field and numerical modeling perspective

Samuel Angiboust, Armel Menant, Taras Gerya, Onno Oncken

► To cite this version:

Samuel Angiboust, Armel Menant, Taras Gerya, Onno Oncken. The rise and demise of deep accretionary wedges: A long-term field and numerical modeling perspective. *Geosphere*, 2021, 10.1130/GES02392.1 . hal-03508442

HAL Id: hal-03508442

<https://hal.science/hal-03508442>

Submitted on 3 Jan 2022

HAL is a multi-disciplinary open access archive for the deposit and dissemination of scientific research documents, whether they are published or not. The documents may come from teaching and research institutions in France or abroad, or from public or private research centers.

L'archive ouverte pluridisciplinaire **HAL**, est destinée au dépôt et à la diffusion de documents scientifiques de niveau recherche, publiés ou non, émanant des établissements d'enseignement et de recherche français ou étrangers, des laboratoires publics ou privés.



Distributed under a Creative Commons Attribution - NonCommercial 4.0 International License

GEOSPHERE

<https://doi.org/10.1130/GES02392.1>

12 figures; 3 tables; 2 sets of supplemental files

CORRESPONDENCE:

samuel.angiboust@ens-lyon.fr

CITATION: Angiboust, S., Menant, A., Gerya, T., and Oncken, O., 2021, The rise and demise of deep accretionary wedges: A long-term field and numerical modeling perspective: *Geosphere*, <https://doi.org/10.1130/GES02392.1>.

Science Editor: Shanaka de Silva
Guest Associate Editor: David William Scholl

Received 22 December 2020
Revision received 18 June 2021
Accepted 6 August 2021

Published online 22 November 2021



This paper is published under the terms of the CC-BY-NC license.

© 2021 The Authors

The rise and demise of deep accretionary wedges: A long-term field and numerical modeling perspective

Samuel Angiboust¹, Armel Menant^{1,2}, Taras Gerya³, and Onno Oncken²

¹Institut de Physique du Globe de Paris (IPGP), Université de Paris, CNRS, F-75005 Paris, France

²GFZ German Center for Geosciences, Helmholtz Zentrum, Potsdam D-14473, Germany

³Institute of Geophysics, Swiss Federal Institute of Technology (ETH), Zürich 8092, Switzerland

ABSTRACT

Several decades of field, geophysical, analogue, and numerical modeling investigations have enabled documentation of the wide range of tectonic transport processes in accretionary wedges, which constitute some of the most dynamic plate boundary environments on Earth. Active convergent margins can exhibit basal accretion (via underplating) leading to the formation of variably thick duplex structures or tectonic erosion, the latter known to lead to the consumption of the previously accreted material and eventually the forearc continental crust. We herein review natural examples of actively underplating systems (with a focus on circum-Pacific settings) as well as field examples highlighting internal wedge dynamics recorded by fossil accretionary systems. Duplex formation in deep paleo-accretionary systems is known to leave in the rock record (1) diagnostic macro- and microscopic deformation patterns as well as (2) large-scale geochronological characteristics such as the downstepping of deformation and metamorphic ages. Zircon detrital ages have also proved to be a powerful approach to deciphering tectonic transport in ancient active margins. Yet, fundamental questions remain in order to understand the interplay of forces at the origin of mass transfer and crustal recycling in deep accretionary systems. We address these questions by presenting a suite of two-dimensional thermo-mechanical experiments that enable unravelling the mass-flow pathways and the long-term distribution of stresses along and above the subduction interface as well as investigating the importance of parameters such as fluids and slab roughness. These results suggest the dynamical instability of fluid-bearing accretionary systems causes either an episodic or a periodic character of subduction erosion and accretion processes as well as their topographic expression. The instability can be partly deciphered through metamorphic and strain records, thus explaining the relative scarcity of paleo-accretionary systems worldwide despite the tremendous amounts of material buried by the subduction process over time scales of tens or hundreds of millions of years. We finally stress that the understanding of the physical processes at the origin of underplating processes as well as the forearc topographic response paves the way for refining our vision of

Samuel Angiboust <https://orcid.org/0000-0002-0207-2927>

long-term plate-interface coupling as well as the rheological behavior of the seismogenic zone in active subduction settings.

INTRODUCTION

Active ocean-continent subduction margins are commonly dominated by one of the two following end-member regimes: tectonic erosion or sediment accretion (e.g., Cloos and Shreve, 1988; McClelland et al., 1992; von Huene and Scholl, 1993; Scholl and von Huene, 2010). Accretionary wedges, which represent a common feature in subduction systems worldwide, form by the recycling of material mostly deposited on the downgoing oceanic plate (e.g., Platt, 1986; Le Pichon et al., 1993; Kukowski et al., 2002; Cawood et al., 2009). Sediments scraped off the top of the downgoing plate may be frontally accreted as large fault-bounded slivers or recycled as underplated nappes forming duplex structures in the basal accretion site (Fig. 1A; e.g., Byrne, 1986; Gutscher et al., 1998; Sick et al., 2006; Menant et al., 2019; Haberland et al., 2020). More than half of the convergent margins worldwide exhibit evidence for consumption of the forearc crust by subduction erosion (Figs. 1B, 1C; von Huene and Scholl, 1991; Ranero and von Huene, 2000; Stern, 2011), with eroded fragments either underplated in the basal accretion site (e.g., Polino et al., 1990) or recycled by melting into the Earth's mantle (Stern, 2011; Ducea and Chapman, 2018). This process, fundamental for mass-balance crustal budgets, is most commonly observed in subduction zones with high convergence rates and sediment-starved trenches (Clift and Vannucchi, 2004; Kukowski and Oncken, 2006).

Erosive margins commonly exhibit crustal thinning (e.g., Contreras-Reyes et al., 2015), subsidence of the outer forearc (e.g., Fisher et al., 2004; Boston et al., 2017, and references therein), as well as long-term arcward retreat of the trench and of the magmatic arc (e.g., Parada et al., 1988; Kay et al., 2005; Clift et al., 2005b; Jicha and Kay, 2018). In most cases, the front of the margin does not exhibit a proper accretionary wedge and the continental slope is rather steep (Clift and Vannucchi, 2004). Removed material may be composed either of a previously accreted (paleo-)accretionary wedge (e.g., Litchfield et al., 2007; Glodny et al., 2006; Moore et al., 2009) or by plutonic rocks from the roots of a former volcanic arc (Kay et al., 2005). Even though tectonic erosion has been identified geophysically mostly at shallow depth ("frontal erosion," 0–5 km

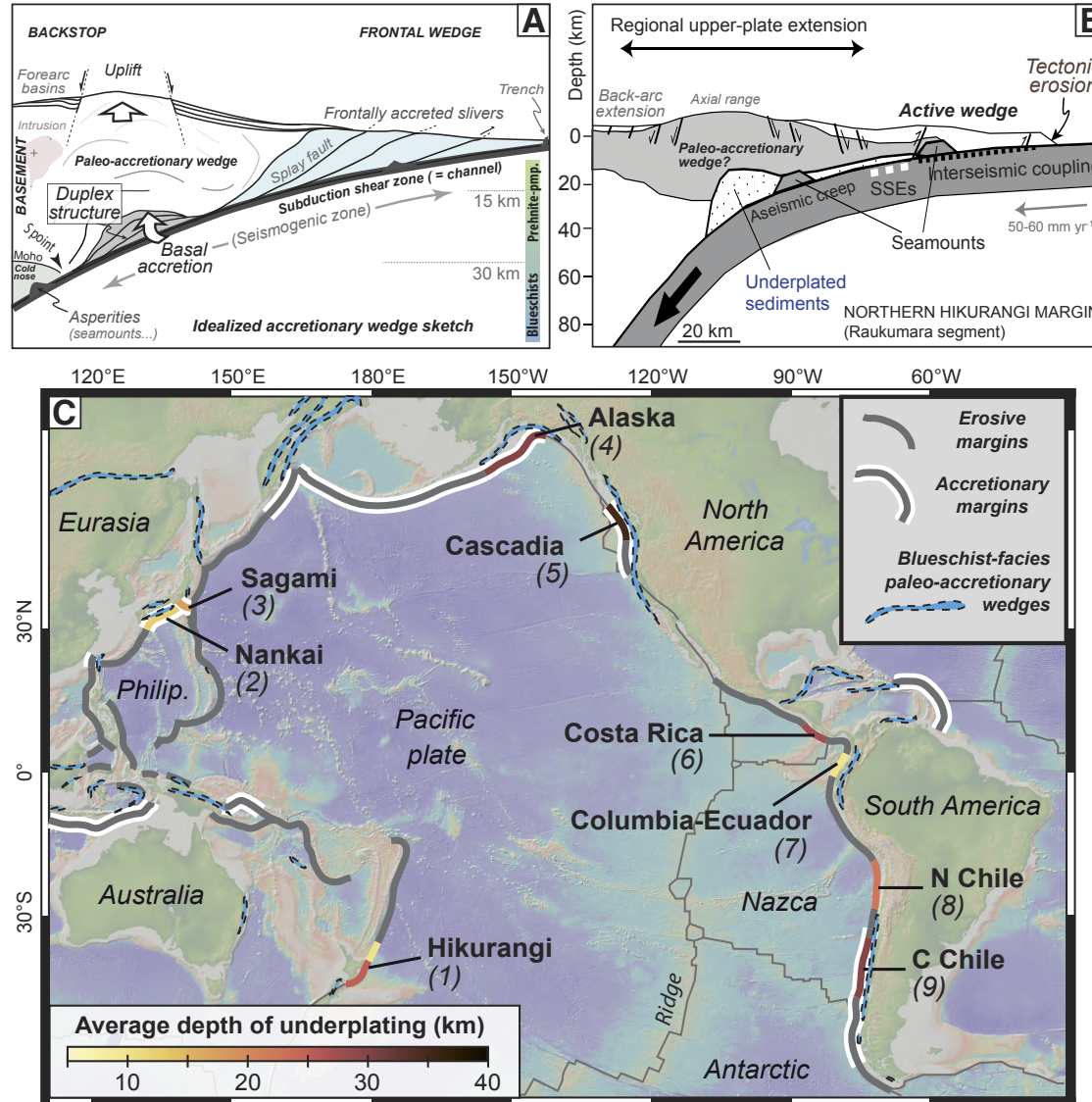


Figure 1. (A) Idealized accretionary wedge sketch locating the main structural features. The S point corresponds to the location of the downdip end of the wedge (see Ellis et al., 1999) for details. pmp.—pumpellyite. (B) Interpretive cross-section of the northern Hikurangi margin (New Zealand) showing the structural features as imaged by geophysical observations (after Litchfield et al., 2007; Williams et al., 2009). SSE—slow-slip events. (C) Map of circum-Pacific ocean-continent active margins showing erosive and accretionary margins as defined by Clift and Vannucchi (2004). Average depth of tectonic underplating along margins where this process has been documented by geophysical observations is also shown (see details in the text and Table 1). Subduction zones: (1)—Hikurangi, New Zealand (Sutherland et al., 2009; Bassett et al., 2010; Henrys et al., 2013); (2)—Nankai, Japan (Tsuji et al., 2017); (3)—Sagami, Japan (Kimura et al., 2010); (4)—Alaska, USA (Moore et al., 1991); (5)—Cascadia, western North America (Calvert et al., 2006); (6)—Costa Rica (Arroyo et al., 2009); (7)—Colombia-Ecuador (Collot et al., 2008); (8)—northern Chile (Husen et al., 2000); (9)—central Chile (Krawczyk et al., 2006; Haberland et al., 2009; Ramos et al., 2018). The location of blueschist-facies paleo-accretionary wedges is also shown (after Maruyama et al., 1996) for comparison with active margins in the circum-Pacific realm.

depth; von Huene and Lallemand, 1990; Bangs et al., 2006), the geological record has demonstrated that this process may occur along the entire interface, down to mantle depth (“basal erosion”; Polino et al., 1990; Wägrich, 1995; Oncken, 1998) with potential implications for forearc topographic evolution.

Effective erosion is strongly controlled by the subduction of rough lower-plate asperities, commonly associated with bathymetric highs such as ridges, seamounts, plateaus, or fracture zones, which increases intraplate mechanical coupling and triggers (seismic) fracturing, playing a critical role in the trimming of the interface hanging wall (e.g., Scholl et al., 1980; Collot et al., 1992, 2008; Lallemand et al., 1992; Clift and Vannucchi, 2004; Gerya et al., 2009; Wang et al., 2010). It has also been proposed that hydrofracturing due to high pore-fluid pressures along the shallow interface could control the thinning of the underside of the margin (e.g., von Huene et al., 2004). However, while the entrance of a single seamount asperity is not expected to impact the margin dynamics at a large scale, the subduction of an entire fracture zone, a large plateau, or a seamount chain (when oblique to the trench direction) can substantially affect its dynamics from accretionary to erosive over a time window of several million years (e.g., Litchfield et al., 2007; von Huene and Ranero, 2009; Clarke et al., 2018). Importantly, tectonic erosion and accretion may occur contemporaneously at different depths along the same subduction interface (e.g., Clift and Hartley 2007; Collot et al., 2008; Contreras-Reyes et al., 2015; St. Clair et al., 2016; Comte et al., 2019), thus making difficult an accurate categorization of active margin types, as shown on Figure 1C. Clift and Hartley (2007) have also underlined that “erosion effectiveness” may also be variable in intensity over space and time scale, leading to a wide palette of erosional patterns transiently alternating with periods of sediment accretion over long geological time scales (e.g., Scholl and von Huene, 2010).

While frontal and shallow basal accretionary and erosional processes are now relatively well imaged and understood in several active subduction settings worldwide (e.g., Alaska, USA: Ye et al., 1997; von Huene et al., 2021; Costa Rica: Ranero and von Huene, 2000; Arroyo et al., 2009; Nankai, Japan: Park et al., 2002), basal underplating and duplex formation mechanisms occurring along and above the interface at depths >20 km require further documentation (e.g., Oncken, 1998; Calvert et al., 2011). Deformation processes occurring in this region of the subduction interface can be assessed thanks to (1) field-based observations from ancient subduction zones now exposed at Earth’s surface (e.g., Bachmann et al., 2009a, 2009b; Angiboust et al., 2014; Liu et al., 2014; Fagereng et al., 2018, and references therein), (2) analogue modeling studies reproducing structures expected in accretionary systems (e.g., Dominguez et al., 2000; Lohrmann et al., 2006; Noda et al., 2020), and (3) long-term and short-term geodynamic numerical modeling illustrating tectonic patterns and kinematics (e.g., Ellis et al., 1999; Selzer et al., 2008; Keppie et al., 2009; van Dinther et al., 2013; Buitier, 2012; Ruh et al., 2015).

The aim of this paper is to provide a synthetic vision of the formation and destruction of deep accretionary systems in ocean-continent settings, (1) providing a review of the existing literature onshore (i.e., the exposed rock record) and offshore (i.e., geological and geophysical information) with

a focus on the circum-Pacific realm, (2) explaining how accretionary and erosive dynamics is recorded in suture zones, using field-based metamorphic and geochronological studies which can help decipher tectonic trajectories during mass-transfer along subduction margins, and (3) discussing the nature of the deep subduction interface and its evolution across geological time scales. The investigation of accretion and erosion mechanisms at depth is supported by a series of new high-resolution numerical models enabling tracking of the trajectories of tectonic slices as well as their thermal and strain evolution and assessing the effect of slab strength on the dynamics and morphology of a forearc margin over tens of millions of years.

■ MARKERS OF DEEP MASS TRANSFER IN ACTIVE SUBDUCTION MARGINS

Because the geological record preserves only a fraction of the past geodynamic picture, the understanding of forearc tectonic processes over geological time scales must be complemented by observations from active systems. From that perspective, the great variety of subduction regimes encountered along the circum-Pacific belt provides the opportunity for documenting mass-transfer processes in both erosional and accretionary systems for a similar fast-spreading-type downgoing oceanic lithosphere. For the sake of coherence, we have discarded from this brief overview ocean-ocean systems (e.g., Marianas) as well as cases with the subduction of a slow-spreading oceanic plate (e.g., Antilles), the latter being not representative of circum-Pacific seafloor material.

Geophysical Highlights of the Deep Forearc Structure and Composition

In forearc settings where coastal morphology enables the development of sufficiently dense seismological networks, it is possible to image the subduction interface, the upper- and lower-plate Moho, structures in the forearc domain, as well as the seismic deformation pattern (Sick et al., 2006; Bostock, 2013; Bassett and Watts, 2015; Scholl, 2019, and references therein). Basal accretion, commonly identified by multichannel seismic reflection profiles, seismic tomography models, gravity anomalies, and high-resolution microseismicity clusters, has been suggested in a number of active subduction segments around the Pacific realm along both accretionary and erosive margins (Fig. 1C). It has been observed to occur at depths between ~5 and ~40 km for temperatures typically ranging between 200 and 400 °C (Table 1).

The Cascadia forearc region (offshore western North America) has been one of the first segments where recent and (likely) active tectonic underplating has been inferred, notably along the northern subduction segment where there are series of landward-dipping reflectors above the plate interface that likely correspond to a stack of mafic or sedimentary bodies (Yorath et al., 1985; Clowes et al., 1987; Calvert et al., 2006). These reflectors likely image

TABLE 1. SUMMARY OF DATA FOR CIRCUM-PACIFIC OCEAN-CONTINENT SUBDUCTION SEGMENTS WHERE BASAL ACCRETION HAS BEEN IDENTIFIED OR SUGGESTED BY GEOPHYSICAL OBSERVATIONS

Locality	Reported depth range for basal underplating (km)	Underplated material	References
Northeastern New Zealand (northern Hikurangi)	10–30	Sediments, forearc crust	Sutherland et al. (2009); Bassett et al. (2010); Scherwath et al. (2010); Henrys et al. (2013)
Southwestern Japan (Nankai)	5–20	Sediments	Park et al. (2002); Tsuji et al. (2017)
Central Japan (Sagami)	15–20	Sediments	Kimura et al. (2010)
Alaska, USA	25–35	Sediments	Moore et al. (1991); Ye et al. (1997)
Cascadia, western North America	25–45	Sediments, mafic rocks, and/or forearc crust	Calvert et al. (2006)
Costa Rica	15–40	Sediments, mafic rocks	Arroyo et al. (2009); St. Clair et al. (2016)
Columbia-Ecuador	5–15	Sediments	Collot et al. (2008)
Northern Chile	15–30	Forearc material (i.e., sediments?)	Husen et al. (2000)
Central Chile	20–40	Sediments	Krawczyk et al. (2006); Haberland et al. (2009); Ramos et al. (2018)

a stack of mafic or sedimentary slivers separated by active and tectonically abandoned shear zones enabling the transfer of detached slab-top material toward the base of the overriding crust (Calvert et al., 2006). The forearc domain is itself composed of a large number of similar slivers (or terranes) previously accreted over the last tens of millions of years, including the Siletz-Crescent terrane, which consists of a >15-km-thick mafic volcanic sequence likely frontally accreted in the middle to late Eocene (McCroory and Wilson, 2013). Between ~25 and 45 km depth, a low-velocity zone imaged by seismic tomography encompasses some of these reflectors and has been interpreted by some authors as deeply accreted sedimentary and mafic rocks (Calvert et al., 2011). A similar seismic signature correlated with a low Bouguer gravity signal has been recently evidenced in the deep forearc crust of the southernmost segment of the Cascadia margin, but not in between, supporting the previous observations and suggesting lateral variations in deep accretion dynamics (Delph et al., 2021). We note, however, that the physical nature of the low-velocity zone remains largely debated (Bostock, 2013). Accreted material at the base of the forearc crust may have been pervasively infiltrated by silica-rich, slab-derived fluids, depositing sufficient amounts of quartz to explain the low V_p/V_s and Poisson's ratios, seismic tremor recurrence intervals, and crustal microseismicity clusters (Audet and Bürgmann, 2014; Savard et al., 2018). It is noteworthy that these observations require, however, the transportation of great amounts of silica and the formation of very large amounts of quartz veins (>15 vol%). Further north in the southern Alaska subduction zone on the Kodiak Island, which exposes at the surface a Mesozoic accretionary complex (Moore et al., 1991; Scholl, 2019), seismic reflection profiles imaged a series of reflectors forming a dome-like structure perhaps 20 km thick on the plate interface. The low-velocity properties of this layered forearc region suggest it is composed of underplated sediments and possibly oceanic and continental fragments (Ye et al., 1997).

Geophysical insights for tectonic underplating have also been reported along the long-lived Chilean subduction zone. Along the south-central Chilean accretionary margin, seismic reflection profiles at 38 °S show reflection

horizons forming a dome-like structure within the forearc domain similar to that associated with the southern Alaska subduction zone (Krawczyk et al., 2006; Ramos et al., 2018). This layering may be the deep expression of the Western Series, a now-exhumed paleo-accretionary complex that was basally accreted in the late Paleozoic (Glodny et al., 2005; Willner, 2005). This interpretation is supported by tomographic images and receiver function analysis suggesting the existence of underplated metasediments between ~20 and 40 km depth at the base of the forearc crust (Haberland et al., 2009; Bishop et al., 2019). Alternatively, the northern Chilean erosive margin does not exhibit clear geophysical imaging of underplated material (e.g., Oncken et al., 2003) despite indirect evidence (see the Surface Expression of Ongoing Basal Accretion section). Nonetheless, seismic tomography models below the Mejillones Peninsula documented a low-velocity zone at ~15–30 km depth above the subducting plate, interpreted by some authors as underplated material previously scraped off the base of the outer forearc region (Patzwahl et al., 1999; Husen et al., 2000). Further north, interpretation of seismic reflection profiles across the Colombia-Ecuador erosive margin suggests active and ancient sedimentary duplexes at shallow depth (i.e., ~5–15 km depth; Sage et al., 2006; Collot et al., 2008). Nonetheless, considering the ~3–4-km-thick trench-filling sediments, tectonic underplating at greater depth is not precluded, coeval with more frontal erosion (Scholl, 2019). Offshore Costa Rica, seismic reflection and refraction surveys suggest stacking from ~15 to ~35–40 km depth of metasediments and/or mafic rocks possibly originated from tectonically eroded material from the outer wedge (e.g., Arroyo et al., 2009; St. Clair et al., 2016).

Geophysical imaging along the western forearc margins of the Pacific realm also documents underplating processes. Landward of the Sagami Trough (central Japan), two seismic reflection profiles show series of reflectors depicting a stack of tectonic slices underplated along the ~15–20-km-depth region of the plate interface where microseismicity and slow-slip events are recorded (Kimura et al., 2010). Further west, seismic profiles across the Nankai accretionary wedge also suggest underplated duplex structures at ~5–20 km depth (Park et al., 2002; Tsuji et al., 2017). In the south, a series of seismic reflection and refraction

surveys and combined magnetic and gravimetric modeling along the Hikurangi margin (New Zealand) support the existence of deep accretionary complexes made of sediments and tectonically eroded crustal rocks at depths between ~10 and ~30 km (Sutherland et al., 2009; Bassett et al., 2010; Scherwath et al., 2010; Henrys et al., 2013). In Sanriku (northeastern Japan), seismicity clusters located above the plate interface in the 25–50 km depth region of the mantle wedge has been interpreted by Uchida et al. (2010) as potentially reflecting active basal accretion of seamounts from the downgoing Pacific plate.

These geophysical pieces of evidence constitute the only remote proxies to have imaged large-scale duplex structures at crustal depth, which are commonly inferred (and likely ubiquitous) along both accretionary and erosive margins (Fig. 1C). The decreasing spatial resolution of geophysical imaging at mantle depth (i.e., >30 km depth) prevents the identification of deeper underplating processes but does not preclude their existence, given that they are commonly recorded in now-exhumed paleo-accretionary systems worldwide (Table 2).

Surface Expression of Ongoing Basal Accretion

Along active circum-Pacific subduction margins, a number of diagnostic tectonic, topographic, and geomorphological observations have been long related with deep-seated processes such as tectonic underplating (e.g., Platt, 1987; Bassett and Watts, 2015, and references therein), offering insights complementary to those provided by deep geophysical imaging. One of the most representative markers of deep duplex formation is coastal uplift and high topography, which is a direct consequence of the huge mass transfer characterizing basal accretion of kilometer-scale tectonic slices. Similarly, outer-arc structural highs are commonly observed trenchward of the above-mentioned coastal topography and may result from accretionary dynamics at shallower depth (Seely, 1979; von Huene et al., 2021). Multiple methods, encompassing a large time window of observation (i.e., from days to millions of years), have long been used to investigate vertical motions along active margins. These include (1) GPS measurements, (2) measurement of uplift of geomorphological features encompassing marine terraces and fluvial incisions, (3) analysis of stratigraphic records in forearc basins, and (4) low-temperature thermochronology. Enhanced uplift rates have thus been locally evidenced all along the Pacific realm and interpreted as a consequence (at least partly) of deep accretionary events, e.g., at Hikurangi (Walcott, 1987; Litchfield et al., 2007; Houlié and Stern, 2017), Nankai (Hasebe and Tagami, 2001), Cascadia (Brandon et al., 1998; Pazzaglia and Brandon, 2001), Costa Rica (Fisher et al., 1998), southern Peru (Regard et al., 2021), northern Chile (Hartley et al., 2000; Cliff and Hartley, 2007), and south-central Chile (Glodny et al., 2005; Saillard et al., 2009; Encinas et al., 2012, 2020). This interpretation is supported by analogue and numerical experiments (Gutscher et al., 1996; Ellis et al., 1999; Lohrmann et al., 2006; Litchfield et al., 2007), but it is also worth noting that other mechanisms occurring at very different time scales contribute to vertical motions of the upper plate. They include cumulative coseismic deformations on the

plate interface or forearc faults (Melnick, 2016; Mouslopoulou et al., 2016) and aseismic crustal deformations (Victor et al., 2011; Noda et al., 2018), both being controlled by variations in subduction-channel properties (Saillard et al., 2017) and plate kinematics (McNeill et al., 2000; Martinod et al., 2016).

Recent high-resolution numerical modeling has shown that the surface signature of active underplating events is characterized by vertical oscillations in the forearc domain with a million-year-scale periodicity and maximum uplift rates ~1–2 mm yr⁻¹ (Menant et al., 2020). This implies that the surface expression of basal accretion is likely inaccessible to short-term geodetic and geomorphological records, although it must be included in the aseismic component of these records (e.g., Victor et al., 2011; Jolivet et al., 2020). Spatial and temporal variations of long-term forearc topography thus appear to be a more reliable marker of deep accretion processes, likely in combination with other deformation mechanisms also driven by the frictional properties of the plate interface (e.g., upper-plate faulting; Roseneau and Oncken, 2009). Accordingly, a coastal topographic high and an inner-forearc depression would support a long-lived duplex at depth, whereas coastal promontories would reflect active (or recent) underplating events underneath (e.g., Bassett and Watts, 2015; Menant et al., 2020).

Faulting in the shallow forearc crust may also provide insights on basal accretion processes along active margins. Normal faults contribute to the exhumation of deep accretionary complexes (Platt, 1987; Ring et al., 1999) and are thought to be part of the crustal response to active tectonic underplating, e.g., at the Hikurangi margin (Böttner et al., 2018) and northern Chile (Adam and Reuther, 2000; Hartley et al., 2000). However, thrust and back-thrust faulting are also predicted along with formation of sedimentary duplexes in sandbox analogue models (Gutscher et al., 1998; Lohrmann et al., 2006), thus supporting the lack of widespread extensional faulting along some active margins where tectonic underplating is suspected (e.g., Cascadia; Brandon et al., 1998). Accretion-related normal or reverse faulting may be thus controlled by the dominant horizontal or vertical mass flow within the forearc wedge, respectively (e.g., Pazzaglia and Brandon, 2001; Menant et al., 2020). This implies that shallow forearc deformation style has to be considered with caution and combined with other observations in order to track deep underplating events along active subduction zones (e.g., Shirzaei et al., 2012). This statement is of paramount importance because an increasing amount of evidence reveals that rocks also record the complex deformation pattern inherent to each seismic cycle (including switches in stress regime; e.g., Loveless et al., 2010).

Forearc Basal Erosion: Potential Examples

While frontal erosion is particularly well imaged along active margins, basal erosion is more challenging to identify due to the low resolution of geophysical methods at greater depths and may only be suspected in present-day subduction margins by the identification of crustal thinning processes (e.g., Scholl et al., 1980; Ranero and von Huene, 2000; Wells et al., 2003; Sage et al., 2006, and

TABLE 2. SUMMARY OF DATA FOR PALEO-ACCRETIONARY SYSTEMS FOR (MOST) OCEAN-CONTINENT SUBDUCTIONS AROUND THE PACIFIC REALM WHERE BASAL ACCRETION IS THE MOST ACCEPTED TECTONIC EMPLACEMENT MODEL, EXCLUDING LOCALITIES AND UNITS WITH HIGH PRESSURE-LOW TEMPERATURE ROCKS EXHUMED IN A SERPENTINIZED CHANNEL

Locality	Basal underplating depth range and age	Peak temperature range (°C)	Underplated material	Reference
Powell Island (South Shetland Islands)	30–40 km (Early Jurassic)	500–550	Pelitic schists	Vinagre da Costa et al. (2019)
Elephant and Smith Islands (South Shetland Islands)	20–30 km (Cretaceous–Paleocene)	300–350	Mafic and pelitic schists	Trouw et al. (1998)
Diego de Almagro Island (Chilean Patagonia)	30–50 km (Cretaceous)	450–700	Mafic and pelitic schists	Willner et al. (2004a); Hyppolito et al. (2016); Angiboust et al. (2018)
Chonos complex, Western belt (southern Chile)	25–35 km (Early Jurassic)	380–550	Mafic and pelitic schists	Willner et al. (2000); Thompson and Hervé (2002)
Valdivia and Pichilemu regions (Western Series, central Chile)	25–35 km (Early Carboniferous)	350–400	Mafic and pelitic schists	Willner et al. (2004b); Willner (2005); Glodny et al. (2005); Hyppolito et al. (2014)
Choapa complex (northern Chile)	20–30 km (Carboniferous)	350–430	Pelitic schists and mafics	Willner et al. (2012)
Arquia complex (central Colombia)	20–30 km (Cretaceous)	400–500	Mafic and pelitic schists	Ríos Reyes et al. (2008); Bustamante et al. (2011); García-Ramírez et al. (2017)
Villa de Cura complex (Venezuela)	15–25 km (Early Cretaceous)	300–400	Mafic and pelitic schists	Smith et al. (1999)
Baja California (Mexico)	20–50(?) km (Cretaceous)	200–600	Serpentine mélange	Kienast and Rangin (1982); Moore (1986); Baldwin and Harrison (1989); Sedlock (1988, 1996)
Santa Catalina Island (southern California, USA)	30–50 km (Cretaceous)	300–550	Serpentine and mafic-sedimentary slivers	Grove and Bebout (1995)
Pelona-Orocopia-Rand Schists (southern California, USA)	30–40 km (Late Cretaceous)	500–700	Pelitic schists with mafic layers	Chapman (2017); Xia and Platt (2017)
Eastern Franciscan belt (California, USA)	20–30 km (Jurassic–Cretaceous)	150–350	Metagraywackes	Dalla Torre et al. (1996); Kimura et al. (1996); Ernst and McLaughlin (2012)
Klamath Mountains (northern California, USA)	20–40 km (Jurassic–Cretaceous)	280–450	Pelitic schists with mafic layers	Helper (1986); Schmidt and Platt (2020); Tewksbury-Christle et al. (2021)
Coast Range, Yolla Bolly (northern California, USA)	25–35 km (Cretaceous)	200–300	Metagraywackes	Ernst (2016)
Liberty Creek–Seldovia (southern Alaska, USA)	40–50 km (Jurassic–Cretaceous)	400–500	Mafic and calcschists	López-Carmona et al. (2011)
Olympic Peninsula (Washington, USA)	10–15 km (Miocene)	200–300	Pelitic schists with mafic layers	Brandon and Calderwood (1990)
Korjakiya (Kamchatka, Russia)	20–30 km (early Mesozoic)	400–500	Mafic and pelitic schists	Dobretsov and Sobolev (1984, and references therein)
Karaginsk (Kamchatka, Russia)	15–20 km (Cretaceous)	400–500	Pelitic schists with mafic layers	Dobretsov and Sobolev (1984, and references therein)
Susunai complex (Sakhalin, Russia)	15–25 km (Cretaceous)	250–400	Pelitic schists with mafic layers	Dobretsov (1974, 1975); Sakakibara et al. (1997); Kimura et al. (1992)
Kamuikotan (Hokkaido, Japan)	20–40 km (Cretaceous)	250–400	Mafic and pelitic schists	Ishizuka et al. (1983); Sakakibara and Ota (1994); Iwasaki et al. (1995)
Sambagawa (non-eclogitized unit; Asemi-Gawa and Bessi, Japan)	20–35 km (Jurassic–Cretaceous)	360–540	Mafic and pelitic schists	Enami et al. (1994)
Shimanto belt (Shikoku, Japan)	15–17 km (Cretaceous)	240–270	Mafic and pelitic schists	Aoki et al. (2008); Raimbourg et al. (2014)
Shimanto belt (Kanto Mountain, Japan)	20–30 km (Cretaceous)	350–550	Mafic and pelitic schists	Hirajima and Banno (1989); Aoki et al. (2011, and references therein)
Suo belt (southwestern Japan)	35–50 km (Triassic)	380–540	Pelitic schists with mafic layers	Nishimura (1998); Ishiwatari and Tsujimori (2003); Li et al. (2017)
Yuli belt (eastern Taiwan)	25–35 km (age unclear, likely Miocene)	350–500	Pelitic schists with (ultra)mafic layers	Liou et al. (1981); Ernst and Jahn (1987); Beyssac et al. (2008); Tsai et al. (2013)

references therein) and long-term, landward migration of the volcanic arc (e.g., Kay et al., 2005; Kukowski and Oncken, 2006, and references therein). Various, more indirect proxies can also be used to identify deep basal erosion. An age gap in the sequential younging toward the base of a well-preserved duplex setting (e.g., Angiboust et al., 2018) could be potentially interpreted as an argument for transient tectonic erosion (e.g., Scholl and von Huene, 2010) but also may well just reflect a temporary cessation of accretion in a continuous underplating history. Transient tectonic erosion could be the consequence of higher stresses related to the downward transport of a topographic high, such as a seamount, plateau, or ridge (see discussion section Wedge Consumption Mechanisms and Transient Dynamics of Accretionary Edifices). For instance, multichannel seismic reflection and gravity anomalies were used by Miura et al. (2004) to propose that a seamount in the Izu-Bonin forearc region has been basally eroded, possibly as a consequence of the subduction of the Ogasawara oceanic plateau.

Vertical motion of the forearc crust investigated at different time scales has been used as a proxy for tracking (long-term) subduction erosion. Using the vertical component of the GPS signal, Heki (2004) proposed that a large section of the forearc crust undergoes basal erosion in northeastern Japan due to a relatively high degree of subsidence ($\sim 15 \text{ mm yr}^{-1}$). For geological time scales, evidence of massive subsidence recorded in forearc basin scientific drillings might also be considered as a good proxy. For instance, the recovery of beach sands at 3 km depth off Tohoku (northeastern Japan) and the progression of paleo-depths in the overlying strata provide a history of Neogene subsidence that can be extended across the shelf and slope with seismic imaging (e.g., von Huene et al., 1982). A similar case study is known in the Lima Basin (Peru) where the shallow forearc is eroded as demonstrated by drilling and multichannel seismic reflection data (Clift et al., 2003). While these two correspond to relatively shallow basal erosion examples, deeper case studies are more challenging to document because seafloor seismic reflection multiples degrades and hinders deep resolution where basal erosion processes are thought to occur.

In fossil systems, the formation of basins (e.g., Gosau Basin in the Austrian Alps) has been attributed to periods of forearc subsidence, possibly related to the removal of material along the base of the forearc crust (e.g., Wagneich, 1995; Vannucchi et al., 2004; see also Oncken, 1998, for similar observations in the Variscan). For the Swiss Alps, Bachmann et al. (2009a, 2009b) have proposed that similar Rb-Sr deformation ages for the sheared base of the crystalline upper plate and sheared upper-plate fragments found in the underlying subduction mélange could indicate, together with the formation of Gosau-type basins, that tectonic erosion was the prevailing mass-transfer mode during the waning deformation stages of the South Penninic–Austroalpine fossilized plate interface. In California (western United States; Condrey Mountain Schist complex), Tewksbury-Christle et al. (2021) reported ultramafic and mafic blocks in basally accreted blueschist-facies metapelites and used geochemistry to suggest that these blocks were tectonically eroded (likely from an obducted ophiolite) in the frontal part of the upper plate.

The Pelona-Orocopia-Rand schist complex in southern California exhibits a primary plate interface contact representative of a peculiar, shallow subduction

environment where the upper-plate Sierran magmatic arc is likely preserved, tectonically overlying a sequence of Franciscan Complex–affiliated pelitic schists (e.g., Chapman, 2017). The entire lower crust and upper mantle beneath the arc were tectonically removed in the process. This strongly foliated Paleocene complex displays a metamorphic imprint (with an inverted metamorphic sequence) typical of a relatively hot subduction setting (mostly amphibolite facies) formed at $\sim 30 \text{ km}$ depth in the basal accretion site (e.g., Kidder and Ducea, 2003). Some authors have invoked the possibility that both tectonic erosion and basal accretion were competing during the Late Cretaceous (Chapman, 2017, and references therein). The debate existing in the literature about the emplacement, exhumation, and significance of the Pelona-Orocopia-Rand complex may be due to the discontinuous nature of exposures as well as to the pervasive exhumation-related overprint that partly reworked prograde, burial-related structural features (e.g., Jacobson et al., 2007; Xia and Platt, 2017).

Basal deformation at depths greater than 40 km remains extremely challenging to detect from surface anomalies because many tectonic variables such as gravitational collapse, large-scale lithospheric buckling, slab rollback, or reactivation of forearc structural lineaments could equally explain these apparently anomalous topographic features. For instance, Tonarini et al. (2011) proposed that mantle-wedge serpentinites could be tectonically recycled (i.e., dragged) deeper at sub-arc depths in order to explain boron isotopic signatures in lavas from the South Sandwich Islands arc volcanoes. Given the extreme scarcity of pristine mantle-wedge structures now exposed at Earth's surface, a considerable number of unknowns remains regarding the physics and dynamics of tectonic erosion of the subcontinental mantle.

■ FIELD AND GEOCHRONOLOGICAL INSIGHTS ON WEDGE DYNAMICS

High pressure–low temperature (HP-LT) belts are widespread along suture zones where oceanic lithosphere has been consumed by subduction. We focus here on the natural record of oceanic-continent systems in the circum-Pacific realm, avoiding settings of ocean-ocean subduction (Cuba–Dominican Republic, Marianas). For the sake of consistency with the geographic focus of this study, HP-LT paleo-accretionary systems outside the circum-Pacific realm are discarded (see the review from Agard et al., 2018, for further details on these other localities). Listed occurrences all belong to the B-type (Cordilleran type) typical of active continental margins as classified by Maruyama et al. (1996).

What Composes a Deep Crustal Wedge?

The extensive amount of literature focusing on paleo-accretionary systems reveals that deep wedges are dominantly composed of metasediments (graywackes, cherts, pelites, and, to a minor extent, reef limestones; Maruyama et al., 1996; Wakita, 2019). It has been proposed that continentally derived

clastic turbidites are preferentially accreted while pelagic sediments are more readily subducted in the mantle (e.g., Moore, 1989; Le Pichon et al., 1993). Variable amounts (never >50 vol%) of mid-ocean-ridge basalts and oceanic island basalts (and locally arc-derived mafic tuffs) are also reported, commonly intercalated within metasedimentary sequences (Fig. 2; e.g., Hashimoto and Kimura, 1999; Hyppolito et al., 2014). Each sliver forming the duplex edifice is generally constituted by laterally coherent bodies ranging in thickness between several tens of meters and a kilometer (e.g., Grove and Bebout, 1995; Kimura et al., 1996; Angiboust et al., 2017; Schmidt and Platt, 2018; Muñoz-Montecinos et al., 2020; Raymond et al., 2020; Tewksbury-Christle et al., 2021; Figs. 3A, 3B, 3C). Kusky et al. (2013) reported the possibility of identifying primary sea-floor lithological contacts in material accreted in paleo-accretionary systems, although this recognition becomes generally more challenging with increasing metamorphic grade. In several localities, some of the slivers forming these deep duplexes exhibit an apparent “mélange” structure, which could have formed either near the trench as olistostromes (Fig. 3B; e.g., Wakabayashi, 2011; Kusky et al., 2013) or tectonically during burial as a consequence of high strain, boudinage, fragmentation, and comminution (Fig. 3A; e.g., Kimura and Mucai, 1991; Wakabayashi and Rowe, 2015; Raimbourg et al., 2019) or via a combination of both processes (Fig. 3C). Underplating of mélange-bearing slivers (comprising semi-brittle deformation) at relatively shallow conditions has been reported on Kii Peninsula and Shikoku island (Japan; e.g., Kimura and Mukai, 1991; Makimine mélange: Ujiie et al., 2018; Fig. 3A) or in some parts of the Franciscan belt in California (Fig. 3B; Underwood and Laughland, 2001; Krohe, 2017). Note that Kato and Godoy (2015), Pavlis and Roeske (2007),

and Amato et al. (2013) have also emphasized that further tectonic mixing may occur along post-accretionary strike-slip structures, thus locally obscuring the structures related to basal accretion history.

Isozaki et al. (1990) and Kimura et al. (1992) have already recognized that deeply underplated metamorphic complexes generally comprise greater amounts of mafic material than shallower ones (i.e., frontally accreted; e.g., Strasser et al., 2009). On one hand, this statement may indicate that a substantial part of the sedimentary cover of the downgoing plate is scraped off and recycled in the upper wedge so that subduction interface strains can be transferred deeper in the downgoing sequence, down to the basaltic crust, thus impacting accretion dynamics and mélange formation (Kusky et al., 1997). On the other hand, massive sediment recycling is at odds with the estimates by Clift and Vannucchi (2004) pointing to relatively minor (<20% on average) sedimentary recycling in accretionary edifices. This apparent paradox, which certainly requires further investigation, may arise from the fact that it remains very challenging to use geophysical methods to evaluate the composition and volume of active deep duplexes in active margins (e.g., Calvert et al., 2011).

Kimura and Ludden (1995) claimed that the material scraped off the top of the downgoing mafic crust is generally in the range of several tens to several hundreds of meters thick. These lenses, now found interlayered with metasediments in paleo-accretionary systems (e.g., Regalla et al., 2018; Raimbourg et al., 2019; Muñoz-Montecinos et al., 2020), may correspond to topographic highs such as the uppermost part of former seamount edifices that were peeled off the downgoing plate and intermixed with sediments or serpentinites within a subduction channel (Fig. 2; e.g., Ueda, 2005; Sang et al., 2020). Note that the

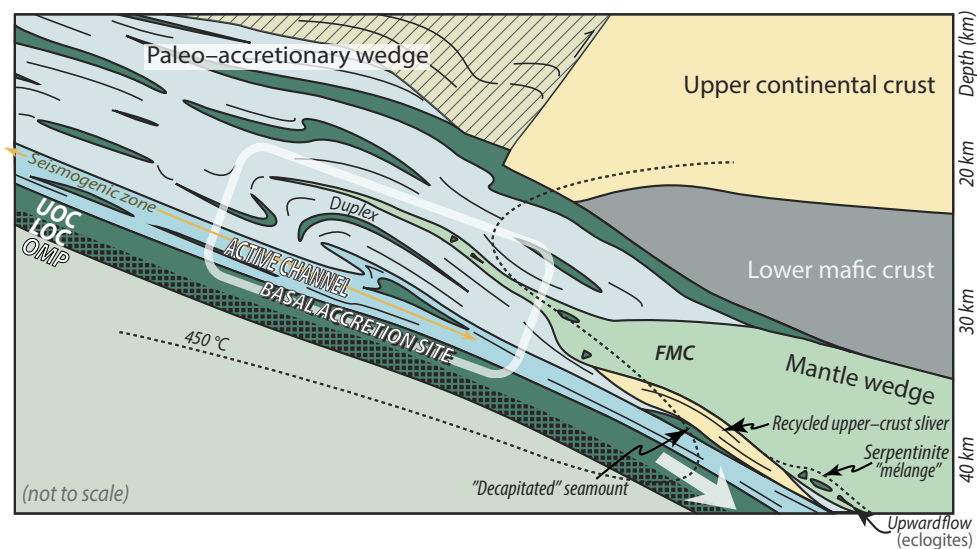


Figure 2. Idealized sketch of accretionary and tectonic processes in the basal accretion region of an ocean-continent subduction zone (inspired from our field observations and numerical modeling results). This sketch combines observations made for paleo-accretionary systems in western, northern, and eastern Pacific margins (references provided in text). UOC—upper oceanic crust; LOC—lower oceanic crust; OMP—oceanic mantle peridotites; FMC—forearc mantle-wedge corner.

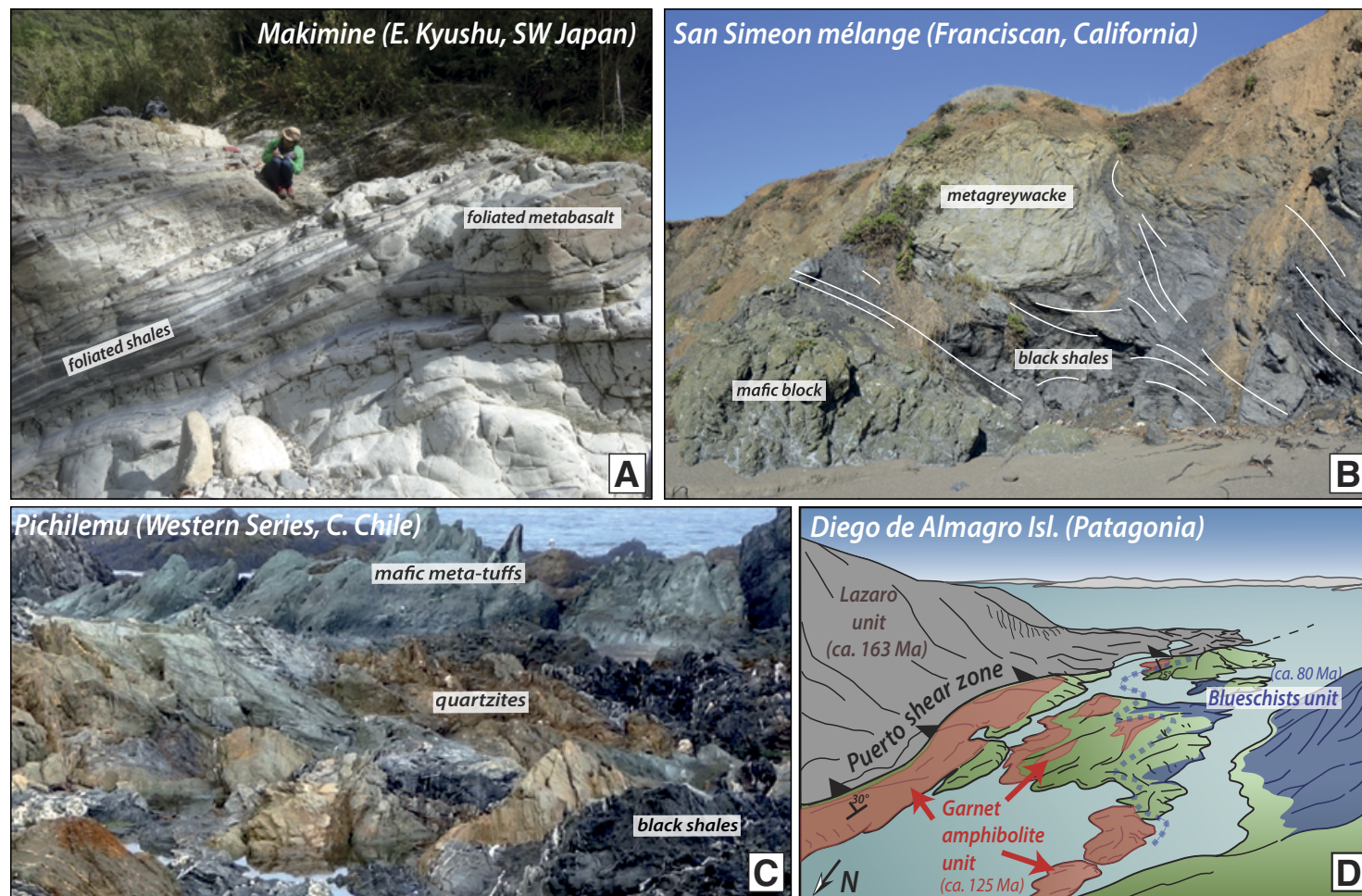


Figure 3. (A) Field view of the Makimine mélangé (eastern coast of the Kyushu island, southwestern Japan; Ujiie et al., 2018) showing lenses of foliated metabasalt wrapped within strongly flattened foliated shales (courtesy H. Raimbourg). (B) Field view of a coastal exposure of the Franciscan mélangé in the San Simeon region (Franciscan Complex, California, USA) where blocks of metagraywacke and metabasalt are tectonically embedded within black shales (courtesy L. Jolivet). Field of view is 20 meters. White lines depict the attitude of the schistosity. (C) Field view of a coastal exposure of the Western Series in central Chile (Infiernillo beach, Pichilemu) showing the complex intercalations of elongated tectonic slivers of mafic tuffs, quartzites, and black shales that were all underplated in the basal accretion site at blueschist-facies conditions (e.g., Muñoz-Montecinos et al., 2020). Field of view is ~100 meters. (D) Field sketch showing the structure of Puerto Bay on Diego de Almagro Island (Patagonia, Chile) where several tectonic slivers with very distinct pressure-temperature-time paths were juxtaposed along the subduction interface (Angiboust et al., 2018; modified after Angiboust and Muñoz, 2018). Green shading indicates vegetation cover; blue dashed line indicates the inferred upper limit of the blueschists unit. Field of view in panel D is ~1 km.

scale of imbrication deduced from field observations is much smaller than that inferred from geophysical studies due to resolution issues (e.g., Moore et al., 1991; St. Clair et al., 2016).

It is interesting to note that natural exposures exhibiting metagabbroic bodies metamorphosed at 20–35 km depth in circum-Pacific paleo-accretionary basal wedges are extremely rare (e.g., Platt, 1986; Nishiyama et al., 2017), confirming that lower-plate deep structural levels are likely rarely involved in the basal underplating process (Fig. 2). Deeper eclogitized metagabbro occurrences are known in the Sambagawa belt (Japan) where they are associated with mantle-wedge serpentinites (e.g., Banno, 2004; Aoya et al., 2006, 2013). The scarcity of gabbros or oceanic peridotites within fossilized mélanges or paleo-accretionary edifices derived from fast-spreading seafloor systems (Fig. 3) indicates that only the uppermost structural levels of the downgoing plate (i.e., sediments, mafic tuffs, and hydrothermally altered basalts) or the top of asperities (i.e., platform carbonates, ocean-island basaltic seamounts; e.g., Wakita, 2019; Bonnet et al., 2020) are tectonically involved in the basal accretion process (Fig. 2). Experiments of Angiboust et al. (2012), Vogt and Gerya (2014a), and Ruh et al. (2015) have shown that extensive oceanic mantle serpentinization is a prerequisite for involvement of the oceanic-plate lower crust into the accretionary edifice, which is generally not the case for most circum-Pacific seafloor material where a thick (5–10 km) basaltic oceanic crust prevails (e.g., Vithana et al., 2019).

What does the physical connection with the deeper serpentinized subduction channel look like? Inside coherent, metasediment-rich paleo-duplexes (e.g., Western Series, Chile), ultramafic material is volumetrically very minor (Fig. 2). In south-central Chile, Godoy and Kato (1990) and Willner et al. (2004a) have indicated that blocks and/or lenses of serpentinized ultramafics are locally found intercalated within the Western Series paleo-accretionary sequence. Similar findings were made in Japan (Nishisonogi area, Kyushu island) where 50–350-m-thick, jadeite-bearing serpentinite mélange slivers are tectonically intercalated within an epidote-blueschist metasedimentary paleo-duplex (e.g., Nishiyama et al., 2017). We postulate that the intercalation of ultramafics—likely derived from the mantle-wedge “cold nose”—is made possible due to the very low viscosity and high buoyancy of serpentinite, which tectonically injects along décollements separating metasedimentary slivers near the forearc “mantle-wedge” corner (FMC; Fig. 2). A similar process—recalling what is well known for evaporitic sequences in foreland basins—has been documented in the Western Alps belt where meter-thick, kilometer-long serpentinite allochthonous slivers systematically line the boundary between deep paleo-accretionary wedge metasediments thrust slices (Schistes Lustrés; Angiboust and Agard, 2010). A slab origin for these serpentinite slivers is likely for the Alps where slow-spreading-type dynamics led to exposure of the oceanic mantle directly on the seafloor (e.g., Lagabrielle and Cannat, 1990). In Pacific-type margins, the involvement of deep-seated (i.e., >6 km below seafloor) slab-derived serpentinites into a deep sediment-rich duplex intuitively appears unlikely (because they would be too deep into the slab for being peeled off on the subduction interface). Even though the identification of

the tectonic origin of serpentinized ultramafics is challenging and debated in several localities (e.g., Deschamps et al., 2013; Barnes et al., 2013; Wakabayashi, 2017), we herein speculate that most serpentinite bodies from circum-Pacific suture zones likely derive from the hydration of the mantle wedge. The finding of serpentinites in paleo-accretionary edifices may thus reflect deep “tectonic insertion” processes from the bottom end of the wedge at the contact area with the upper end of the serpentinized subduction channel (as depicted on Fig. 2; e.g., González-Jiménez et al., 2017).

In several circum-Pacific localities, it has been noted that higher-grade (>400 °C) blocks are also documented in mélange-like, block-in-matrix structure within lower-grade series, pointing to substantial pressure-temperature (*P-T*) difference between them and their encapsulating host (e.g., Kato and Godoy, 1995; Ukar and Cloos, 2014, and references therein; Nishiyama et al., 2020). In the Diego de Almagro Island (Patagonia, Chile), Hyppolito et al. (2016) and Angiboust et al. (2018) have identified the presence of a 100-m-thick tectonic sliver (“garnet amphibolite unit”) that reached eclogite-facies conditions before, several tens of millions of years later, being juxtaposed with epidote blueschists in the basal accretion region (Fig. 3D). Again, an extrusion of these blocks and/or slivers, traveling via transient return-flow episodes in a weak sedimentary or serpentinite-rich environment from the updip termination of the deep subduction channel (forming along the slab top at the base of the mantle wedge), represents one possible model to explain the *P-T* jumps occasionally visible in the exhumed material (Fig. 2). This model shares similarities with what has been recently proposed for the exhumation of the (poorly exposed) Cabaña HP ultramafics in south-central Chile that were juxtaposed together with lower-grade metasediments (e.g., González-Jiménez et al., 2017). Overall, the dynamics and tectonic transport processes that occur in this deep region remain poorly documented, calling for further investigation.

The Pressure-Temperature-Time-Strain Record of Basal Accretion Processes

While prehnite-pumpellyite- to lower greenschist-facies conditions (typically <0.4 GPa; i.e., <10 km of overburden) are expected for frontal accretion processes, HP-LT metamorphism—typically at lower blueschist-facies conditions—appears to be a characteristic metamorphic imprint left during the basal accretion process. A review of available *P-T* paths for some localities where basal accretion has been identified (or inferred) is presented in Table 2 and in Figure 4. This compilation may suggest at a first sight that relatively warm subduction environments (e.g., Nankai, Cascadia) represent a more favorable environment for enabling deep duplex formation. Note that this statement is compatible with the finding from Heki (2004), who identified basal erosion as the dominant mass-transfer mode in northeastern Japan, a thermally stable, notably cold active margin (Fig. 4). Some of the *P-T* paths where deep duplex formation has been identified follow a nearly isothermal decompression stage, implying an increase in the local geothermal gradient as the exhuming material

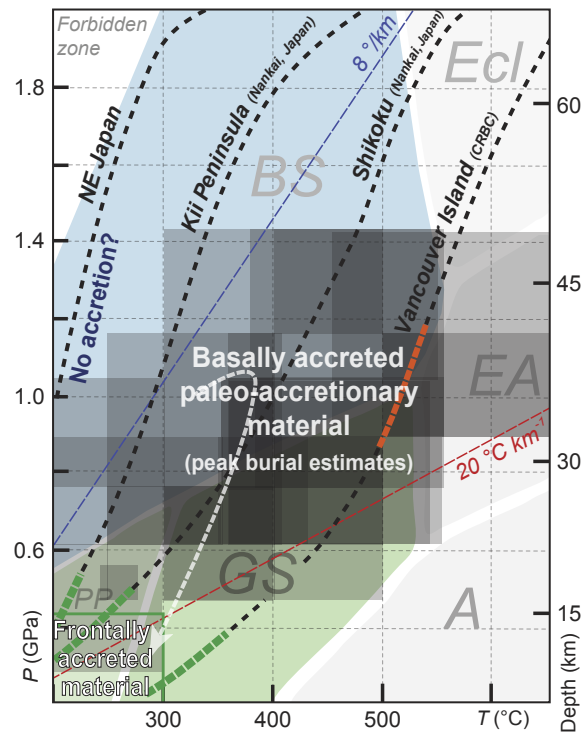


Figure 4. Compilation of peak burial pressure-temperature (P - T) conditions for 25 circum-Pacific paleo-accretionary wedges where slivers were basally accreted (gray boxes; see Table 2 for references and further information). P - T paths are from Peacock and Wang (1999) and Peacock (2009). The forbidden zone corresponds to the domain where pressure and temperature conditions are not expected on Earth. Orange thick dashed line denotes active basal accretion (Cascadia; Calvert et al., 2011), and thick green dashed lines, active margins where frontal accretion has been identified (e.g., Park et al., 2002; Adam et al., 2004). Red dashed line indicates geothermal gradient calculated for a value of 20 °/km; BS—blueschist facies; CRBC—Cascadia Range, British Columbia (Canada); Ecl—eclogite facies; EA—epidote amphibolite facies; GS—greenschist facies; A—amphibolite facies; PP—prehnite-pumpellyite facies.

is transported away from the cooled plate interface (see the white dashed arrow on Fig. 4, calculated for the Western Series in south-central Chile, a representative crustal-scale duplex sequence, by Willner [2005]). This exhumation mode strongly differs from that at localities (e.g., Marianas, Franciscan belt, eastern Australia) dominated by fast and buoyant, serpentinite-driven uplift of material, where interface-parallel exhumation along a P - T path as cool as the burial path is known and documented (e.g., Tsujimori et al., 2006; Tamblyn et al., 2020).

One of the most iconic processes in basally accreted metamorphic sequences is the gradual downstepping of deformation ages, generally decreasing toward the base (e.g., Silver et al., 1985; Platt, 1987; Kimura et al., 1992; Wakabayashi, 1999; Angiboust et al., 2018). Among the various existing geochronological techniques, the Rb-Sr multi-mineral method for mylonites (i.e., plastically deformed samples) has proven to be a very powerful and accurate way of evaluating end-of-deformation ages when samples are devoid of isotopic inheritance, i.e., fully dynamically recrystallized (e.g., Glodny et al., 2005). The combination of field, structural, and Rb-Sr studies has revealed a decrease of deformation ages toward the base of the paleo-duplex, confirming (1) the gradual downstepping invoked for building the duplex and (2) the abandonment of the shear zones bounding the thrust contacts between basally accreted slices (e.g., Angiboust et al., 2017). Out-of-sequence thrusting does exist in nature but is challenging to document from a geochronological point of view due to the mutual partial overprinting of deformation events. At a very large scale, Isozaki et al. (2010) have shown that the southern Japanese active margin has been formed after a very long, protracted history of terrane accretion that started in the early Paleozoic and proceeded trenchward until the end of the Cenozoic (Fig. 5; see also Wakita, 2013, 2019). There, slivers with a HP-LT imprint are interleaved with terranes devoid of HP-LT imprint and separated by age gaps on the order of several tens of millions of years. This region of Japan has been variably overprinted over the entire accretion history by a protracted sequence of out-of-sequence thrusting, normal faulting, and strike-slip faulting that was not sufficient to shuffle the first-order age trend depicted in Figure 5. Transient episodes of tectonic erosion, likely related to plateau or ridge subduction, could also have increased the complexity of the structural record (e.g., Raimbourg et al., 2014) and/or disrupted the continuum of the accretionary sequence (see also Scholl and von Huene, 2010, and Aouizerat et al., 2020, for other examples).

A similar pattern is known on Santa Catalina Island (California; Grove and Bebout, 1995; Grove et al., 2008), where several million years separate the various slivers accreted in the basal accretion site during the Cretaceous. Also, the Diego de Almagro Island exhibits a similar—but much longer—discontinuous accretion history, spanning almost 100 m.y. of subduction history over the late Mesozoic (Angiboust et al., 2018). Given the present state of knowledge, it is extremely challenging to assess whether these long gaps in the accretionary sequence at these localities are the consequence of the destruction of the base of the previously formed duplex structure by tectonic erosion between two episodes of accretion (e.g., Isozaki et al., 2010; Aoki et al., 2012) or whether other factors (i.e., increase in trench-fill sediment income, change in slab dip, thermal structure fluctuation, convergence velocity variations) played a role in producing these “non-accretionary gaps.” Among these factors, the evolution of the margin thermal regime over million-year time scales (e.g., Grove and Bebout, 1995; Hyppolito et al., 2014, 2016) certainly has a paramount importance in controlling plate-interface strength, which is itself controlled by the distribution of fluids generated by prograde mineral dehydration reactions (e.g., Saffer and Tobin, 2011). The thickness of trench-fill sediments capping the top of the downgoing plate has also been considered by Cliff and Vannucchi

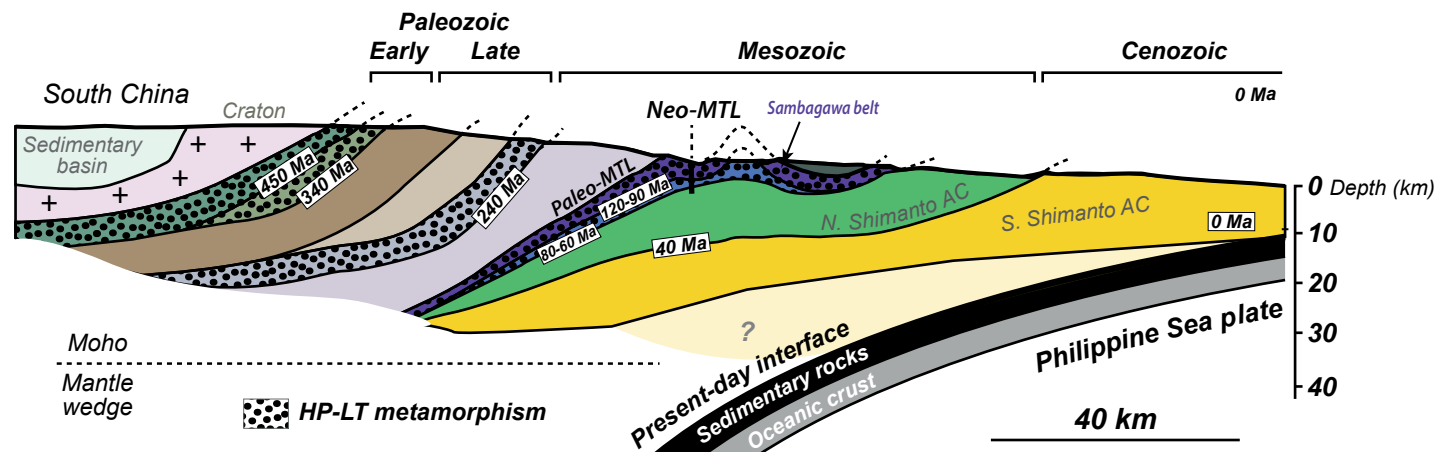


Figure 5. Large-scale simplified and idealized cross-section of southwestern Japan (modified from Isozaki et al., 2010; slab geometry has been updated based on the Slab2 model, Hayes, 2018) showing how the island has been built via long-term accretion of terranes against the South China margin from the early Paleozoic until the present day (along the trench to the east of the archipelago). Deformation ages also reveal substantial age gaps (some of them as long as several tens of millions of years) between each accretion event. Dotted domains correspond to slivers where high pressure–low temperature (HP-LT) metamorphism (i.e., blueschist or eclogite facies) has been identified. Colors are arbitrary. MTL—Median Tectonic Line (Neo- is active; Paleo- is fossil); AC—accretionary complex.

(2004) and Scholl and von Huene (2007) as critical in switching mass-transfer mode from non-accretionary or erosive to accretionary. In that sense, numerical modeling certainly represents a promising research direction that may provide some answers to this issue (e.g., Ruh, 2020; see also section Modeling Insights on Rock Records of Episodic Accretion and Erosion Events).

Field studies conducted on the Western Series in south-central Chile enabled a high-resolution understanding of kinematics and deformation patterns associated with the transport of underplated material from the interface itself up to subsurface conditions in the case of a very thick (>30 km) paleo-accretionary wedge (e.g., Hervé, 1988; Glodny et al., 2005; Richter et al., 2007). There, a common feature ubiquitously observed across 2500 km along strike is the presence of a first foliation acquired during prograde shearing (at temperatures as high as 400 °C) that is overprinted by a tight crenulation cleavage together with a new, flat-lying transposition foliation in which remnants of prograde veins occur as dismembered intrafolial, rootless folds (Richter et al., 2007; Muñoz-Montecinos et al., 2020). This pervasive deformation record that formed within the duplex during exhumation (at rates of 0.2–0.6 km/m.y.; Glodny et al., 2005; Willner, 2005) is commonly referred to as “ductile thinning” and produces at the end of the record some brittle, localized normal faulting as the rocks finally cross the brittle-ductile transition, typically above 10–15 km depth (e.g., Feehan and Brandon, 1999; Glodny et al., 2005; Ring and Brandon, 2008; Schmidt and Platt, 2018). Similar exhumation patterns were identified on discrete islands further south in Patagonia and the Antarctic Peninsula (Wilson et al., 1989; Tranter, 1992). When duplexing occurs at temperatures

<300 °C (a range common for frontal accretion but much rarer for basal accretion; Fig. 3), deformation occurs mostly by cataclastic flow along fault zones, which together with pressure solution appear to be the prevalent deformation patterns (e.g., Oncken et al., 2021), as reported, for instance, in the Kii Peninsula and the Franciscan suture by Hashimoto et al. (2002) and Regalla et al. (2018), respectively (see also Sample and Fisher, 1986, for similar features in the Kodiak Islands, Alaska).

Evidence for Mass Transfer and Crustal Recycling

The increasing use of detrital zircon geochronology has been challenging the common belief that subduction accretionary complexes preserve only accretionary periods of subduction activity. A common approach is the comparison of age distribution patterns and maximum ages of deposition inferred for the youngest grains in a distinct sample. This methodology, when applied for each of the subunits forming paleo-duplexes, is known to enable an efficient tracking of the source of accreted material as well as identification of age gaps and potential episodes of tectonic erosion (e.g., Cawood et al., 2012; Žák et al., 2020). For the Franciscan Complex, Snow et al. (2010) have demonstrated using detrital zircon U-Pb ages a decrease in maximum sedimentation ages from Cretaceous for the uppermost underplated slivers to Eocene for the structurally lowermost thrust sheets. Similar findings by Dumitru et al. (2010) and Grove et al. (2008) for the northern and southern parts of the Franciscan

Complex also pointed to transient periods of duplexing during the entire Franciscan subduction history that lasted >100 m.y. (e.g., Mulcahy et al., 2018). Only few exotic terranes of limited size exhibit peak burial ages back to middle Jurassic times while most other Franciscan ages span middle Cretaceous times. Through a compilation of existing peak metamorphism ages and zircon age dating, Dumitru et al. (2010) and Mulcahy et al. (2018) emphasized how discrete and relatively short-lived the accretionary record is within the Franciscan Complex compared with the full duration of subduction history there. Detailed processes explaining the detachment and preservation of these older outliers and their involvement in the main Cretaceous accretionary edifice remain a matter of discussion. From the extensive geochronological data set available, abrupt switches in mass-transfer mode (e.g., erosive to accretionary, basally to frontally accreted) appear to be a widespread mechanism in subduction history around the Pacific realm (e.g., Franciscan: Dumitru et al., 2010; south-central Chile: Glodny et al., 2006; Richter et al., 2007; Shimanto belt, Japan: Aoki et al., 2012).

For instance, in the Alaskan Chugach paleo-accretionary complex, Roeske et al. (1989), Clift et al. (2005a), Amato and Pavlis (2010), and Amato et al. (2013) have identified two episodes of subduction erosion: one in the middle Jurassic that ended at ca. 169 Ma, accompanied by an inboard migration of arc magmatism, and another one in the Early Cretaceous (125–101 Ma) as demonstrated by detrital zircon geochronology. Despite post-accretionary overprinting of accretion-related structures due to large-scale strike-slip shearing, the age gaps existing in the available data for the Chugach paleo-accretionary complex (together with the identification of a 125 Ma trondhjemitic magmatism) may reveal the past subduction of an oceanic ridge during the Early Cretaceous, given that such objects are known to be very efficient transient erosional agents (e.g., von Huene and Scholl, 1991). Later during middle Cretaceous (101–91 Ma), the mass-transfer mode along the southern Alaskan margin switched back to a basal accretionary mode as shown by the thick McHugh Creek formation (Amato et al., 2013). A rather similar scenario with two discrete subduction erosion events of Cretaceous age (associated with trench and arc magmatism retreat) has been identified in the southern Japan Shimanto belt by Aoki et al. (2012). There, ridge subduction is also suspected as a trigger for massive basal erosion of the previously accreted accretionary sequence.

In southern Chile, various coastal paleo-accretionary complexes are exposed (including the Chonos, the Madre de Dios, and the Diego de Almagro Metamorphic Complexes), providing an opportunity to decipher subduction dynamics and mass transfers during early Mesozoic times along this long-lived active margin (Hervé et al., 2008; Calderón et al., 2016; Fig. 6A). The Madre de Dios Metamorphic Complex is composed of pelagic limestones, pillow basalts, cherts, and turbidites that were frontally accreted under very low-grade metamorphic conditions (260 °C, <0.5 GPa) to the western Gondwana margin before the Early Jurassic (Thompson and Hervé, 2002; Sepúlveda et al., 2008; Hervé et al., 2008, and references therein). The Chonos Complex exhibits slightly deeper accretion conditions near the Triassic-Jurassic boundary, as revealed by Late Triassic detrital zircons and Early Jurassic fission-track zircon ages (Hervé and Fanning,

2001; Willner et al., 2000; Thompson and Hervé, 2002; Table 2). During Early Jurassic times, the Madre de Dios and Chonos Metamorphic Complexes were thus forming the westernmost part of the Patagonian paleo-accretionary wedge. The eastern part of the Diego de Almagro Metamorphic Complex is formed by the Lazaro unit, a several-kilometers-thick, pervasively deformed stack of mafic and pelitic schists that comprises remnants of transitional upper amphibolitic to HP granulite-facies metamorphism with evidence for partial melting of this paleo-accretionary material during Middle Jurassic times (Angiboust et al., 2017). Recently, Angiboust et al. (2017, 2018) have shown using field and petrological investigations together with sensitive high-resolution ion microprobe (SHRIMP) U-Pb metamorphic rim and detrital zircon ages that the material now forming the Lazaro unit exhibits similar age distribution patterns and seafloor lithologies as those from the Madre de Dios Metamorphic Complex further east. From these observations, it has been proposed that a frontally accreted sliver from the Madre de Dios Metamorphic Complex has been tectonically eroded during Early Jurassic times and dragged down to the basal accretion site at 35–40 km depth (~1.2 GPa and 750 °C) at 160–165 Ma in a hot subduction environment (Figs. 6B, 6C). There, the Lazaro unit has remained in a plate-interface hanging-wall position for several tens of millions of years (Fig. 6B) during which younger tectonic slivers with various metamorphic histories became underplated at 120 Ma and 80 Ma (Willner et al., 2004b; Hyppolito et al., 2016; Angiboust et al., 2018) and the shear zone bounding the base of the Lazaro unit was abandoned.

This list, far from being exhaustive, of natural laboratories where detrital zircon geochronology can be used for deciphering subduction dynamics demonstrates the great potential of the method to identify punctuated episodes of tectonic erosion in long-lived accretionary edifices (see also Žák et al., 2020, and references therein for further reading).

■ MODELING INSIGHTS ON ROCK RECORDS OF EPISODIC ACCRETION AND EROSION EVENTS

As described in the section Forearc Basal Erosion: Potential Examples, the modalities of basal erosion processes as well as their connection with crustal recycling are more challenging to document than for frontal erosion processes. Physically constrained, high-resolution numerical modeling can thus provide valuable insights into the dynamics of these deep mass transfers. In the following section, we present the results of numerical experiments highlighting with unprecedented detail the forearc dynamics and the pressure-temperature-time-strain (P - T - t - ϵ) record characterizing episodic accretion and erosion events in ocean-continent subduction zones.

Numerical Approach and Initial Setup

A set of two-dimensional thermo-mechanical experiments have been carried out, solving the continuity, momentum, and heat conservation equations,

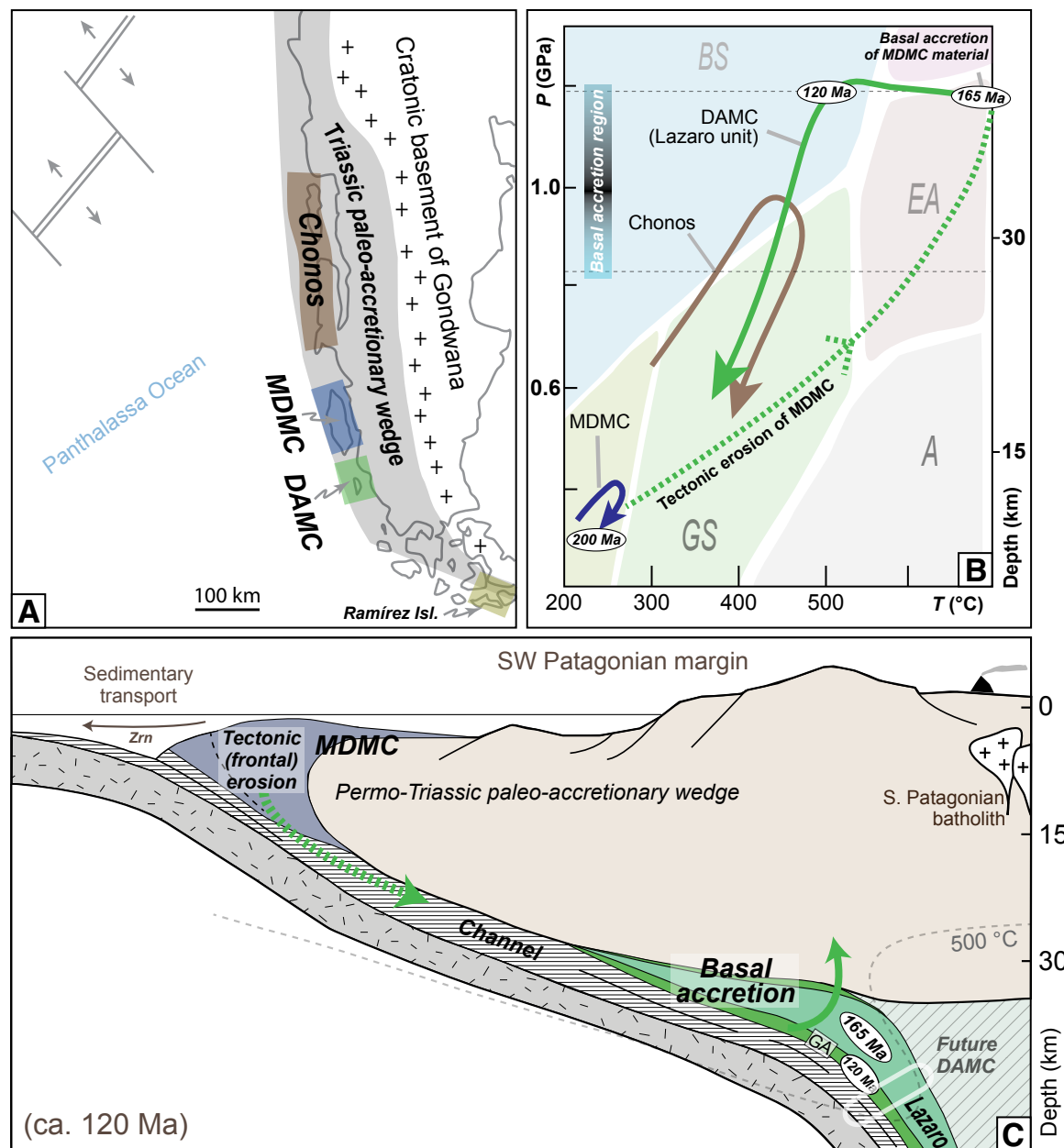


Figure 6. (A) Simplified geodynamic reconstruction of the South American subduction margin during early Mesozoic times showing the respective location of accretionary systems mentioned in text. MDMC—Madre de Dios Metamorphic Complex; DAMC—Diego de Almagro Metamorphic Complex. Modified after Rapalini et al. (2001). (B) Pressure-temperature-time (P - T - t) paths of the various complexes forming the southwestern Gondwana paleo-accretionary margin. BS—blueschist facies; EA—epidote amphibolite facies; GS—greenschist facies; A—amphibolite facies. (C) Schematic reconstruction of the southwestern Patagonian margin at ca. 120 Ma locating the various tectonic elements presented in text (modified after Angiboust et al., 2018). Fragments from the Permo-Triassic paleo-accretionary wedge are frontally eroded and tectonically dragged along the interface before underplating in the basal accretion site. The stack of slices, accreted during Cretaceous times, will after exhumation have formed the Diego de Almagro Metamorphic Complex. Dashed green and solid arrows, prograde and early exhumation paths for DAMC rocks, respectively. Zrn—zircon; GA—garnet amphibolite unit.

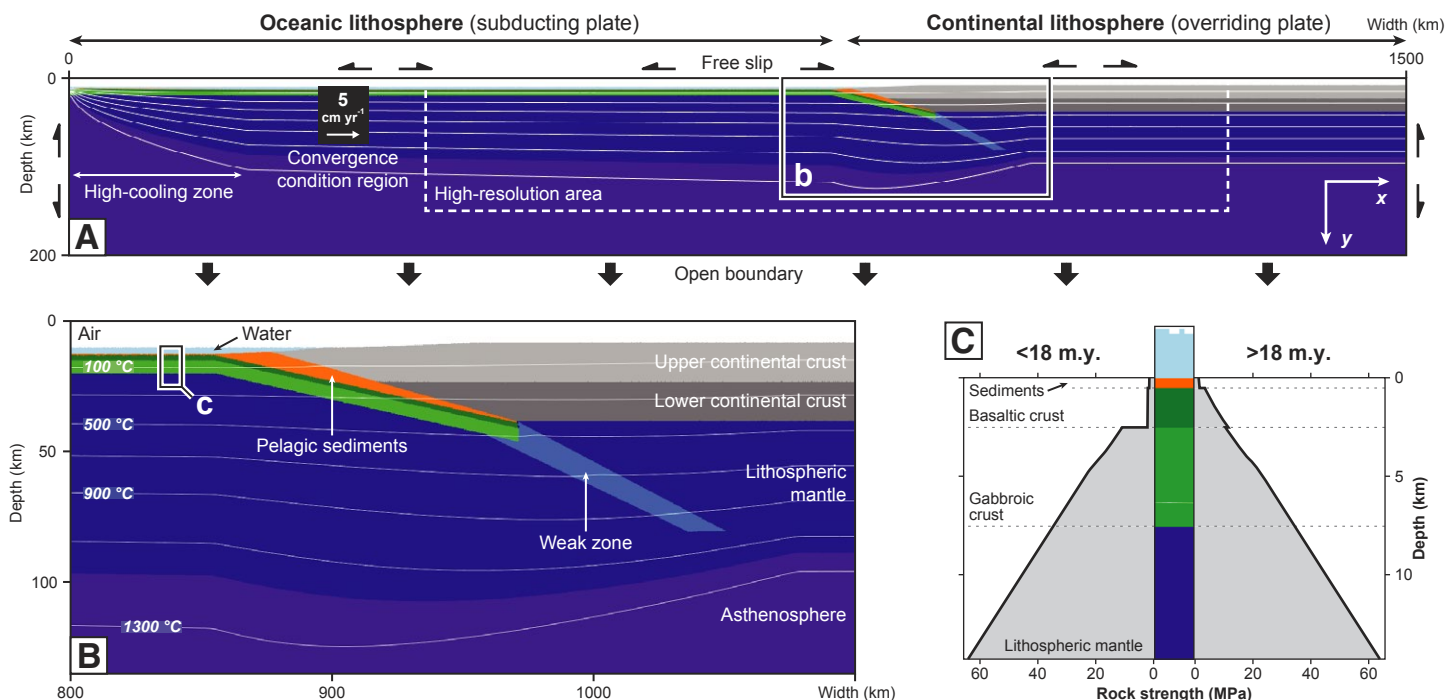


Figure 7. Two-dimensional numerical modeling setup for the reference experiment. (A) Compositional map of the whole computational domain (1500 × 200 km). (B) Magnification of the compositional map on the initial plate boundary zone (see A for location). (C) Graph showing the prescribed rheological layering for the oceanic lithosphere and emphasizing the increasing strength of subducted sediments and basaltic crust after 18 m.y. (in the reference experiment). These rheological profiles are calculated by considering an ~13 °C km⁻¹ geothermal gradient and 10⁻¹⁵ s⁻¹ strain rate. Note that only Drucker-Prager plastic (i.e., brittle) deformation is activated at such shallow depths.

based on a finite-difference scheme and a non-diffusive marker-in-cell technique and assuming non-Newtonian, visco-elasto-plastic rheologies (Gerya and Yuen, 2007). Physicochemical processes such as hydration-dehydration and fluid transport are also considered by implementing fluid expulsion by compaction and thermodynamically constrained metamorphic reactions (Connolly, 2005). This comes along with fluid effects on rock density and viscosity (i.e., weakening due to high pore-fluid pressure), which play a critical role in the frictional strength of the subduction interface and therefore on accretion-erosion dynamics and associated tectonic processes at convergent margins (Peacock, 1990; Saffer and Tobin, 2011; Gerya and Meilick, 2011; Angiboust et al., 2012; Menant et al., 2019). To accurately reproduce topographic variations resulting from subduction-related tectonic processes, the model follows the sticky-air method (Schmeling et al., 2008), which solves the top of the lithospheres as an internal free surface where sedimentation and erosion processes are also considered, providing a reasonable estimation of

topographic variations. Details on governing equations, fluid implementation, and surface calculation are available in the Supplemental Material¹.

Models have been set up to reproduce a typical ocean-continent subduction system where the rheological properties of the downgoing plate can vary through time, impacting margin dynamics (i.e., accretional versus erosive mode). The computational domain measures 1500 × 200 km in the x and y directions, respectively (Fig. 7A). It is discretized using an irregularly spaced Eulerian grid of 1467 × 271 nodes with a resolution of 0.5 × 0.5 km in the vicinity of the plate boundary (i.e., the area subjected to the largest deformation) and of 2.0 × 1.5 km elsewhere. Additionally, approximately eight million randomly distributed Lagrangian markers are initially prescribed for advecting material

¹Supplemental Material. Methods and supplemental figures of the numerical experiments. Please visit <https://doi.org/10.1130/GEOS.S.16746337> to access the supplemental material, and contact editing@geosociety.org with any questions.

properties and computing water release, transport, and consumption. The initial setup is designed with a 30-km-thick overriding continental crust composed of 15 km of felsic upper crust and 15 km of mafic lower crust and with a 7.5-km-thick subducting oceanic crust made up of 0.5 km of pelagic sediments, 2 km of hydrated basaltic crust, and 5 km of gabbroic crust (Figs. 7B, 7C). A temperature threshold of 1200 °C is used to distinguish the underlying lithospheric mantle from the asthenosphere. To initiate subduction, the oceanic crust is initially underthrust below the continental margin and a 10-km-thick weak zone is prescribed at the interface between the two plates. The convergence between the two domains is defined by prescribing a fixed-convergence-condition region belonging to the subducting oceanic lithosphere (e.g., $\sim 5 \text{ cm yr}^{-1}$ for the reference model; Fig. 7A). The velocity boundary conditions are free slip for the left, right, and upper boundaries while the lower boundary is open to ensure mass conservation in the computational domain. An internal free surface is prescribed at the top of the oceanic and continental lithospheres, allowing modeling of the topography. The thermal structure of the oceanic lithosphere is calculated by applying a half-space cooling-age model from 10 k.y. ($x = 0$; i.e., simulating a mid-oceanic ridge on the left boundary of the computational domain) to 53 m.y. ($x = 854 \text{ km}$; i.e., initial location of the subduction zone). To limit the size of the computational domain, the cooling of the oceanic lithosphere is prescribed as 10 times faster for $0 \leq x \leq 200 \text{ km}$. This high-cooling zone is located at $\sim 600 \text{ km}$ away from the subduction zone, which avoids any thermal or mechanical effects on forearc dynamics. A geothermal gradient of $\sim 15 \text{ }^\circ\text{C km}^{-1}$ down to 90 km is defined for the continental lithosphere. Below, the asthenospheric geothermal gradient is set to $\sim 0.5 \text{ }^\circ\text{C km}^{-1}$.

Modeling Strategy

The set of numerical simulations presented herein aims at evaluating the role of varying subduction regime on accretion and erosion processes and brings to light the associated geological records (i.e., from the underplated duplex to the surface evolution). A reference model is first designed to reproduce a long-lived, steady-state accretionary margin (model *Steady-5*). In an alternative experiment, we strengthen the subducting oceanic plate (and hence the subduction interface) by removing permanently the initial water content in the sediments and basaltic crust after $\sim 18 \text{ m.y.}$, therefore preventing fluid weakening (model *Transient-5*; Fig. 7C). The effect of the size of this “subducting rheological asperity” is also investigated by only prescribing an $\sim 100\text{-km-wide}$, dry and strong oceanic crust subducting at $\sim 18 \text{ m.y.}$ (model *Transient100-5*). Finally, different plate-convergence rates are imposed to evaluate the impact of convergence rate on the changing subduction regime from accretional to erosive (models *Transient-10* and *Transient-2*).

Description of the numerical results is presented hereafter with an emphasis on deep accretion and erosion dynamics, metamorphic rock records, and topography evolution. Further details on the whole parametric study are available in the Supplemental Material (footnote 1).

Modeled Steady-State versus Transient Underplating Dynamics

In the reference steady-state experiment (model *Steady-5*; see also Movie S1² and Menant et al., 2019, for further details on model evolution), frontal and basal accretion is predicted during the entire model duration (i.e., $>70 \text{ m.y.}$; Fig. 8). At the front, an $\sim 50\text{-km-wide}$ sedimentary prism develops associated with splay fault–like thrusting events (Figs. 8A, 8B). At $\sim 15\text{--}30 \text{ km}$ depth, the succession of slicing events results in the growth of an $\sim 75\text{-km-wide}$ dome-shaped duplex composed of sedimentary and basaltic material, which is progressively exhumed by the joint action of ongoing underplating, localized shallow normal faulting, and surface erosion. Resulting deformation patterns consist of horizontal then vertical contraction from the base to the top of the nappe pile (see contraction strain axes on Fig. 8B) in agreement with conceptual models (Platt, 1987; Ring et al., 1999). Resulting finite deformation is then characterized by kilometer-scale nappe folding and boudinage, as well as symmetric and asymmetric shearing mostly acquired during the exhumation stage (Fig. 8C). Landward, minor back-thrusting events are predicted in the shallow crust, contributing to the overall forearc in response to protracted frontal and basal accretion processes. At mantle depth, transient detachment of basaltic slices is promoted by the vigorously flowing serpentinite-rich mantle wedge (Fig. 8A; see also Movie S1 [footnote 2]). The persistence of a weak serpentinite layer atop these basaltic slivers seems to prevent their permanent insertion to the overriding plate.

The evolution of the model *Transient-5*, where the subducting oceanic lithosphere is strengthened during the simulation, may be described in three main stages (Fig. 9; see also Movie S2 [footnote 2]). The first stage ($\sim 0\text{--}18 \text{ m.y.}$) is similar to the reference experiment and is dominated by (1) frontal accretion leading to the growth of an $\sim 60\text{-km-wide}$ sedimentary prism and (2) tectonic underplating of thick basaltic tectonic slices with minor sedimentary material forming a deep accretionary complex (i.e., duplex #1, Fig. 9A). The second stage ($\sim 18\text{--}40 \text{ m.y.}$) starts immediately after the inception of subduction of the dry and strong oceanic crust and is characterized by the downdip propagation of a tectonic erosion front (Fig. 9B). Frontal and basal erosion then significantly decreases the size of the frontal prism (from ~ 60 to $\sim 25 \text{ km}$ wide) and dismembers the duplex #1. Coevally, a second nappe stack develops at $\sim 25\text{--}45 \text{ km}$ depth (duplex #2), mostly composed of tectonically eroded sediments and basaltic crust from the former duplex #1 as well as minor continental crust. These deeper accretion events are triggered by the sudden increase of mass flux (i.e., the downgoing crust plus the rapidly eroding former accretionary wedge), which cannot be entirely consumed in the subduction channel while rocks are dragged down to mantle depth. Material in excess is then underplated during this second, deeper accretion stage, which results in an overall doming of the overlying forearc crust associated with high-angle normal faulting (Fig. 9D). This model thus shows that a drastic change in the rheological properties of the subducting lithosphere results in an $\sim 23\text{-m.y.}$ -long transient period during

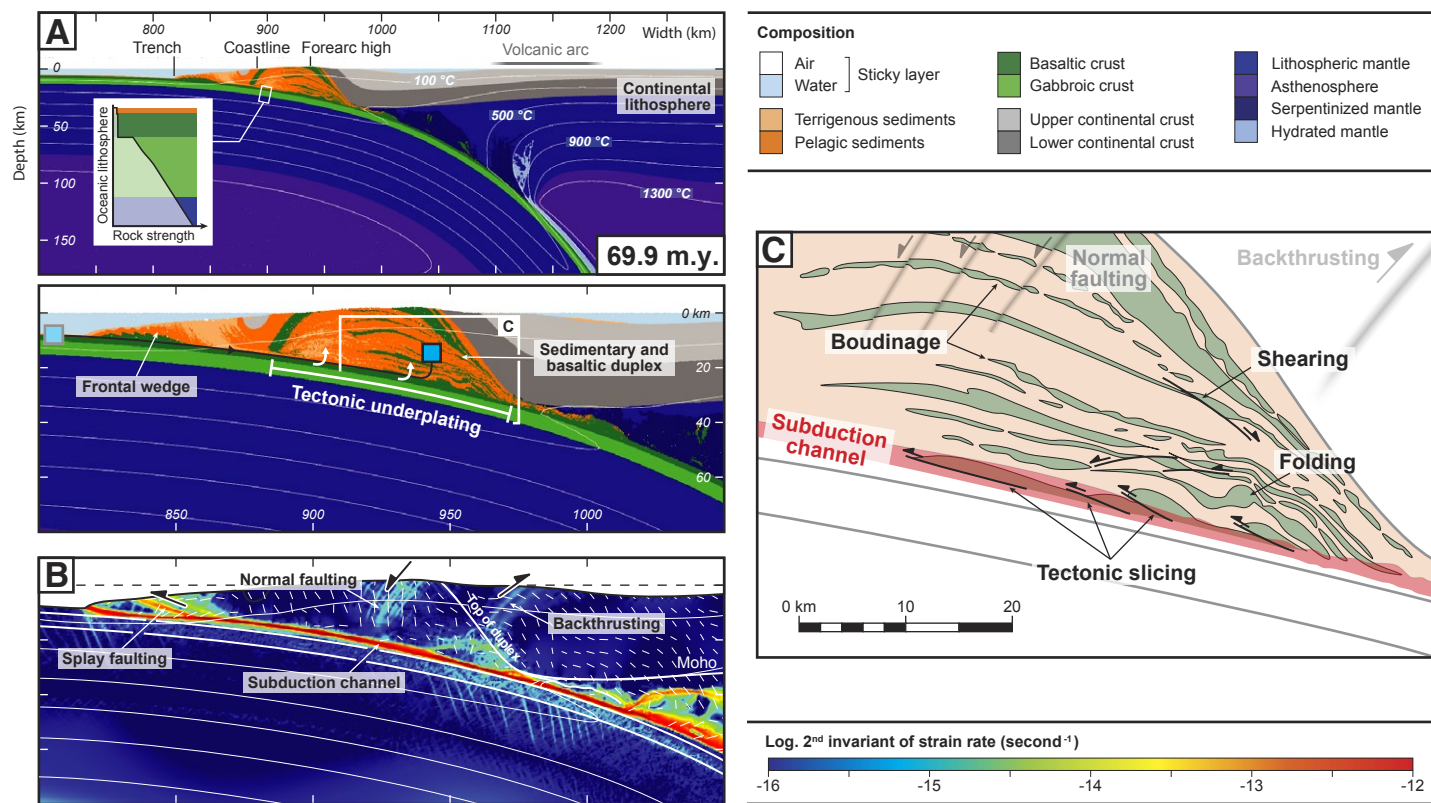
²Supplemental Videos. Five movies (S1–S5) of the numerical experiments. Please visit <https://doi.org/10.1130/GEOS.S.16746349> to access the supplemental material, and contact editing@geosociety.org with any questions.

which frontal and basal erosion in the outer forearc domain is concomitant with underplating in the inner forearc domain. Afterward, the downdip migration of the basal erosion front eventually leads to the consumption of the duplex #2 itself, and the margin becomes completely erosive after ~40 m.y. (Fig. 9C).

Predicted Tectono-Metamorphic Rock Record

To compare with the geological rock record of basal accretion and basal erosion, we extracted from the numerical experiments *P-T-t-ε* paths for a set of Lagrangian markers tracking underplated material (Fig. 10).

The *P-T-t-ε* trajectories for both pelagic sediment and basaltic crust in the reference experiment *Steady-5* show prograde and retrograde paths following a similar ~10 °C km⁻¹ geothermal gradient (Figs. 8A, 10A). Pressure and temperature peak conditions lie between ~0.5–0.9 GPa and ~200–300 °C for rocks inserted into the duplex, except for some markers tracking material transiently accreted at mantle depth (>1.5 GPa and >300 °C). Differences between pelagic sediment and basaltic crust mostly come from their deformation record. Indeed, the prograde path for the sediments occurs under a high strain rate (~10⁻¹² s⁻¹) while it is commonly marked by a medium strain rate for the basaltic crust (~10⁻¹⁴–10⁻¹³ s⁻¹) preceding a more intense deformation stage near peak conditions (Fig. 10A). This discrepancy is explained by the fact that the sedimentary



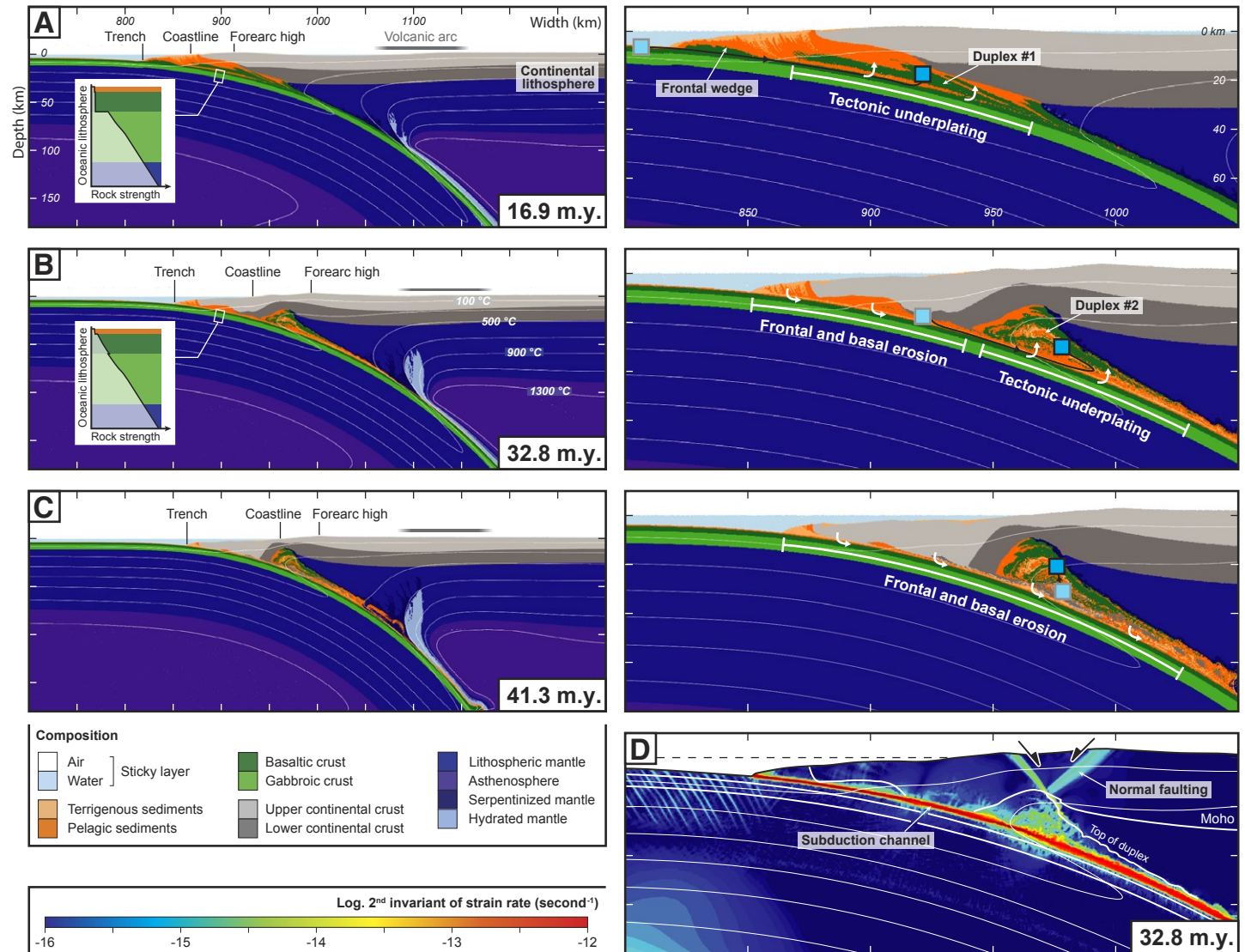


Figure 9. Numerical results of model *Transient-5* where the rheological properties of the subducting oceanic crust have been modified after ~18 m.y. to reproduce an accretionary-then-erosive margin. (A) Composition maps of the first accretionary stage (large-scale view [left] and magnification of the forearc domain [right]) predicting the formation of a frontal and basal accretionary wedge. (B) Composition maps of the second, transient erosive stage (large-scale view [left] and magnification of the forearc domain [right]) where frontal and shallow basal erosion are coeval with deep underplating, resulting in the formation of the deep duplex #2. Insets on left panels in A and B show the relative strength of the subducting lithosphere during these two stages. (C) Composition maps of the erosive stage (large-scale view [left] and magnification of the forearc domain [right]) where frontal and basal erosion lead to the dismembering of the outer forearc crust and deep duplex #2. White arrows locate the key erosional and accretionary domains along the subduction interface. The blue squares and black arrows on right panels of A–C depict the trajectory of the sediment tracer used as a reference on the pressure-temperature diagram of Figure 10B. (D) Strain-rate map showing the typical deformation pattern affecting the forearc domain during the erosive stage (same area as right panel of B).

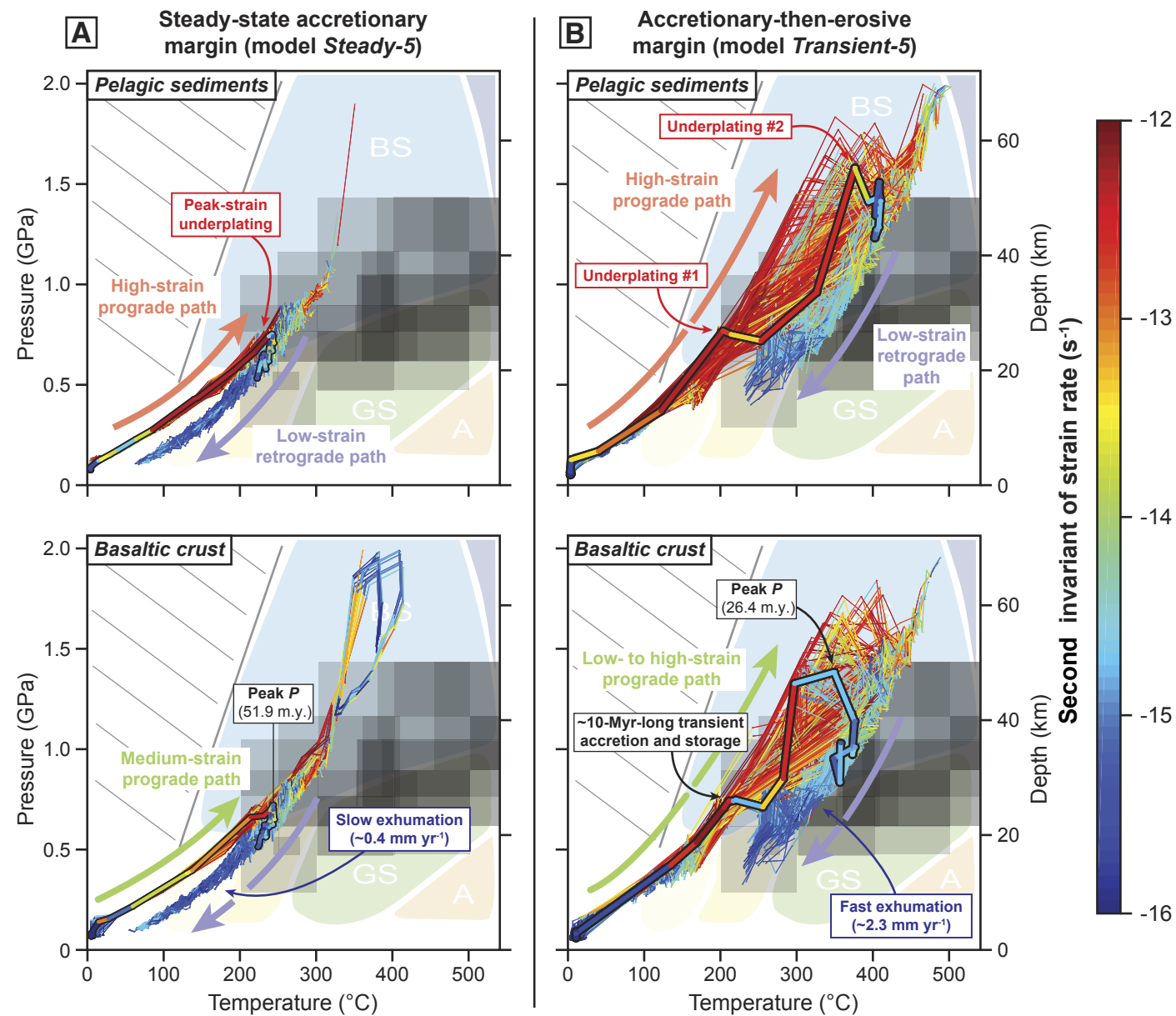


Figure 10. Predicted pressure-temperature (*P-T*) paths for a set of Lagrangian markers from the subducting pelagic sediments (upper panels) and basaltic crust (lower panel) in models *Steady-5* (A) and *Transient-5* (B) (i.e., ~350 markers for each panel). The *P-T* lines are colored as a function of the strain rate during their tectonic transport, depicting the *P-T*-time-strain record of metamorphic rocks from deep duplex structures. Diagonal hatching: Domain not realized on Earth. Grey boxes in the background correspond to peak burial estimates of basally accreted material from the compilation shown on Figure 4. BS—blueschist facies; GS—greenschist facies; A—amphibolite facies.

cover is buried within the high-strain subduction channel while the oceanic crust is mostly subducted underneath and becomes part of the channel only during the deep slicing event (i.e., near peak conditions; Fig. 8B). Conversely, the retrograde path for both rock types is characterized by a low strain rate ($\sim 10^{-16}$ – 10^{-15} s $^{-1}$) and slow exhumation (~ 0.4 mm yr $^{-1}$).

In the experiment *Transient-5*, the *P-T-t-ε* trajectories depict a more complex pattern marked by pressure peak conditions mostly between ~ 1.0 and 1.7 GPa and between ~ 300 and 400 °C, although some rock markers reach ~ 1.9 GPa and ~ 450 °C (Fig. 10B; see also the representative marker trajectory on Figs. 9A, 9B). While the peak pressure conditions characterize the second stage of underplating (duplex #2), transient storage, lasting ~ 10 m.y., is commonly predicted during the prograde path, reflecting the first stage of underplating (duplex #1) at ~ 0.6 – 0.8 GPa and ~ 200 – 250 °C. According to our model results, rock burial occurs following a typical subduction geothermal gradient of ~ 9 °C km $^{-1}$ at crustal depth, while it shows a considerably higher variability at mantle depth (i.e., ~ 4 – 15 °C km $^{-1}$), probably because of the temperature increase associated with the rapid mass flux that characterizes the sudden basal erosion and underplating events after 18 m.y. (Movie S2 [footnote 2]). As for the reference experiment, strain rates during the prograde path are higher in the sediments (buried within the subduction channel) than in the basaltic crust (Fig. 10B).

The latter, however, records two peaks in the strain rate ($\sim 10^{-12}$ s $^{-1}$), which mark the two successive underplating stages. The retrograde path records the incomplete exhumation of deeply accreted rocks and is characterized by low strain rates ($\sim 10^{-16}$ – 3.10^{-15} s $^{-1}$) and a faster exhumation (~ 2.3 mm yr $^{-1}$) than for the reference model. Note also that an ~ 30 – 50 °C temperature increase is commonly predicted during the first step of the retrograde path, reflecting the higher temperatures, and therefore the inverted geothermal gradient, in the overriding plate atop the subduction channel.

Diagnostic Forearc Topographic Evolution

Predicted forearc topography in experiments *Steady-5* and *Transient-5* (for both accretionary and erosional stages) is consistently characterized by a coastal high with an ~ 2000 to ~ 4000 m maximum elevation spatially followed by an inner-forearc depression (Figs. 11A, 11C). Major discrepancies between the two models arise, however, when looking at the temporal evolution of the topography.

Long-lived frontal and basal accretion dynamics in the reference simulation lead to the overall growth of the forearc margin, marked by the seaward

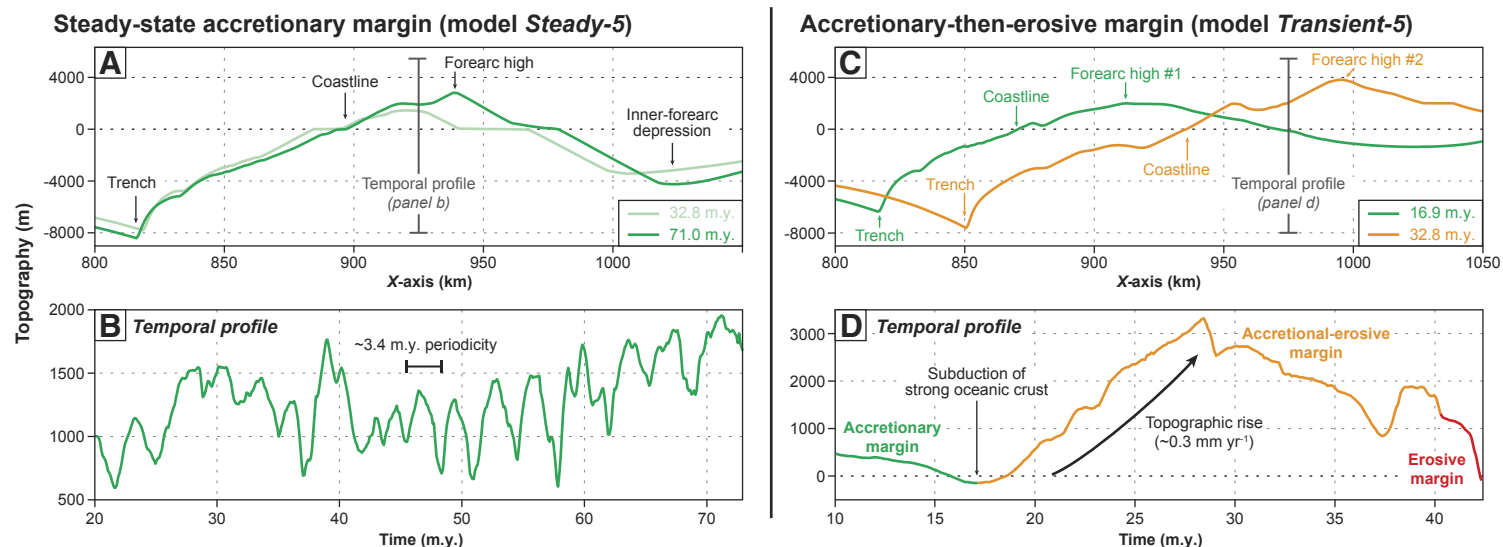


Figure 11. Comparison of the forearc-topography evolution predicted in models *Steady-5* (A, B) and *Transient-5* (C, D). (A, C) Forearc topographic profiles at two different time steps for the two experiments, all showing a typical high coastal topography spatially followed by an inner-forearc depression. (B, D) Temporal profile of forearc surface for the two experiments. See the exact location of the profile on panels A and C. The forearc topography in model *Steady-5* is marked by periodic vertical oscillations as a response to basal accretion processes (panel B), while it is characterized by a long-term rise in model *Transient-5* during the transient accretionary-erosive subduction regime, in response to deep duplex growth (panel D; see details in the text). Note that the elevation in the experiments is relative to a fixed sea level, implying that topographic variations and vertical surface velocities are more relevant indicators of topography dynamics than absolute elevations.

migration of the trench and the long-term rise of the forearc high achieved by a succession of uplift-then-subsidence sequences (Fig. 11B). These topographic pulses are characterized by uplift (and subsidence) rates ranging from ~ 0.5 to ~ 1.5 mm yr⁻¹ and a robust periodicity of ~ 3.4 m.y., which reflects the underplating dynamics at depth (see also Menant et al., 2020, for further details on this accretion-related topographic signal).

Alternatively, no periodic signal is predicted in experiment *Transient-5*, which rather shows a rapid landward migration of the trench and the forearc high, coevally with an increase of the tectonic relief, triggered by the subduction of a stronger oceanic crust and associated changing margin dynamics (Figs. 9, 11C). From ~ 18 m.y., the forearc high #1 subsides due to the basal erosion of duplex #1, while the forearc high #2 rises (i.e., ~ 3000 m increase in ~ 10 m.y.) in response to the growth of the duplex #2 underneath (Fig. 11D). After ~ 30 m.y., this newly formed high coastal topography starts to subside as the basal erosion front propagates downdip along the plate interface and eventually starts to dismember the deep duplex structure.

Some Parametric Investigations

The modeling results presented in the previous section place emphasis on the critical effect of the permanent strengthening of the subducting plate on forearc dynamics. In an alternative simulation, the subduction of an only 100-km-wide, dry and strong oceanic crust segment after 18 m.y. (model *Transient100-5*) does not disturb the overall accretion dynamics. Despite a brief interruption, the protracted frontal and basal accretion result in the growth of a wide sedimentary prism and a deep duplex and the long-term rise of a high coastal topography (Fig. S1 [footnote 2]). This suggests that the subduction of small “asperities” unlike drastic and sustained changes of the rheological properties of the downgoing plate, does not significantly modify the margin dynamics.

From the model *Transient-5*, different plate kinematics have been imposed in two additional experiments. With an increase in the convergence rate (~ 10 cm yr⁻¹; model *Transient-10*), the margin evolution is akin to a dominant accretional then erosive regime and the development of two successive duplex structures at crustal then crustal-mantle depth (Fig. S2 [footnote 2]). It is worth noting that the transient accretionary-erosive period starts earlier than in the *Transient-5* model (i.e., ~ 11 m.y.) and is associated with a more rapid growth (and dismembering) of the deep nappe stack and a faster topographic rise (and demise) of the high forearc topography. Alternatively, with a decrease in the convergence rate (~ 2 cm yr⁻¹; model *Transient-2*), basal accretion is achieved by a mostly horizontal mass flow at the base of the forearc domain, which allows more basaltic crust to be scraped off the subducting plate (Fig. S3 [footnote 2]). Accretion processes then prevail until ~ 42 m.y. and the subduction of the stronger oceanic crust, which changes the margin dynamics to erosive. The former accretionary wedge is then slowly dismembered and the whole of the remobilized material is progressively consumed in the subduction channel and dragged at depth, preventing the growth of a second, deeper duplex structure.

Further details on the modeling results of these additional experiments, including their topographic evolution, are available in the Supplemental Material (footnote 1).

DISCUSSION

Insights on Wedge Growth Processes in the Basal Accretion Region

The pioneering return-flow model described by Cloos and Shreve (1988) has been widely applied to study wedge formation mechanisms and deformation processes, in particular to illuminate the recycling of shallow, frontally accreted material, explaining olistostromes and chaotic block-in-matrix mixing such as in the Franciscan belt (e.g., Ernst, 2016). However, the extent of tectonic mixing within mélange-like slivers such as in the Cuban ophiolitic belt (e.g., Diaz et al., 2017) or on Santa Catalina (California) or Syros (Greek Cyclades) Islands remains controversial and debated (e.g., Grove et al., 2008; Laurent et al., 2016; Harvey et al., 2020). In other words, it remains unclear whether (1) meter-sized blocks can independently travel atop the slab interface over tens of kilometers in a rheologically weak matrix, or (2) the apparent block-in-matrix mélange characteristic feature is the protracted result of superimposed sedimentary and tectonic deformation processes (e.g., Wakabayashi, 1999; Krohe, 2017).

The recognition of coherent nappe stacking all along circum-Pacific ancient (and active) accretionary systems (Figs. 1, 3) as well as the analogue and numerical outputs predicting tectonic slicing and duplex growth both in wedge- and lithosphere-scaled models (Fig. 8; Gutscher et al., 1996; Ellis et al., 1999; Lohrmann et al., 2006; Malavieille, 2010; Vogt and Gerya, 2014a; Ruh et al., 2015; Menant et al., 2019; Ruh, 2020) challenge this vision of a widespread chaotic mixing process within the subduction channel and overriding accretionary wedge. Instead, these physically constrained studies (1) allow comparison of the return-flow concept (as an overall mass flow) and transport of coherent slices through strain localization processes and (2) shed light on the mechanisms responsible for the off-scraping and recycling of the downgoing oceanic crust at the base of the wedge. Menant et al. (2019) have thus evidenced that local, along-dip shear-stress increase along the interface—as a consequence of variability of fluid availability (see also Moreno et al., 2018)—critically controls the location of the slab-peeling event and the composition and thickness of the formed tectonic slice. A relative stability of underplating sites over multiple basal-accretion cycles (i.e., commonly predicted at 15–20 km and 25–30 km depth among the various parametric experiments undertaken; Fig. 8A; see also Menant et al., 2019) can be suspected from the compilation shown in Figure 4. A number of factors explains the dispersion of estimates, including (1) the uncertainties in pressure estimates from natural samples and (2) the variability of the subduction-zone geometry and of the rheological and thermal state recorded in subduction channels worldwide, which likely tends to result in distribution of underplating events at all crustal depths. Also, given that large and steady-state accretionary systems as modeled in our study are rather rare

in the geological record, we emphasize that the basal accretion segments at 15–20 km and 25–30 km depth may not be systematically identified in active and fossil accretionary wedge systems (see also Oncken, 1998). Nonetheless, preferential tectonic underplating approaching the subcontinental Moho (see the preferential basal underplating depth in Fig. 4) appears to be a reasonable assumption given that differential stress increase is expected in this region corresponding to the resistance peak of the upper-plate rheological envelope (also called the “S point”; e.g., Ellis et al., 1999; Fig. 1A), where the cool lower crust and lithospheric mantle mechanically close (at least partially) the connection with the deeper serpentinized interface. Although such a differential stress increase is likely limited along the plate interface (i.e., a few megapascals, in agreement with the low stress drops invariably associated with seismic ruptures in subduction environments; e.g., Ruff, 1999), it appears to be large enough to localize tectonic slicing in weak lithologies (Ruh et al., 2015; Menant et al., 2019). However, it is worth noting that significantly higher differential stresses (i.e., on the order of several hundreds of megapascals) probably accumulate in particularly strong and relatively dry lithologies (e.g., gabbroic or peridotitic crust, continental granulites) that act as rheological asperities at the base of the crustal wedge. This is geologically supported by the formation of pseudotachylytes (i.e., seismically generated frictional melts) during brittle, blueschist-facies deformation of the alpine subduction complex (Austrheim and Andersen, 2004; Menant et al., 2018) and by the high differential stresses (i.e., >100 MPa) numerically predicted in the deepest part of the forearc crust (see Menant et al., 2019, their figure 1d).

The tracking of strain-rate evolution of rock markers in numerical experiments throughout subduction and exhumation of the downgoing slab top confirms that high-strain rock fabrics, including mylonites, cataclases, sheath folds, and vein networks, are mostly acquired in these basal accretion regions (Fig. 10A), in line with field and microstructural studies (e.g., Hashimoto et al., 2002; Richter et al., 2007; Ring, 2008; Meneghini et al., 2009; Behr and Bürgmann, 2021; Fig. 3). Previous prograde, burial-related deformation stages (in the form of schistosity and vein networks) may be variably affected by subsequent shearing and underplating (e.g., Muñoz-Montecinos et al., 2020) depending on the pervasiveness of peak burial deformation. Numerical investigations predict that the material subsequently transported from the interface upward into the duplex travels at relatively low velocities (on the order of $\sim 0.4 \text{ mm yr}^{-1}$, in line with geological estimates; Glodny et al., 2005), associated with strain rates several orders of magnitude lower than during the underplating event, changing the main deformation mechanisms recorded in exhuming duplexes (most likely from brittle or semi-brittle creep to pressure-solution and locally dislocation creep; Fig. 10A; Oncken et al., 2021). Resulting internal duplex deformation appears as distributed folding and boudinage and localized extensional shearing, in agreement with field fabric descriptions in paleo-accretionary systems, notably reporting crenulation cleavage, which does not fully overprint the fabrics formed along the subduction interface (Figs. 3, 8C; e.g., Onishi et al., 2001; Richter et al., 2007; Regalla et al., 2018). In nature, however, local domains (too small to be resolved in our models) may exhibit

full overprint during exhumation, as expected in particular along the duplex roof, the deep back-thrusts, or normal fault systems as seen for instance on Figure 8B. Note that the modeled absolute strain-rate values (Fig. 10A) cannot be directly compared with those geophysically and geologically estimated (e.g., Angiboust et al., 2015; Oncken et al., 2021) because of a scaling issue due to the resolution of the models. Nonetheless, it is interesting to track strain rate evolution using model markers because strain rates also impact fabric formation and likely mineral-reaction and isotopic-equilibration rates. This approach predicts the emplacement along the P - T path where fabric formation, mineral equilibrium, and age freezing would occur, hence enabling further comparison with subduction-related (and potentially, a reassessment of) P - T data in literature.

When the system reaches a steady-state equilibrium, the slab-top peeling process is predicted to occur with a strikingly constant periodicity on the order of several millions of years (Menant et al., 2020; Figs. 8B, 11C), giving rise to a very thick and stable accretionary edifice (e.g., Konstantinovskaya and Malavieille, 2011). The growth and *preservation* of such an extremely thick wedge (>35 km thick) formed by protracted basal accretion events as recorded in south-central Chile during the late Paleozoic (Western Series; e.g., Willner, 2005) may appear at first sight as a quite unusual phenomenon in Earth's Phanerozoic subduction history. This process could be interpreted as reflecting a “steady-state” subduction regime along the Gondwana margin over the second half of the Paleozoic. Two key factors that may have led to this situation are (1) a relatively smooth Panthalassa oceanic plate, devoid of large asperities that would act as effective tectonic erosion agents, and (2) a relatively stable climatic regime given that the amount of trench-filling material—susceptible to impacting plate-interface coupling and margin dynamics (see also the following section Wedge Consumption Mechanisms and Transient Dynamics of Accretionary Edifices)—is known to be influenced by climatic changes and glaciations (e.g., Lamb and Davis, 2003; Kukowski and Oncken, 2006).

Wedge Consumption Mechanisms and Transient Dynamics of Accretionary Edifices

When the long-term mechanical coupling between the two plates becomes too high, the previously formed wedge is eroded from its base and the connection with the deep serpentinized channel broadens (Fig. 9B). The growth (or destruction) of a wedge thus reflects a peculiar stress state of the interface as well as its structural stability over geological time. Indeed, our new modeling investigations demonstrate that an increase in the subduction interface strength on a limited spatial extent (i.e., small asperities) does not significantly affect the margin dynamics (compare models *Transient-5* and *Transient100-5*; Fig. 9 and Fig. S1 [footnote 2]). Punctuated basal erosion episodes (e.g., associated with the subduction of an isolated seamount) could transiently unlock the “S point” and open the updip end of the serpentinized channel. Once such an asperity were passed, this deep connection would close and the mass-transfer mode

return to accretionary. These short-lived (≤ 2 m.y.) changes likely leave only few imprints in the long-term geological records (Fig. S1). However, we stress that such events could allow for the extrusion (from the top of the deep channel; Fig. 2) and intercalation of higher-grade (generally serpentinite-bearing) material within lower-grade, basally accreted duplex structures as documented in the thick Carboniferous Chilean paleo-accretionary wedge (Los Pabilos; e.g., Willner et al., 2004a) and elsewhere (Liberty Creek–Seldovia, Alaska: López-Carmona et al., 2011; Sambagawa, Japan: Wallis, 1998).

Alternatively, drastic and long-lived changes in the rheological properties of the plate interface resulting from climate-related variations of sedimentary input at the trench or subduction of large asperities such as plateaus, ridges, large seamount chains, or widespread oceanic fracture zones (e.g., Ranero and von Huene, 2000; Sisson et al., 2003; Gerya et al., 2009; Moreno et al., 2014) have a major impact on accretion-erosion dynamics, leading to switches between deep accretionary wedge growth and dismembering during accretionary-erosive periods tens of millions of years long (Fig. 12). In addition to these external parameters, wedge-internal dynamics also appears to be a critical factor affecting the spatial and temporal variations of the mass-transfer mode.

Evolving density distribution in the growing duplex, strain and fluid weakening, and/or the development of a fabric anisotropy may also promote spatial and temporal switches between accretion and erosion without involving external changes (see the duplex dynamics for the steady-state subduction model in Movie S1 [footnote 2]). This non-exhaustive list of extrinsic and intrinsic parameters reflects the multiplicity of factors that can explain, for instance, the multiple gaps in the accretionary history along the Japanese archipelago (Fig. 5) since the Cambrian period (Isozaki et al., 2010). These transient tectonic erosion events (and the associated consumption of previously formed duplexes) explain why very large accretionary edifices are much rarer in the geological record than expected from the widespread and long-term subduction history on Earth. Studies from Bangs and Cande (1997) and Clift and Hartley (2007) have also tended to show that the “aggressiveness” of tectonic erosion is a non-steady factor in subduction history over time scales of tens of millions of years, capable of removing large amounts of previously accreted sediments at rates faster than accretion. In this highly dynamic plate-interface environment, frontal erosion (and outer forearc subsidence) and basal underplating (and inner forearc uplift) may be concomitant (Fig. 12; Comte et

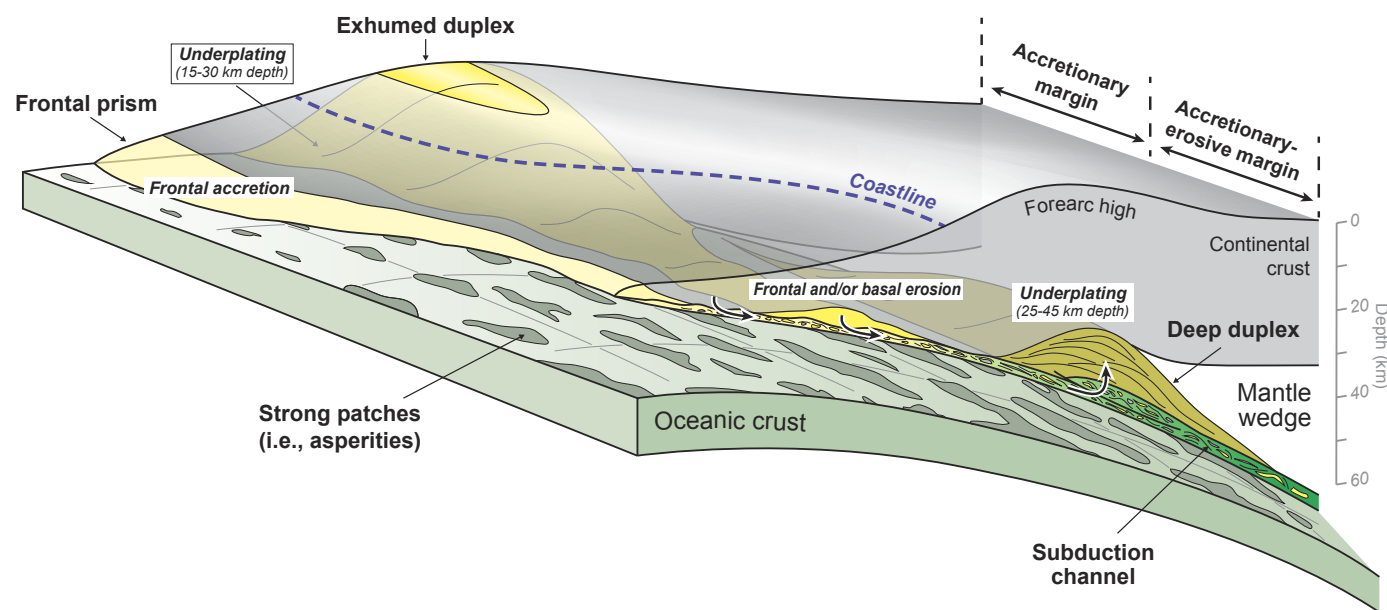


Figure 12. Three-dimensional sketch (not to scale) showing the morphology of the subduction system for accretionary and erosive environments based on geological observations and model predictions. The long-term accretionary margin (in the background) is marked by a wide frontal wedge and thick duplex (in yellow) that may be exposed at the surface in the region of high coastal topography. The erosive margin (in the foreground) shows the transient growth of a deep duplex (in orange) made of material previously scraped off the base of the outer forearc region in response to coeval frontal and basal erosion. The change of subduction regime (i.e., from accretionary to erosive or vice versa) requires a drastic change in the rheological properties of the downgoing plate, here illustrated by the subduction of asperities (in dark green; see details in the text).

al., 2019; see also Tewksbury-Christle et al., 2021, for a fossil example in California) due to the balance between the mass flux and the amount of material that can be consumed by the subduction channel, which is notably controlled by the plate-convergence rate (see parametric investigations in the Supplemental Material [footnote 1]). The erosive northern Chilean margin and its high coastal topography may well illustrate this “hybrid” subduction regime (Clift and Hartley, 2007), with transient underplating at 30–50 km depth of tectonically eroded forearc material driving the long-term coastal uplift and associated forearc-basin exposure since the lower to middle Miocene (Courdurier-Curveur et al., 2015; Evenstar et al., 2017). Coeval increasing aridity in the Atacama Desert (Chile; Lamb and Davis, 2003; Armijo et al., 2015; Rech et al., 2019), likely associated with a decreasing amount of sediment entering the trench, thus provides a plausible mechanism for triggering the switch in the subduction regime and the subsequent deep-duplex growth and forearc topography rise in ~10–15 m.y. as predicted numerically (Figs. 9B, 11D).

A particularly vigorous coastal uplift recently also occurred in the Mejillones Peninsula in a long-term context of frontal erosion of the northern Chilean margin and arcward trench retreat. There, a sequence of first terrestrial sedimentation on arc basement is succeeded by marine sedimentation and a return to uplift with terrestrial sedimentation and erosion (e.g., Victor et al., 2011) over a few million years. The spatial persistence of this uplift event in the same location over the last few million years discounts the subduction of a topographic high as an explanation for this peninsula formation. Instead, a spatially stable high-shear-stress region, with variable degrees of coupling of the plate interface segment under the uplifted region (i.e., a “barrier” at seismological time scales; e.g., Victor et al., 2011; Saillard et al., 2017), could explain the observed topographic feature (in northern Chile but also along the entire margin) by involvement of transient basal accretion events (Fig. 12; see also Menant et al., 2020, and references therein). Alternatively, Encinas et al. (2020) noted that the uplift of the Coastal Cordilleras in south-central Chile may be decreased where a strongly hydrated seafloor (such as a fracture zone) is subducted under the wedge (in line with previous geophysical data from Moreno et al. [2014]). Although debated, the question of the critical role of deep accretionary processes on the formation of these coastal promontories deserves to be addressed, notably through further geophysical investigations (e.g., Bassett and Watts, 2015).

Another noteworthy implication from these numerical experiments is that temporal switches from basal accretion to basal erosion (as well as the along-strike variations in mass-transfer regime in active margins) may be used as a proxy to constrain the long-term frictional properties of the plate interface over geological time scales (Fig. 12). As a consequence, active margins where duplexing is identified near the subcontinental Moho could be viewed as reflecting a transition from decoupled to coupled segments along the subduction interface, which appears, however, at odds with GPS-based locking maps exhibiting a common decrease in plate coupling approaching the forearc mantle corner (e.g., Moreno et al., 2018). This suggests a “time scale-dependent” frictional pattern along the plate interface. Such pattern,

typically at the seismic-cycle time scale, precludes the recognition of sites of million-year-long basal accretion events from the distribution of GPS-monitored frictional heterogeneities (Bassett and Watts, 2015), which rather reflect short-term processes associated with the seismic cycle or slow slip processes (e.g., Obara and Kato, 2016).

Insights on the Structure and Dynamics of the Forearc Mantle Corner

Field studies confirm that a large number of suture zones where an oceanic realm has been closed by subduction exhibit tectonic slivers scraped off and stacked (in the presence of a duplex structure or not) in the 30–50 km depth range, i.e., at the base of the “cold nose” region (e.g., Bostock, 2013; Despaigne-Díaz et al., 2017; Bebout and Penniston-Dorland, 2016; Agard et al., 2018). These slivers, generally metamorphosed at blueschist- to eclogite-facies or amphibolitic conditions, exhibit thicknesses ranging between several hundred meters and kilometers (Fig. 2; e.g., Vitale-Brovarone et al., 2013; Angiboust et al., 2014, 2018; Plunder et al., 2015; Despaigne-Díaz et al., 2017). This observation reveals that the forearc lithospheric mantle in the forearc mantle-wedge corner (FMC) region may not always be in direct contact with the slab top but instead may be separated from the downgoing plate by a series of previously accreted slivers, remaining relatively immobile along the interface hanging wall for periods that can last as long as several tens of millions of years (Fig. 2; Franciscan: Wakabayashi, 1990; Diego de Almagro Island, Patagonia: Angiboust et al., 2018). These slivers may be constituted of ocean-derived material (plateaus, extensional continental allochthons, thick and coherent packages of mafic or sedimentary material) but also of shallow upper-plate continental crust frontally eroded near the trench (e.g., Fig. 6C; Cluzel et al., 2001; Beltrando et al., 2010; Angiboust et al., 2017). In our models, a several kilometers-thick layer of mixed sedimentary-(ultra)mafic material can develop atop the subduction interface down to 50–60 km depth (Figs. 8, 9; see also Menant et al., 2019). This layer (which may be viewed as a subduction channel in the sense of Guillot et al., 2009) is never permanently attached to the base of the FMC because of the persistence of a weak serpentinite layer in between. Instead, our models suggest that this transiently accreted material package is regularly dragged deeper in the mantle by enhanced basal erosion due to fluctuations in plate interface shear stresses, which are mostly controlled by fluid distribution, slab strength, or the presence of asperities. Such a process would be extremely challenging to identify in the rock record and require subsequent exhumation and exposure of key outcrops at the surface. One possibility for preservation may be a burial and a fast, buoyant exhumation of a large continental sliver (or an oceanic plateau) against a deep wedge that may freeze such deep-seated, transient structures (e.g., Vogt and Gerya, 2014b). Note also that the transport via basal erosion of such “mélange” packages (or “subduction channel” fragments) down to sub-arc depths (as inferred, e.g., in Central Mexico; Ducea and Chapman, 2018) may bear implications because their preferential melting would likely enhance magmatism and volcanism

and hence contribute to the growth of continental crust (e.g., Plank and Langmuir, 1993; Stern, 2011; Cruz-Uribe et al., 2018). A link may thus exist between episodes of continental crust growth along active margins and fluctuations in mass-transfer modes along the adjacent subduction interface.

Lastly, we conclude that the occurrence of a deep accretion process of large coherent slices along the FMC, as seen in current models and field examples (Fig. 2), perhaps calls for a reassessment of the common vision of the rheological segmentation of the plate interface where the presence of weak hydrated mantle minerals such as serpentinite and talc are expected to control the depth of the downdip end of the seismogenic zone (e.g., Peacock and Hyndman, 1999; Hippchen and Hyndman, 2008). Indeed, an accreted metasedimentary sliver (or an interlayered mafic-sedimentary pile; Fig. 9B) is likely mechanically less “weak” than a hydrated, serpentinite, and/or talc-rich “cold nose” environment (e.g., Hilaiet et al., 2007; Agard et al., 2018). Thus, in active margins where a package of blueschist-facies material is accreted at mantle depth, the downdip end of the locked seismogenic zone may be controlled by the rheological behavior of the accreted material—where fluid-saturated conditions are likely (e.g., Oleskevich et al., 1999; Palazzin et al., 2016; Fagereng et al., 2018)—rather than by the rheology of the hydrated FMC itself (see also discussions in Heuret et al., 2011; Abers et al., 2017). Reconsidering the compositional environment of the deep subduction interface is of paramount importance for setting the rheological framework, which controls the seismic behavior and acts together with mass fluxes to drive the long-term evolution of active margins.

Remaining Questions and Future Challenges

Undeniable progress was made in the 1980s and 1990s toward understanding basal accretion processes from a field and structural perspective. Over the past 20 years, a number of important tectonic and kinematic issues have been resolved using analogue and numerical modeling tools as well as geodetic methods. A summary of diagnostic criteria typical for each mass-transfer mode, including the transient accretionary-erosive subduction regime (Figs. 9B, 12), has been tentatively compiled in Table 3. This non-exhaustive review evidences a widespread occurrence of basal tectonic underplating at active margins both in space and time (Fig. 1A) and underscores a need to integrate this wealth of geological and geophysical data in order to understand forearc dynamics and rheology in a comprehensive way, bridging space and time scales, aiming at providing critical insights on a region of the plate interface where most megathrust ruptures ($M_w > 8$) nucleate (e.g., Bassett and Watts, 2015). Some first-order aspects appear to stand out of the crowd of remaining issues to be addressed by future studies:

- (1) Temperatures between 300 and 550 °C are typically inferred from basally accreted paleo-accretionary material (Fig. 4). This range encompasses the typical 350 °C threshold classically considered for the downdip end of locking at the plate interface (e.g., Oleskevich et al., 1999) where basal accretion commonly occurs (e.g., Bassett and Watts, 2015). The matter of peak burial temperatures warmer in rocks than in geophysical

TABLE 3. SUMMARY OF DIAGNOSTIC CRITERIA CHARACTERIZING EACH MASS-TURNFER MODE IN ACCRETIONARY, EROSIIVE, AND TRANSIENT ACCRETIONARY-EROSIVE CONTEXTS (MODIFIED AFTER ONCKEN, 1998)

Features	Mass-flow mode		
	Accretion	Tectonic erosion	Transient accretion-erosion
Accretionary wedge	Complete	Frontal wedge is missing in models; a tiny wedge may locally develop in natural systems	Small frontal wedge; deep duplex formation
Fore-arc deformation			
Offshore	Shortening, imbrication; peninsula formation	Extension, surface collapse in case of frontal erosion; embayments of shoreline	Compression at the toe of the margin, extension landward with local thrusting
Onshore	Deep duplexing at depth >15 km; formation of fore-thrust and back-thrusts; extension at the top of the duplex	Extension, surface collapse in case of basal erosion	Extension
Surface motion	Periodic uplift and erosion; exhumation of a blueschist-facies duplex	Rapid subsidence, forearc basin formation; local uplift in the inner forearc when a deep duplex forms	Rapid subsidence, uplift above exhuming blueschist-facies duplex
Trench and volcanic front displacement	Toward the ocean	Toward the continent	Toward the continent
Seismic reflectivity	Reflective imbricate fan	Interface-parallel reflections in the duplex zone; truncated reflections at the base	Interface-parallel reflections in the duplex zone; truncated reflections at the base
Shear-zone rocks, mélanges	Only lower-plate crust (or trench-fill sediments)	Tectonic mixing of material from both plates	Tectonic mixing of material from both plates (likely also involving trench-fill material)
Provenance of high-pressure rocks	Only lower plate	Lower and upper plate	Lower and upper plate
Basement of upper plate	Thickened, possibly eroded at surface	Lacking or too thin to accommodate neritic or subaerial sedimentation	Lacking or too thin to accommodate neritic or subaerial sedimentation

and numerical models has been extensively debated in the last few years (e.g., Penniston-Dorland et al., 2015; van Keken et al., 2018) and unsurprisingly recurs in our compilation as well. Does this mean that petrological studies on these rocks systematically overestimate temperatures, as a consequence of very long residence times in a hanging-wall position that caused full re-equilibration of assemblages at temperatures greater than the conditions at which each slice detached from the downgoing plate? Or does underplating preferentially occur in nature during transient warming of the subduction environment (e.g., decrease of convergence rate, subduction of a warmer seafloor)? The latter option is clearly not supported by our modeling approach, which, despite temperatures slightly cooler than in the compilation (Fig. 10), does not reveal such control for triggering deep duplex formation. Refining our understanding of subduction thermal structures, incorporating the plethora of factors that contribute to the heat budget (e.g., shear heating, effect of fluids, exothermic mantle wedge hydration reactions, etc.), certainly represents a first-order scientific challenge to solving this apparent discrepancy and refining our vision of rheological processes that control the position of the downdip end of the seismogenic zone (e.g., Peacock, 2020).

- (2) What are the strain rates during slice accretion, and what would be the dominant deformation mechanism under these relatively fast-slipping, water-saturated conditions? For Japan, Kimura et al. (2010), Hashimoto et al. (2002), and Onishi et al. (2001) have tentatively correlated the tectonic underplating process with slow slip events and cataclastic fabrics. While ductile shearing should prevail in relatively warm and young environments (e.g., Xia and Platt, 2017), brittle or semi-brittle creep is expected below 400 °C in the basal accretion region for most mature subduction systems (e.g., Onishi et al., 2001; Angiboust et al., 2015; Oncken et al., 2021; Behr and Bürgmann, 2021). The wide deformation spectrum potentially associated with accretion processes also calls for a reassessment, through further multidisciplinary investigations, of the origin of (micro)seismicity nests above the plate interface, i.e., where duplex structures likely develop and grow (e.g., Uchida et al., 2010; Menant et al., 2018; Savard et al., 2018; Comte et al., 2019). Future field studies should finally focus on the hydro-mechanical regime during slice detachment and more generally identify markers of periodicity in basally accreted material as a potential consequence of transient shear-zone activity as well as transient fluid pulses associated with enhanced strain rates (e.g., Bürgmann, 2018; Fagereng et al., 2018; Taetz et al., 2018).
- (3) Understanding the physical processes acting on the main subduction shear zone during each basal accretion event is crucial for interpreting the significance of vertical motion of the forearc crust across time scales (e.g., Sieh et al., 2008; Mouslopoulou et al., 2016). Efforts should be made in the identification of permanent-deformation signals included in the geodetically measured surface displacements during the various stages of the seismic cycle, which may in part correspond to finite strain

permanently recorded during duplexing sequences (e.g., Houlié and Stern, 2017; Jolivet et al., 2020).

- (4) We lack near-surface geological markers unambiguously indicating tectonic underplating at the base of active forearc margins. This is especially true because the accretion-related million-year-scale forearc topographic signal (Fig. 11B; Menant et al., 2020) interferes with long-term, climate-related variations in the sediment input at the trench, which partly control the subduction regime. Nonetheless, we stress that detailed stratigraphic investigations on forearc basins located above potential underplating sites (e.g., Mountney and Westbrook, 1997; Encinas et al., 2012), coupled with robust estimations of climatic variations, are crucial for tracking recent (or active) underplating events as well as potential switches in mass-transfer mode over millions of years.
- (5) The long-term modeling approach followed in studying accretion processes in subduction systems fails at addressing the question of their potential short-term (seismic-related?) signature. Future studies should aim at bridging this gap, using, e.g., numerical modeling accounting for time-stepping refinement and rate(-and-state)-dependent, fluid pressure-sensitive friction formulation (e.g., van Dinther et al., 2013; Dal Zilio et al., 2018; Herrendörfer et al., 2018; Petrini et al., 2020), as well as further detailed field investigations. Linking models with field structures will also inevitably (1) require a dramatic enhancement of the spatial resolution of the existing models, overcoming current computational limitations, and (2) require a fully coupled analytical and numerical development satisfactorily reproducing the rheological effect of fluids on plate-interface mechanical processes at various time scales.

ACKNOWLEDGMENTS

Michael Bostock, Robin Lacassin, Martine Simoes, and Raphael Grandin are acknowledged for insightful discussions. The guest editor Dave Scholl is acknowledged for encouraging us to write this contribution and for the handling of the manuscript, which benefited from helpful comments from Roland von Huene and John Platt. Special thanks to Hugues Raimbourg and Laurent Jolivet for sharing field photographs. This work has been funded with a research chair grant 16C538 (granted by ANR, agence nationale de la recherche) to S.A. in the frame of the IDEX-2018-0001 grant from the Université de Paris.

REFERENCES CITED

- Abers, G.A., Van Keken, P.E., and Hacker, B.R., 2017, The cold and relatively dry nature of mantle forearcs in subduction zones: *Nature Geoscience*, v. 10, p. 333–337, <https://doi.org/10.1038/ngeo2922>.
- Adam, J., and Reuther, C.-D., 2000, Crustal dynamics and active fault mechanics during subduction erosion: Application of frictional wedge analysis on to the North Chilean Forearc: *Tectonophysics*, v. 321, p. 297–325, [https://doi.org/10.1016/S0040-1951\(00\)00074-3](https://doi.org/10.1016/S0040-1951(00)00074-3).
- Adam, J., Klaeschen, D., Kukowski, N., and Flueh, E., 2004, Upward delamination of Cascadia Basin sediment infill with landward frontal accretion thrusting caused by rapid glacial age material flux: *Tectonics*, v. 23, <https://doi.org/10.1029/2002TC001475>.
- Agard, P., Plunder, A., Angiboust, S., Bonnet, G., and Ruh, J., 2018, The subduction plate interface: Rock record and mechanical coupling (from long to short timescales): *Lithos*, v. 320, p. 537–566, <https://doi.org/10.1016/j.lithos.2018.09.029>.

- Amato, J.M., and Pavlis, T.L., 2010, Detrital zircon ages from the Chugach terrane, southern Alaska, reveal multiple episodes of accretion and erosion in a subduction complex: *Geology*, v. 38, p. 459–462, <https://doi.org/10.1130/G30719.1>.
- Amato, J.M., Pavlis, T.L., Clift, P.D., Kochelek, E.J., Hecker, J.P., Worthman, C.M., and Day, E.M., 2013, Architecture of the Chugach accretionary complex as revealed by detrital zircon ages and lithologic variations: Evidence for Mesozoic subduction erosion in south-central Alaska: *Geological Society of America Bulletin*, v. 125, p. 1891–1911, <https://doi.org/10.1130/B30818.1>.
- Angiboust, S., and Agard, P., 2010, Initial water budget: The key to detaching large volumes of eclogitized oceanic crust along the subduction channel?: *Lithos*, v. 120, p. 453–474, <https://doi.org/10.1016/j.lithos.2010.09.007>.
- Angiboust, S., and Muñoz, J., 2018, Field report: Sailing around the exhumed roots of the Mesozoic Patagonian paleo-accretionary wedge (Diego de Almagro Island, Chile): *Geoscience Frontiers*, v. 9, p. 1591–1594, <https://doi.org/10.1016/j.gsf.2018.05.003>.
- Angiboust, S., Wolf, S., Burov, E., Agard, P., and Yamato, P., 2012, Effect of fluid circulation on subduction interface tectonic processes: Insights from thermo-mechanical numerical modelling: *Earth and Planetary Science Letters*, v. 357, p. 238–248, <https://doi.org/10.1016/j.epsl.2012.09.012>.
- Angiboust, S., Glodny, J., Oncken, O., and Chopin, C., 2014, In search of transient subduction interfaces in the Dent Blanche–Sesia Tectonic System (W. Alps): *Lithos*, v. 205, p. 298–321, <https://doi.org/10.1016/j.lithos.2014.07.001>.
- Angiboust, S., Kirsch, J., Oncken, O., Glodny, J., Monié, P., and Rybacki, E., 2015, Probing the transition between seismically coupled and decoupled segments along an ancient subduction interface: *Geochemistry Geophysics Geosystems*, v. 16, p. 1905–1922, <https://doi.org/10.1002/2015GC005776>.
- Angiboust, S., Hyppolito, T., Glodny, J., Cambeses, A., Garcia-Casco, A., Calderón, M., and Juliani, C., 2017, Hot subduction in the middle Jurassic and partial melting of oceanic crust in Chilean Patagonia: *Gondwana Research*, v. 42, p. 104–125, <https://doi.org/10.1016/j.gr.2016.10.007>.
- Angiboust, S., Cambeses, A., Hyppolito, T., Glodny, J., Monié, P., Calderón, M., and Juliani, C., 2018, A 100-m.y.-long window onto mass-flow processes in the Patagonian Mesozoic subduction zone (Diego de Almagro Island, Chile): *Geological Society of America Bulletin*, v. 130, p. 1439–1456, <https://doi.org/10.1130/B31891.1>.
- Aoki, K., Itaya, T., Shibuya, T., Masago, H., Kon, Y., Terabayashi, M., Kaneko, Y., Kawai, T., and Maruyama, S., 2008, The youngest blueschist belt in SW Japan: Implication for the exhumation of the Cretaceous Sanbagawa high-*P/T* metamorphic belt: *Journal of Metamorphic Geology*, v. 26, p. 583–602, <https://doi.org/10.1111/j.1525-1314.2008.00777.x>.
- Aoki, K., Maruyama, S., Isozaki, Y., Otoh, S., and Yanai, S., 2011, Recognition of the Shimanto HP metamorphic belt within the traditional Sanbagawa HP metamorphic belt: New perspectives of the Cretaceous–Paleogene tectonics in Japan: *Journal of Asian Earth Sciences*, v. 42, p. 355–369, <https://doi.org/10.1016/j.jseas.2011.05.001>.
- Aoki, K., Isozaki, Y., Yamamoto, S., Maki, K., Yokoyama, T., and Hirata, T., 2012, Tectonic erosion in a Pacific-type orogen: Detrital zircon response to Cretaceous tectonics in Japan: *Geology*, v. 40, p. 1087–1090, <https://doi.org/10.1130/G33414.1>.
- Aouizerat, A., Xiao, W., Schulmann, K., Windley, B.F., Zhou, J., Zhang, J., Ao, S., Song, D., Monie, P., and Liu, K., 2020, Accretion, subduction erosion, and tectonic extrusion during late Paleozoic to Mesozoic orogenesis in NE China: *Journal of Asian Earth Sciences*, v. 194, 104258, <https://doi.org/10.1016/j.jseas.2020.104258>.
- Aoya, M., Tsuboi, M., and Wallis, S.R., 2006, Origin of eclogitic metagabbro mass in the Sambagawa belt: Geological and geochemical constraints: *Lithos*, v. 89, p. 107–134, <https://doi.org/10.1016/j.lithos.2005.10.001>.
- Aoya, M., Endo, S., Mizukami, T., and Wallis, S.R., 2013, Paleo-mantle wedge preserved in the Sambagawa high-pressure metamorphic belt and the thickness of forearc continental crust: *Geology*, v. 41, p. 451–454, <https://doi.org/10.1130/G33834.1>.
- Armijo, R., Lacassin, R., Coudurier-Curveur, A., and Carrizo, D., 2015, Coupled tectonic evolution of Andean orogeny and global climate: *Earth-Science Reviews*, v. 143, p. 1–35, <https://doi.org/10.1016/j.earscirev.2015.01.005>.
- Arroyo, I.G., Husen, S., Flueh, E.R., Gossler, J., Kissling, E., and Alvarado, G.E., 2009, Three-dimensional *P*-wave velocity structure on the shallow part of the Central Costa Rican Pacific margin from local earthquake tomography using off- and onshore networks: *Geophysical Journal International*, v. 179, p. 827–849, <https://doi.org/10.1111/j.1365-246X.2009.04342.x>.
- Audet, P., and Bürgmann, R., 2014, Possible control of subduction zone slow-earthquake periodicity by silica enrichment: *Nature*, v. 510, p. 389–392, <https://doi.org/10.1038/nature13391>.
- Austrheim, H., and Andersen, T.B., 2004, Pseudotachylites from Corsica: Fossil earthquakes from a subduction complex: *Terra Nova*, v. 16, p. 193–197, <https://doi.org/10.1111/j.1365-3121.2004.00551.x>.
- Bachmann, R., Glodny, J., Oncken, O., and Seifert, W., 2009a, Abandonment of the South Penninic–Austroalpine palaeosubduction zone, Central Alps, and shift from subduction erosion to accretion: Constraints from Rb/Sr geochronology: *Journal of the Geological Society, London*, v. 166, no. 2, p. 217–231.
- Bachmann, R., Oncken, O., Glodny, J., Seifert, W., Georgieva, V., and Sudo, M., 2009b, Exposed plate interface in the European Alps reveals fabric styles and gradients related to an ancient seismogenic coupling zone: *Journal of Geophysical Research*, v. 114, B05402, <https://doi.org/10.1029/2008JB005927>.
- Baldwin, S.L., and Harrison, T.M., 1989, Geochronology of blueschists from west-central Baja California and the timing of uplift in subduction complexes: *The Journal of Geology*, v. 97, p. 149–163, <https://doi.org/10.1086/629291>.
- Bangs, N.L., and Cande, S.C., 1997, Episodic development of a convergent margin inferred from structures and processes along the southern Chile margin: *Tectonics*, v. 16, p. 489–503, <https://doi.org/10.1029/97TC00494>.
- Bangs, N.L.B., Gulick, S.P.S., and Shipley, T.H., 2006, Seamount subduction erosion in the Nankai Trough and its potential impact on the seismogenic zone: *Geology*, v. 34, p. 701–704, <https://doi.org/10.1130/G22451.1>.
- Banno, S., 2004, Ultramafic rocks and associated eclogites of the Sanbagawa schists, Japan: A review: *International Geology Review*, v. 46, p. 693–704, <https://doi.org/10.2747/0020-6814.46.8.693>.
- Barnes, J.D., Eldam, R., Lee, C.-T.A., Errico, J.C., Loewy, S., and Cisneros, M., 2013, Petrogenesis of serpentinites from the Franciscan Complex, western California, USA: *Lithos*, v. 178, p. 143–157, <https://doi.org/10.1016/j.lithos.2012.12.018>.
- Bassett, D., and Watts, A.B., 2015, Gravity anomalies, crustal structure, and seismicity at subduction zones: 2. Interrelationships between fore-arc structure and seismogenic behavior: *Geochemistry Geophysics Geosystems*, v. 16, p. 1541–1576, <https://doi.org/10.1002/2014GC005685>.
- Bassett, D., Sutherland, R., Henrys, S., Stern, T., Scherwath, M., Benson, A., Toulmin, S., and Henderson, M., 2010, Three-dimensional velocity structure of the northern Hikurangi margin, Raukumara, New Zealand: Implications for the growth of continental crust by subduction erosion and tectonic underplating: *Geochemistry Geophysics Geosystems*, v. 11, Q10013, <https://doi.org/10.1029/2010GC003137>.
- Bebout, G.E., and Penniston-Dorland, S.C., 2016, Fluid and mass transfer at subduction interfaces—The field metamorphic record: *Lithos*, v. 240, p. 228–258, <https://doi.org/10.1016/j.lithos.2015.10.007>.
- Behr, W.M., and Bürgmann, R., 2021, What's down there? The structures, materials and environment of deep-seated tremor and slip: *Philosophical Transactions of the Royal Society of London A*, v. 379, 20200218, <https://doi.org/10.1098/rsta.2020.0218>.
- Beltrando, M., Rubatto, D., and Manatschal, G., 2010, From passive margins to orogens: The link between ocean-continent transition zones and (ultra) high-pressure metamorphism: *Geology*, v. 38, p. 559–562, <https://doi.org/10.1130/G30768.1>.
- Beysac, O., Negro, F., Simoes, M., Chan, Y.C., and Chen, Y.G., 2008, High-pressure metamorphism in Taiwan: From oceanic subduction to arc-continent collision?: *Terra Nova*, v. 20, p. 118–125, <https://doi.org/10.1111/j.1365-3121.2008.00796.x>.
- Bishop, B.T., Beck, S.L., and Zandt, G., 2019, Segmentation in continental forearcs: Links between large-scale overriding plate structure and seismogenic behavior associated with the 2010 M_w 8.8 Maule, Chile earthquake: *Tectonophysics*, v. 767, 228164, <https://doi.org/10.1016/j.tecto.2019.228164>.
- Bonnet, G., Agard, P., Angiboust, S., Monié, P., Fournier, M., Caron, B., and Omrani, J., 2020, Structure and metamorphism of a subducted seamount (Zagros suture, Southern Iran): *Geosphere*, v. 16, p. 62–81, <https://doi.org/10.1130/GES02134.1>.
- Bostock, M.G., 2013, The Moho in subduction zones: *Tectonophysics*, v. 609, p. 547–557, <https://doi.org/10.1016/j.tecto.2012.07.007>.
- Boston, B., Moore, G.F., Nakamura, Y., and Kodaira, S., 2017, Forearc slope deformation above the Japan Trench megathrust: Implications for subduction erosion: *Earth and Planetary Science Letters*, v. 462, p. 26–34, <https://doi.org/10.1016/j.epsl.2017.01.005>.
- Böttner, C., Gross, F., Geersen, J., Crutchley, G.J., Mountjoy, J.J., and Krastel, S., 2018, Marine forearc extension in the Hikurangi margin: New insights from high-resolution 3-D seismic data: *Tectonics*, v. 37, p. 1472–1491, <https://doi.org/10.1029/2017TC004906>.
- Brandon, M.T., and Calderwood, A.R., 1990, High-pressure metamorphism and uplift of the Olympic subduction complex: *Geology*, v. 18, p. 1252–1255, [https://doi.org/10.1130/0091-7613\(1990\)018<1252:HPMAUO>2.3.CO;2](https://doi.org/10.1130/0091-7613(1990)018<1252:HPMAUO>2.3.CO;2).

- Brandon, M.T., Roden-Tice, M.K., and Garver, J.I., 1998, Late Cenozoic exhumation of the Cascadia accretionary wedge in the Olympic Mountains, northwest Washington State: *Geological Society of America Bulletin*, v. 110, p. 985–1009, [https://doi.org/10.1130/0016-7606\(1998\)110<0985:LCEOTC>2.3.CO;2](https://doi.org/10.1130/0016-7606(1998)110<0985:LCEOTC>2.3.CO;2).
- Buiter, S.J., 2012, A review of brittle compressional wedge models: *Tectonophysics*, v. 530, 1–17, <https://doi.org/10.1016/j.tecto.2011.12.018>.
- Bürgmann, R., 2018, The geophysics, geology and mechanics of slow fault slip: *Earth and Planetary Science Letters*, v. 495, p. 112–134, <https://doi.org/10.1016/j.epsl.2018.04.062>.
- Bustamante, A., Juliani, C., Hall, C.M., and Essene, E.J., 2011, $^{40}\text{Ar}/^{39}\text{Ar}$ ages from blueschists of the Jambaló region, Central Cordillera of Colombia: Implications on the styles of accretion in the Northern Andes: *Geologica Acta*, v. 9, p. 351–362, <https://doi.org/10.1344/105.000001697>.
- Byrne, T., 1986, Eocene underplating along the Kodiak shelf, Alaska: Implications and regional correlations: *Tectonics*, v. 5, p. 403–421, <https://doi.org/10.1029/TC005i003p00403>.
- Calderón, M., Hervé, F., Fuentes, F., Fosdick, J.C., Sepúlveda, F., and Galaz, G., 2016, Tectonic evolution of Paleozoic and Mesozoic Andean metamorphic complexes and the Rocas Verdes ophiolites in southern Patagonia, in Ghiglione, M.C., ed., *Geodynamic Evolution of the Southernmost Andes: Connections with the Scotia Arc*: Cham, Switzerland, Springer, p. 7–36, https://doi.org/10.1007/978-3-319-39727-6_2.
- Calvert, A.J., Ramachandran, K., Kao, H., and Fisher, M.A., 2006, Local thickening of the Cascadia forearc crust and the origin of seismic reflectors in the uppermost mantle: *Tectonophysics*, v. 420, p. 175–188, <https://doi.org/10.1016/j.tecto.2006.01.021>.
- Calvert, A.J., Preston, L.A., and Farahbod, A.M., 2011, Sedimentary underplating at the Cascadia mantle-wedge corner revealed by seismic imaging: *Nature Geoscience*, v. 4, p. 545–548, <https://doi.org/10.1038/ngeo1195>.
- Cawood, P.A., Kröner, A., Collins, W.J., Kusky, T.M., Mooney, W.D., and Windley, B.F., 2009, Accretionary orogens through Earth history, in Cawood, P.A., and Kröner, A., eds., *Earth Accretionary Systems in Space and Time*: Geological Society of London Special Publication 318, p. 1–36, <https://doi.org/10.1144/SP318.1>.
- Cawood, P.A., Hawkesworth, C.J., and Dhuime, B., 2012, Detrital zircon record and tectonic setting: *Geology*, v. 40, p. 875–878, <https://doi.org/10.1130/G32945.1>.
- Chapman, A.D., 2017, The Pelona–Orocopia–Rand and related schists of southern California: A review of the best-known archive of shallow subduction on the planet: *International Geology Review*, v. 59, p. 664–701, <https://doi.org/10.1080/00206814.2016.1230836>.
- Clarke, A.P., Vannucchi, P., and Morgan, J., 2018, Seamount chain–subduction zone interactions: Implications for accretionary and erosive subduction zone behavior: *Geology*, v. 46, p. 367–370, <https://doi.org/10.1130/G40063.1>.
- Clift, P.D., and Hartley, A.J., 2007, Slow rates of subduction erosion and coastal underplating along the Andean margin of Chile and Peru: *Geology*, v. 35, p. 503–506, <https://doi.org/10.1130/G23584A.1>.
- Clift, P., and Vannucchi, P., 2004, Controls on tectonic accretion versus erosion in subduction zones: Implications for the origin and recycling of the continental crust: *Reviews of Geophysics*, v. 42, RG2001, <https://doi.org/10.1029/2003RG000127>.
- Clift, P.D., Pecher, I., Kukowski, N., and Hampel, A., 2003, Tectonic erosion of the Peruvian forearc, Lima Basin, by subduction and Nazca Ridge collision: *Tectonics*, v. 22, 1023, <https://doi.org/10.1029/2002TC001386>.
- Clift, P.D., Draut, A.E., Kelemen, P.B., Blusztajn, J., and Greene, A., 2005a, Stratigraphic and geochemical evolution of an oceanic arc upper crustal section: The Jurassic Talkeetna Volcanic Formation, south-central Alaska: *Geological Society of America Bulletin*, v. 117, p. 902–925, <https://doi.org/10.1130/B25638.1>.
- Clift, P.D., Pavlis, T., DeBari, S.M., Draut, A.E., Rioux, M., and Kelemen, P.B., 2005b, Subduction erosion of the Jurassic Talkeetna–Bonanza arc and the Mesozoic accretionary tectonics of western North America: *Geology*, v. 33, p. 881–884, <https://doi.org/10.1130/G21822.1>.
- Cloos, M., and Shreve, R.L., 1988, Subduction-channel model of prism accretion, melange formation, sediment subduction, and subduction erosion at convergent plate margins: 1. Background and description: *Pure and Applied Geophysics*, v. 128, p. 455–500, <https://doi.org/10.1007/BF00874548>.
- Clowes, R.M., Yorath, C.J., and Hyndman, R.D., 1987, Reflection mapping across the convergent margin of western Canada: *Geophysical Journal International*, v. 89, p. 79–84, <https://doi.org/10.1111/j.1365-246X.1987.tb04391.x>.
- Cluzel, D., Aitchison, J.C., and Picard, C., 2001, Tectonic accretion and underplating of mafic terranes in the Late Eocene intraoceanic fore-arc of New Caledonia (Southwest Pacific): Geodynamic implications: *Tectonophysics*, v. 340, p. 23–59, [https://doi.org/10.1016/S0040-1951\(01\)00148-2](https://doi.org/10.1016/S0040-1951(01)00148-2).
- Collot, J.-Y., Lallemand, S., Pelletier, B., Bissen, J.-P., Glaçon, G., Fisher, M.A., Greene, H.G., Boulon, J., Daniel, J., and Monzier, M., 1992, Geology of the d'Entrecasteaux–New Hebrides Arc collision zone: Results from a deep subsurface survey: *Tectonophysics*, v. 212, p. 213–241, [https://doi.org/10.1016/0040-1951\(92\)90292-E](https://doi.org/10.1016/0040-1951(92)90292-E).
- Collot, J.-Y., Agudelo, W., Ribodetti, A., and Marcaillou, B., 2008, Origin of a crustal splay fault and its relation to the seismogenic zone and underplating at the erosional north Ecuador–south Colombia oceanic margin: *Journal of Geophysical Research*, v. 113, B12102, <https://doi.org/10.1029/2008JB005691>.
- Comte, D., Farias, M., Roecker, S., and Russo, R., 2019, The nature of the subduction wedge in an erosive margin: Insights from the analysis of aftershocks of the 2015 Mw 8.3 Illapel earthquake beneath the Chilean Coastal Range: *Earth and Planetary Science Letters*, v. 520, p. 50–62, <https://doi.org/10.1016/j.epsl.2019.05.033>.
- Connolly, J.A., 2005, Computation of phase equilibria by linear programming: A tool for geodynamic modeling and its application to subduction zone decarbonation: *Earth and Planetary Science Letters*, v. 236, p. 524–541, <https://doi.org/10.1016/j.epsl.2005.04.033>.
- Contreras-Reyes, E., Ruiz, J.A., Becerra, J., Kopp, H., Reichert, C., Maksymowicz, A., and Arriagada, C., 2015, Structure and tectonics of the central Chilean margin (31°–33°S): Implications for subduction erosion and shallow crustal seismicity: *Geophysical Journal International*, v. 203, p. 776–791, <https://doi.org/10.1093/gji/ggv309>.
- Coudurier-Curveur, A., Lacassin, R., and Armijo, R., 2015, Andean growth and monsoon winds drive landscape evolution at SW margin of South America: *Earth and Planetary Science Letters*, v. 414, p. 87–99, <https://doi.org/10.1016/j.epsl.2014.12.047>.
- Cruz-Uribe, A.M., Marschall, H.R., Gaetani, G.A., and Le Roux, V., 2018, Generation of alkaline magmas in subduction zones by partial melting of mélange diapirs—An experimental study: *Geology*, v. 46, p. 343–346, <https://doi.org/10.1130/G39956.1>.
- Dalla Torre, M., De Capitani, C., Frey, M., Underwood, M.B., Mullis, J., and Cox, R., 1996, Very low-temperature metamorphism of shales from the Diablo Range, Franciscan Complex, California: New constraints on the exhumation path: *Geological Society of America Bulletin*, v. 108, p. 578–601, [https://doi.org/10.1130/0016-7606\(1996\)108<0578:VLTMO>2.3.CO;2](https://doi.org/10.1130/0016-7606(1996)108<0578:VLTMO>2.3.CO;2).
- Dal Zilio, L., van Dinther, Y., Gerya, T.V., and Pranger, C.C., 2018, Seismic behaviour of mountain belts controlled by plate convergence rate: *Earth and Planetary Science Letters*, v. 482, p. 81–92, <https://doi.org/10.1016/j.epsl.2017.10.053>.
- Delph, J.R., Thomas, A.M., and Levander, A., 2021, Subcretionary tectonics: Linking variability in the expression of subduction along the Cascadia forearc: *Earth and Planetary Science Letters*, v. 556, 116724, <https://doi.org/10.1016/j.epsl.2020.116724>.
- Deschamps, F., Godard, M., Guillot, S., and Hattori, K., 2013, Geochemistry of subduction zone serpentinites: A review: *Lithos*, v. 178, p. 96–127, <https://doi.org/10.1016/j.lithos.2013.05.019>.
- Despaigne-Diaz, A.I., Casco, A.G., Govea, D.C., Wilde, S.A., and Trujillo, G.M., 2017, Structure and tectonic evolution of the southwestern Trinidad dome, Escambray complex, Central Cuba: Insights into deformation in an accretionary wedge: *Tectonophysics*, v. 717, p. 139–161, <https://doi.org/10.1016/j.tecto.2017.07.024>.
- Dobretsov, N.L., 1974, Glaucofane Schists and Eclogite-Glaucofane Schist Complexes in the USSR: Novosibirsk, Nauka, 460 p. (in Russian).
- Dobretsov, N.L., 1975, The glaucofane schist facies, in Dobretsov, N.L., Sobolev, V.S., Sobolev, N.V., and Khlestov, V.V., eds., *The Facies of Regional Metamorphism at High Pressures* [translated by D.A. Brown]: Canberra, Australian National University, p. 84–153.
- Dobretsov, N.L., and Sobolev, N.V., 1984, Glaucofane schists and eclogites in the folded systems of northern Asia: *Ophiolite*, v. 9, p. 401–423.
- Dominguez, S., Malavieille, J., and Lallemand, S.E., 2000, Deformation of accretionary wedges in response to seamount subduction: Insights from sandbox experiments: *Tectonics*, v. 19, p. 182–196, <https://doi.org/10.1029/1999TC000055>.
- Ducea, M.N., and Chapman, A.D., 2018, Sub-magmatic arc underplating by trench and forearc materials in shallow subduction systems: A geologic perspective and implications: *Earth-Science Reviews*, v. 185, p. 763–779, <https://doi.org/10.1016/j.earscirev.2018.08.001>.
- Dumitru, T.A., Wakabayashi, J., Wright, J.E., and Wooden, J.L., 2010, Early Cretaceous transition from nonaccretionary behavior to strongly accretionary behavior within the Franciscan subduction complex: *Tectonics*, v. 29, TC5001, <https://doi.org/10.1029/2009TC002542>.
- Ellis, S., Beaumont, C., and Pffiffer, O.A., 1999, Geodynamic models of crustal-scale episodic tectonic accretion and underplating in subduction zones: *Journal of Geophysical Research*, v. 104, p. 15,169–15,190, <https://doi.org/10.1029/1999JB900071>.

- Enami, M., Wallis, S.R., and Banno, Y., 1994, Paragenesis of sodic pyroxene-bearing quartz schists: Implications for the *P-T* history of the Sanbagawa belt: Contributions to Mineralogy and Petrology, v. 116, p. 182–198, <https://doi.org/10.1007/BF00310699>.
- Encinas, A., Finger, K.L., Buatois, L.A., and Peterson, D.E., 2012, Major forearc subsidence and deep-marine Miocene sedimentation in the present Coastal Cordillera and Longitudinal Depression of south-central Chile (38°30'S–41°45'S): Geological Society of America Bulletin, v. 124, p. 1262–1277, <https://doi.org/10.1130/B305671>.
- Encinas, A., Sagripanti, L., Rodríguez, M.P., Orts, D., Anavalón, A., Giroux, P., Otero, J., Echaurren, A., Zambrano, P., and Valencia, V., 2020, Tectonosedimentary evolution of the Coastal Cordillera and Central Depression of south-Central Chile (36°30'–42°S): Earth-Science Reviews, v. 213, 103465, <https://doi.org/10.1016/j.earscirev.2020.103465>.
- Ernst, W.G., 2016, Franciscan mélanges: Coherent blocks in a low-density, ductile matrix: International Geology Review, v. 58, p. 626–642, <https://doi.org/10.1080/00206814.2015.1108879>.
- Ernst, W.G., and Jahn, B.M., 1987, Crustal accretion and metamorphism in Taiwan, a post-Palaeozoic mobile belt: Philosophical Transactions of the Royal Society of London: Series A, Mathematical and Physical Sciences, v. 321, p. 129–161, <https://doi.org/10.1098/rsta.1987.0008>.
- Ernst, W.G., and McLaughlin, R.J., 2012, Mineral parageneses, regional architecture, and tectonic evolution of Franciscan metagraywackes, Cape Mendocino–Garberville–Covelo 30' x 60' quadrangles, northwest California: Tectonics, v. 31, TC1001, <https://doi.org/10.1029/2011TC002987>.
- Evenstar, L.A., Mather, A.E., Hartley, A.J., Stuart, F.M., Sparks, R.S.J., and Cooper, F.J., 2017, Geomorphology on geologic timescales: Evolution of the late Cenozoic Pacific paleosurface in Northern Chile and Southern Peru: Earth-Science Reviews, v. 171, p. 1–27, <https://doi.org/10.1016/j.earscirev.2017.04.004>.
- Fagereng, Å., Diener, J.F.A., Ellis, S., and Remitti, F., 2018, Fluid-related deformation processes at the up- and downdip limits of the subduction thrust seismogenic zone: What do the rocks tell us?, in Byrnie, T., Underwood, M.B., III, Fisher, D., McNeill, L., Saffer, D., Ujiie, K., and Yamaguchi, A., eds., Geology and Tectonics of Subduction Zones: A Tribute to Gaku Kimura: Geological Society of America Special Paper 534, p. 187–215, [https://doi.org/10.1130/2018.2534\(12\)](https://doi.org/10.1130/2018.2534(12)).
- Feehan, J.G., and Brandon, M.T., 1999, Contribution of ductile flow to exhumation of low-temperature, high-pressure metamorphic rocks: San Juan–Cascade nappes, NW Washington State: Journal of Geophysical Research, v. 104, p. 10,883–10,902, <https://doi.org/10.1029/1998JB900054>.
- Fisher, D.M., Gardner, T.W., Marshall, J.S., Sak, P.B., and Protti, M., 1998, Effect of subducting seafloor roughness on fore-arc kinematics, Pacific coast, Costa Rica: Geology, v. 26, p. 467–470, [https://doi.org/10.1130/0091-7613\(1998\)026<0467:EOSSFR>2.3.CO;2](https://doi.org/10.1130/0091-7613(1998)026<0467:EOSSFR>2.3.CO;2).
- Fisher, D.M., Gardner, T.W., Sak, P.B., Sanchez, J.D., Murphy, K., and Vannucchi, P., 2004, Active thrusting in the inner forearc of an erosive convergent margin, Pacific coast, Costa Rica: Tectonics, v. 23, TC2007, <https://doi.org/10.1029/2002TC001464>.
- García-Ramírez, C.A., Ríos-Reyes, C.A., Castellanos-Alarcón, O.M., and Mantilla-Figueroa, L.C., 2017, Petrology, geochemistry and geochronology of the Arquíia Complex's metabasites at the Pijao-Génova sector, Central Cordillera, Colombian Andes: Boletín de Geología, v. 39, no. 1, p. 105–126, <https://doi.org/10.18273/revbol.v39n1-2017005>.
- Gerya, T.V., and Meilick, F.I., 2011, Geodynamic regimes of subduction under an active margin: Effects of rheological weakening by fluids and melts: Journal of Metamorphic Geology, v. 29, p. 7–31, <https://doi.org/10.1111/j.1525-1314.2010.00904.x>.
- Gerya, T.V., and Yuen, D.A., 2007, Robust characteristics method for modelling multiphase visco-elasto-plastic thermo-mechanical problems: Physics of the Earth and Planetary Interiors, v. 163, p. 83–105, <https://doi.org/10.1016/j.pepi.2007.04.015>.
- Gerya, T.V., Fossati, D., Cantieni, C., and Seward, D., 2009, Dynamic effects of aseismic ridge subduction: Numerical modelling: European Journal of Mineralogy, v. 21, p. 649–661, <https://doi.org/10.1127/0935-1221/2009/0021-1931>.
- Glodny, J., Lohrmann, J., Echter, H., Gräfe, K., Seifert, W., Collao, S., and Figueroa, O., 2005, Internal dynamics of a paleoaccretionary wedge: Insights from combined isotope tectono-chronology and sandbox modelling of the South-Central Chilean forearc: Earth and Planetary Science Letters, v. 231, p. 23–39, <https://doi.org/10.1016/j.epsl.2004.12.014>.
- Glodny, J., Echter, H., Figueroa, O., Franz, G., Gräfe, K., Kemnitz, H., Kramer, W., Krawczyk, C., Lohrmann, J., Lucassen, F., Melnick, D., Rosenau, M., and Seifert, W., 2006, Long-term geological evolution and mass-flow balance of the south-central Andes, in Oncken, O., Chong, G., Franz, G., Giese, P., Götze, H.-J., Ramos, V.A., Strecker, M.R., and Wigger, P., eds., The Andes: Active Subduction Orogeny: Berlin, Heidelberg, Springer, p. 401–428, https://doi.org/10.1007/978-3-540-48684-8_19.
- Godoy, E., and Kato, T., 1990, Late Paleozoic serpentinites and mafic schists from the Coast Range accretionary complex, central Chile: Their relation to aeromagnetic anomalies: Geologische Rundschau, v. 79, p. 121–130, <https://doi.org/10.1007/BF01830451>.
- González-Jiménez, J.M., Plissart, G., Garrido, L.N., Padrón-Navarra, J.A., Aiglsperger, T., Romero, R., Marchesi, C., Moreno-Abril, A.J., Reich, M., Barra, F., and Morata, D., 2017, Titanian clinohumite and chondrodite in antigorite serpentinites from Central Chile: Evidence for deep and cold subduction: European Journal of Mineralogy, v. 29, p. 959–970, <https://doi.org/10.1127/ejm/2017/0029-2668>.
- Grove, M., and Bebout, G.E., 1995, Cretaceous tectonic evolution of coastal southern California: Insights from the Catalina Schist: Tectonics, v. 14, p. 1290–1308, <https://doi.org/10.1029/95TC01931>.
- Grove, M., Bebout, G.E., Jacobson, C.E., Barth, A.P., Kimbrough, D.L., King, R.L., Zou, H., Lovera, O.M., Mahoney, B.J., and Gehrels, G.E., 2008, The Catalina Schist: Evidence for middle Cretaceous subduction erosion of southwestern North America, in Draut, A.E., Clift, P.D., and Scholl, D.W., eds., Formation and Applications of the Sedimentary Record in Arc Collision Zones: Geological Society of America Special Paper 436, p. 335–361, [https://doi.org/10.1130/2008.2436\(15\)](https://doi.org/10.1130/2008.2436(15)).
- Guillot, S., Hattori, K., Agard, P., Schwartz, S., and Vidal, O., 2009, Exhumation processes in oceanic and continental subduction contexts: A review, in Lallemand, S., and Funicello, F., eds., Subduction Zone Geodynamics: Berlin, Heidelberg, Springer, p. 175–205, https://doi.org/10.1007/978-3-540-87974-9_10.
- Gutscher, M.-A., Kukowski, N., Malavieille, J., and Lallemand, S., 1996, Cyclical behavior of thrust wedges: Insights from high basal friction sandbox experiments: Geology, v. 24, p. 135–138, [https://doi.org/10.1130/0091-7613\(1996\)024<0135:CBOTWI>2.3.CO;2](https://doi.org/10.1130/0091-7613(1996)024<0135:CBOTWI>2.3.CO;2).
- Gutscher, M.-A., Kukowski, N., Malavieille, J., and Lallemand, S., 1998, Episodic imbricate thrusting and underthrusting: Analog experiments and mechanical analysis applied to the Alaskan accretionary wedge: Journal of Geophysical Research, v. 103, p. 10,161–10,176, <https://doi.org/10.1029/97JB03541>.
- Haberland, C., Rietbrock, A., Lange, D., Bataille, K., and Dahm, T., 2009, Structure of the seismogenic zone of the southcentral Chilean margin revealed by local earthquake traveltime tomography: Journal of Geophysical Research, v. 114, B01317, <https://doi.org/10.1029/2008JB005802>.
- Haberland, C., Mokhtari, M., Babaei, H.A., Ryberg, T., Masoodi, M., Partabian, A., and Lauterjung, J., 2020, Anatomy of a crustal-scale accretionary complex: Insights from deep seismic sounding of the onshore western Makran subduction zone, Iran: Geology, v. 49, p. 3–7, <https://doi.org/10.1130/G47700.1>.
- Hartley, A.J., May, G., Chong, G., Turner, P., Kape, S.J., and Jolley, E.J., 2000, Development of a continental forearc: A Cenozoic example from the Central Andes, northern Chile: Geology, v. 28, p. 331–334, [https://doi.org/10.1130/0091-7613\(2000\)28<331:DOACFA>2.0.CO;2](https://doi.org/10.1130/0091-7613(2000)28<331:DOACFA>2.0.CO;2).
- Harvey, K.M., Penniston-Dorland, S.C., Kohn, M.J., and Piccoli, P.M., 2020, Assessing *P-T* variability in mélange blocks from the Catalina Schist: Is there differential movement at the subduction interface?: Journal of Metamorphic Geology, v. 39, p. 271–295, <https://doi.org/10.1111/jmg.12571>.
- Hasebe, N., and Tagami, T., 2001, Exhumation of an accretionary prism—Results from fission track thermochronology of the Shimanto Belt, southwest Japan: Tectonophysics, v. 331, p. 247–267, [https://doi.org/10.1016/S0040-1951\(00\)00282-1](https://doi.org/10.1016/S0040-1951(00)00282-1).
- Hashimoto, Y., and Kimura, G., 1999, Underplating process from melange formation to duplexing: Example from the Cretaceous Shimanto Belt, Kii Peninsula, southwest Japan: Tectonics, v. 18, p. 92–107, <https://doi.org/10.1029/1998TC900014>.
- Hashimoto, Y., Enjoji, M., Sakaguchi, A., and Kimura, G., 2002, *P-T* conditions of cataclastic deformation associated with underplating: An example from the Cretaceous Shimanto complex, Kii Peninsula, SW Japan: Earth, Planets, and Space, v. 54, p. 1133–1138, <https://doi.org/10.1186/BF03353314>.
- Hayes, G., 2018, Slab2—A comprehensive subduction zone geometry model: U.S. Geological Survey data release, <https://doi.org/10.5066/F7PV6JNV>.
- Heki, K., 2004, Space geodetic observation of deep basal subduction erosion in northeastern Japan: Earth and Planetary Science Letters, v. 219, p. 13–20, [https://doi.org/10.1016/S0012-821X\(03\)00693-9](https://doi.org/10.1016/S0012-821X(03)00693-9).
- Helper, M.A., 1986, Early Cretaceous metamorphic ages for high *P/T* schists in the Condrey Mountain Window, Klamath Mountains, northern California: An inlier of Franciscan: Geological Society of America Abstracts with Programs, v. 18, p. 634.
- Henry, S., Wech, A., Sutherland, R., Stern, T., Savage, M., Sato, H., Mochizuki, K., Iwasaki, T., Okaya, D., Seward, A., Tozer, B., Townend, J., Kurashimo, E., Iidaka, T., and Ishiyama, T., 2013, SAHKE geophysical transect reveals crustal and subduction zone structure at the southern

- Hikurangi margin, New Zealand: *Geochemistry Geophysics Geosystems*, v. 14, p. 2063–2083, <https://doi.org/10.1002/ggge.20136>.
- Herrendörfer, R., Gerya, T., and van Dinther, Y., 2018, An invariant rate- and state-dependent friction formulation for viscoelastoplastic earthquake cycle simulations: *Journal of Geophysical Research: Solid Earth*, v. 123, p. 5018–5051, <https://doi.org/10.1029/2017JB015225>.
- Hervé, F., 1988, Late Paleozoic subduction and accretion in southern Chile: *Episodes*, v. 11, p. 183–188, <https://doi.org/10.18814/epiiugs/1988/v11i3/005>.
- Hervé, F., and Fanning, C.M., 2001, Late Triassic detrital zircons in meta-turbidites of the Chonos Metamorphic Complex, southern Chile: *Revista Geológica de Chile*, v. 28, p. 91–104, <https://doi.org/10.4067/S0716-02082001000100005>.
- Hervé, F., Calderón, M., and Faúndez, V., 2008, The metamorphic complexes of the Patagonian and Fuegian Andes: *Geologica Acta*, v. 6, p. 43–53, <https://doi.org/10.1344/105.000000240>.
- Heuret, A., Lallemand, S., Funicello, F., Piromallo, C., and Faccenna, C., 2011, Physical characteristics of subduction interface type seismogenic zones revisited: *Geochemistry Geophysics Geosystems*, v. 12, Q01004, <https://doi.org/10.1029/2010GC003230>.
- Hilaret, N., Reynard, B., Wang, Y., Daniel, I., Merkel, S., Nishiyama, N., and Petitgirard, S., 2007, High-pressure creep of serpentine, interseismic deformation, and initiation of subduction: *Science*, v. 318, p. 1910–1913, <https://doi.org/10.1126/science.1148494>.
- Hippchen, S., and Hyndman, R.D., 2008, Thermal and structural models of the Sumatra subduction zone: Implications for the megathrust seismogenic zone: *Journal of Geophysical Research*, v. 113, B12103, <https://doi.org/10.1029/2008JB005698>.
- Hirajima, T., and Banno, S., 1989, Records of high pressure metamorphism in the so-called “superficial nappe” in the Chichibu belt, Japan: *Bulletin de la Société Géologique de France*, v. 5, p. 661–664, <https://doi.org/10.2113/gssgfbull.V.3.661>.
- Houlié, N., and Stern, T.A., 2017, Vertical tectonics at an active continental margin: *Earth and Planetary Science Letters*, v. 457, p. 292–301, <https://doi.org/10.1016/j.epsl.2016.10.018>.
- Husen, S., Kissling, E., and Flueh, E.R., 2000, Local earthquake tomography of shallow subduction in north Chile: A combined onshore and offshore study: *Journal of Geophysical Research*, v. 105, p. 28,183–28,198, <https://doi.org/10.1029/2000JB900229>.
- Hyppolito, T., García-Casco, A., Juliani, C., Meira, V.T., and Hall, C., 2014, Late Paleozoic onset of subduction and exhumation at the western margin of Gondwana (Chilena Terrane): Counterclockwise P-T paths and timing of metamorphism of deep-seated garnet–mica schist and amphibolite of Punta Sirena, Coastal Accretionary Complex, central Chile (34° S): *Lithos*, v. 206, p. 409–434, <https://doi.org/10.1016/j.lithos.2014.07.023>.
- Hyppolito, T., Angiboust, S., Juliani, C., Glodny, J., García-Casco, A., Calderón, M., and Chopin, C., 2016, Eclogite- and blueschist-facies rocks from Diego de Almagro Island (Patagonia): Episodic accretion and thermal evolution of the Chilean subduction interface during the Cretaceous: *Lithos*, v. 264, p. 422–440, <https://doi.org/10.1016/j.lithos.2016.09.001>.
- Ishiwatari, A., and Tsujimori, T., 2003, Paleozoic ophiolites and blueschists in Japan and Russian Primorye in the tectonic framework of East Asia: A synthesis: *Island Arc*, v. 12, 190–206, <https://doi.org/10.1046/j.1440-1738.2003.00390.x>.
- Ishizuka, H., Imaizumi, M., Gouchi, N., and Banno, S., 1983, The Kamuikotan zone in Hokkaido, Japan: Tectonic mixing of high-pressure and low-pressure metamorphic rocks: *Journal of Metamorphic Geology*, v. 1, p. 263–275, <https://doi.org/10.1111/j.1525-1314.1983.tb00275.x>.
- Isozaki, Y., Maruyama, S., and Furuoka, F., 1990, Accreted oceanic materials in Japan: *Tectonophysics*, v. 181, p. 179–205, [https://doi.org/10.1016/0040-1951\(90\)90016-2](https://doi.org/10.1016/0040-1951(90)90016-2).
- Isozaki, Y., Aoki, K., Nakama, T., and Yanai, S., 2010, New insight into a subduction-related orogen: A reappraisal of the geotectonic framework and evolution of the Japanese Islands: *Gondwana Research*, v. 18, p. 82–105, <https://doi.org/10.1016/j.gr.2010.02.015>.
- Iwasaki, I., Watanabe, T., Itaya, T., Yamazaki, M., and Takigami, Y., 1995, Palaeogene K-Ar ages from the Kamuikotan metamorphic rocks, southern area of the Kamuikotan Gorge, central Hokkaido, northern Japan: *Geological Journal*, v. 30, p. 281–295, <https://doi.org/10.1002/gj.3350300308>.
- Jacobson, C.E., Grove, M., Vučić, A., Pedrick, J.N., and Ebert, K.A., 2007, Exhumation of the Orocoopia Schist and associated rocks of southeastern California: Relative roles of erosion, synsubduction tectonic denudation, and middle Cenozoic extension, *in* Cloos, M., Carlson, W.D., Gilbert, M.C., Liou, J.G., and Sorensen, S.S., eds., *Convergent Margin Terranes and Associated Regions: A Tribute to W.G. Ernst*: Geological Society of America Special Paper 419, p. 1–37, [https://doi.org/10.1130/2007.2419\(01\)](https://doi.org/10.1130/2007.2419(01)).
- Jicha, B.R., and Kay, S.M., 2018, Quantifying arc migration and the role of forearc subduction erosion in the central Aleutians: *Journal of Volcanology and Geothermal Research*, v. 360, p. 84–99, <https://doi.org/10.1016/j.jvolgeores.2018.06.016>.
- Jolivet, R., Simons, M., Duputel, Z., Olive, J.-A., Bhat, H.S., and Bletery, O., 2020, Interseismic loading of subduction megathrust drives long-term uplift in northern Chile: *Geophysical Research Letters*, v. 47, e2019GL085377, <https://doi.org/10.1029/2019GL085377>.
- Kato, T.T., and Godoy, E., 1995, Petrogenesis and tectonic significance of Late Paleozoic coarse-crystalline blueschist and amphibolite boulders in the Coastal Range of Chile: *International Geology Review*, v. 37, p. 992–1006, <https://doi.org/10.1080/00206819509465437>.
- Kato, T.T., and Godoy, E., 2015, Middle to late Triassic mélange exhumation along a pre-Andean transpressional fault system: Coastal Chile (26°–42°S): *International Geology Review*, v. 57, p. 606–628, <https://doi.org/10.1080/00206814.2014.1002119>.
- Kay, S.M., Godoy, E., and Kurtz, A., 2005, Episodic arc migration, crustal thickening, subduction erosion, and magmatism in the south-central Andes: *Geological Society of America Bulletin*, v. 117, p. 67–88, <https://doi.org/10.1130/B25431.1>.
- Keppie, D.F., Currie, C.A., and Warren, C., 2009, Subduction erosion modes: Comparing finite element numerical models with the geological record: *Earth and Planetary Science Letters*, v. 287, p. 241–254, <https://doi.org/10.1016/j.epsl.2009.08.009>.
- Kidder, S., and Ducea, M.N., 2006, High temperatures and inverted metamorphism in the schist of Sierra de Salinas, California: *Earth and Planetary Science Letters*, v. 241, p. 422–437, <https://doi.org/10.1016/j.epsl.2005.11.037>.
- Kienast, J.-R., and Rangin, C., 1982, Mesozoic blueschists and mélanges of Cedros Island (Baja California, Mexico): A consequence of nappe emplacement or subduction? *Earth and Planetary Science Letters*, v. 59, p. 119–138, [https://doi.org/10.1016/0012-821X\(82\)90121-2](https://doi.org/10.1016/0012-821X(82)90121-2).
- Kimura, G., and Ludden, J., 1995, Peeling oceanic crust in subduction zones: *Geology*, v. 23, p. 217–220, [https://doi.org/10.1130/0091-7613\(1995\)023<0217:POCISZ>2.3.CO;2](https://doi.org/10.1130/0091-7613(1995)023<0217:POCISZ>2.3.CO;2).
- Kimura, G., and Mukai, A., 1991, Underplated units in an accretionary complex: Melange of the Shimanto Belt of eastern Shikoku, southwest Japan: *Tectonics*, v. 10, p. 31–50, <https://doi.org/10.1029/90TC00799>.
- Kimura, G., Sakakibara, M., Ofuka, H., Ishizuka, H., Miyashita, S., Okamura, M., Melnikov, O.A., and Lushchenko, V., 1992, A deep section of accretionary complex: Susunai Complex in Sakhalin island, northwest Pacific margin: *Island Arc*, v. 1, p. 166–175, <https://doi.org/10.1111/j.1440-1738.1992.tb00067.x>.
- Kimura, G., Maruyama, S., Isozaki, Y., and Terabayashi, M., 1996, Well-preserved underplating structure of the jadeitized Franciscan complex, Pacheco Pass: *California Geology*, v. 24, p. 75–78, [https://doi.org/10.1130/0091-7613\(1996\)024<0075:WPUSOT>2.3.CO;2](https://doi.org/10.1130/0091-7613(1996)024<0075:WPUSOT>2.3.CO;2).
- Kimura, H., Takeda, T., Obara, K., and Kasahara, K., 2010, Seismic evidence for active underplating below the megathrust earthquake zone in Japan: *Science*, v. 329, p. 210–212, <https://doi.org/10.1126/science.1187115>.
- Konstantinovskaya, E., and Malavieille, J., 2011, Thrust wedges with décollement levels and syntectonic erosion: A view from analog models: *Tectonophysics*, v. 502, p. 336–350, <https://doi.org/10.1016/j.tecto.2011.01.020>.
- Krawczyk, C.M., Mechie, J., Lüth, S., Tašárová, Z., Wigger, P., Stiller, M., Brasse, H., Ehtler, H.P., Aranedo, M., and Bataille, K., 2006, Geophysical signatures and active tectonics at the south-central Chilean margin, *in* Oncken, O., Chong, G., Franz, G., Giese, P., Götze, H.-J., Ramos, V.A., Strecker, M.R., and Wigger, P., eds., *The Andes: Active Subduction Orogeny*: Berlin, Heidelberg, Springer, p. 171–192, https://doi.org/10.1007/978-3-540-48684-8_8.
- Krohe, A., 2017, The Franciscan Complex (California, USA)—The model case for return-flow in a subduction channel put to the test: *Gondwana Research*, v. 45, p. 282–307, <https://doi.org/10.1016/j.gr.2017.02.003>.
- Kukowski, N., and Oncken, O., 2006, Subduction erosion—The “normal” mode of fore-arc material transfer along the Chilean margin?, *in* Oncken, O., Chong, G., Franz, G., Giese, P., Götze, H.-J., Ramos, V.A., Strecker, M.R., and Wigger, P., eds., *The Andes: Active Subduction Orogeny*: Berlin, Heidelberg, Springer, p. 217–236, https://doi.org/10.1007/978-3-540-48684-8_10.
- Kukowski, N., Lallemand, S.E., Malavieille, J., Gutscher, M.-A., and Reston, T.J., 2002, Mechanical decoupling and basal duplex formation observed in sandbox experiments with application to the Western Mediterranean Ridge accretionary complex: *Marine Geology*, v. 186, p. 29–42, [https://doi.org/10.1016/S0025-3227\(02\)00171-8](https://doi.org/10.1016/S0025-3227(02)00171-8).
- Kusky, T.M., Bradley, D.C., Haessler, P.J., and Karl, S., 1997, Controls on accretion of flysch and mélange belts at convergent margins: Evidence from the Chugach Bay thrust and Iceworm mélange, Chugach accretionary wedge, Alaska: *Tectonics*, v. 16, p. 855–878, <https://doi.org/10.1029/97TC02780>.
- Kusky, T.M., Windley, B.F., Safonova, I., Wakita, K., Wakabayashi, J., Polat, A., and Santosh, M., 2013, Recognition of ocean plate stratigraphy in accretionary orogens through Earth history:

- A record of 3.8 billion years of sea floor spreading, subduction, and accretion: *Gondwana Research*, v. 24, p. 501–547, <https://doi.org/10.1016/j.gr.2013.01.004>.
- Lagabrielle, Y., and Cannat, M., 1990, Alpine Jurassic ophiolites resemble the modern central Atlantic basement: *Geology*, v. 18, p. 319–322, [https://doi.org/10.1130/0091-7613\(1990\)018<0319:AJORTM>2.3.CO;2](https://doi.org/10.1130/0091-7613(1990)018<0319:AJORTM>2.3.CO;2).
- Lallemant, S.E., Schnurle, P., and Manoussis, S., 1992, Reconstruction of subduction zone paleogeometries and quantification of upper plate material losses caused by tectonic erosion: *Journal of Geophysical Research*, v. 97, p. 217–239, <https://doi.org/10.1029/91JB02342>.
- Lamb, S., and Davis, P., 2003, Cenozoic climate change as a possible cause for the rise of the Andes: *Nature*, v. 425, p. 792–797, <https://doi.org/10.1038/nature02049>.
- Laurent, V., Jolivet, L., Roche, V., Augier, R., Scaillet, S., and Cardello, G.L., 2016, Strain localization in a fossilized subduction channel: Insights from the Cycladic Blueschist Unit (Syros, Greece): *Tectonophysics*, v. 672, p. 150–169, <https://doi.org/10.1016/j.tecto.2016.01.036>.
- Le Pichon, X., Henry, P., and Lallemant, S., 1993, Accretion and erosion in subduction zones: The role of fluids: *Annual Review of Earth and Planetary Sciences*, v. 21, p. 307–331, <https://doi.org/10.1146/annurev.ea.21.050193.001515>.
- Li, W., Kabir, M.F., Liu, Y., Guo, X., and Takasu, A., 2017, Metamorphism of the blueschists in the Suo metamorphic belt, Gotsu area, SW Japan: *Earth Science (Chikyū Kagaku)*, v. 71, p. 17–25, https://doi.org/10.15080/agcjchikyukagaku.71.1_17.
- Liou, J.G., Ernst, W.G., and Moore, D.E., 1981, Geology and petrology of some polymetamorphosed amphibolites and associated rocks in northeastern Taiwan: Summary: *Geological Society of America Bulletin*, v. 92, p. 219–224, [https://doi.org/10.1130/0016-7606\(1981\)92<219:GAOSP>2.0.CO;2](https://doi.org/10.1130/0016-7606(1981)92<219:GAOSP>2.0.CO;2).
- Litchfield, N., Ellis, S., Berryman, K., and Nicol, A., 2007, Insights into subduction-related uplift along the Hikurangi Margin, New Zealand, using numerical modeling: *Journal of Geophysical Research*, v. 112, F02021, <https://doi.org/10.1029/2006JF005353>.
- Liu, X., Su, W., Gao, J., Li, J., Jiang, T., Zhang, X., and Ge, X., 2014, Paleozoic subduction erosion involving accretionary wedge sediments in the South Tianshan Orogen: Evidence from geochronological and geochemical studies on eclogites and their host metasediments: *Lithos*, v. 210, p. 89–110, <https://doi.org/10.1016/j.lithos.2014.09.017>.
- Lohrmann, J., Kukowski, N., Krawczyk, C.M., Oncken, O., Sick, C., Sobiesiak, M., and Rietbro, A., 2006, Subduction channel evolution in brittle fore-arc wedges—A combined study with scaled sandbox experiments, seismological and reflection seismic data and geological field evidence, in Oncken, O., Chong, G., Franz, G., Giese, P., Götze, H.-J., Ramos, V.A., Strecker, M.R., and Wigger, P., eds., in *The Andes: Active Subduction Orogeny*: Berlin, Heidelberg, Springer, p. 237–262, https://doi.org/10.1007/978-3-540-48684-8_11.
- López-Carmona, A., Kusky, T.M., Santosh, M., and Abati, J., 2011, *P-T* and structural constraints of lawsonite and epidote blueschists from Liberty Creek and Seldovia: Tectonic implications for early stages of subduction along the southern Alaska convergent margin: *Lithos*, v. 121, p. 100–116, <https://doi.org/10.1016/j.lithos.2010.10.007>.
- Loveless, J.P., Allmendinger, R.W., Pritchard, M.E., and González, G., 2010, Normal and reverse faulting driven by the subduction zone earthquake cycle in the northern Chilean fore arc: *Tectonics*, v. 29, TC2001, <https://doi.org/10.1029/2009TC002465>.
- Malavieille, J., 2010, Impact of erosion, sedimentation, and structural heritage on the structure and kinematics of orogenic wedges: Analog models and case studies: *GSA Today*, v. 20, no. 1, p. 4–10, <https://doi.org/10.1130/GSATG48A.1>.
- Martinod, J., Regard, V., Letourmy, Y., Henry, H., Hassani, R., Baratchart, S., and Carretier, S., 2016, How do subduction processes contribute to forearc Andean uplift? Insights from numerical models: *Journal of Geodynamics*, v. 96, p. 6–18, <https://doi.org/10.1016/j.jog.2015.04.001>.
- Maruyama, S., Liou, J.G., and Terabayashi, M., 1996, Blueschists and eclogites of the world and their exhumation: *International Geology Review*, v. 38, p. 485–594, <https://doi.org/10.1080/00206819709465347>.
- McClelland, W.C., Gehrels, G.E., and Saleeby, J.B., 1992, Upper Jurassic–lower Cretaceous basinal strata along the Cordilleran margin: Implications for the accretionary history of the Alexander-Wrangellia-Peninsular terrane: *Tectonics*, v. 11, p. 823–835, <https://doi.org/10.1029/92TC00241>.
- McCrory, P.A., and Wilson, D.S., 2013, A kinematic model for the formation of the Siletz-Crescent forearc terrane by capture of coherent fragments of the Farallon and Resurrection plates: *Tectonics*, v. 32, p. 718–736, <https://doi.org/10.1002/tect.20045>.
- McNeill, L.C., Goldfinger, C., Kulm, L.D., and Yeats, R.S., 2000, Tectonics of the Neogene Cascadia forearc basin: Investigations of a deformed late Miocene unconformity: *Geological Society of America Bulletin*, v. 112, p. 1209–1224, [https://doi.org/10.1130/0016-7606\(2000\)112<1209:TOTNCF>2.0.CO;2](https://doi.org/10.1130/0016-7606(2000)112<1209:TOTNCF>2.0.CO;2).
- Melnick, D., 2016, Rise of the central Andean coast by earthquakes straddling the Moho: *Nature Geoscience*, v. 9, p. 401–407, <https://doi.org/10.1038/ngeo2683>.
- Menant, A., Angiboust, S., Monié, P., Oncken, O., and Guigner, J.-M., 2018, Brittle deformation during Alpine basal accretion and the origin of seismicity nests above the subduction interface: *Earth and Planetary Science Letters*, v. 487, p. 84–93, <https://doi.org/10.1016/j.epsl.2018.01.029>.
- Menant, A., Angiboust, S., and Gerya, T., 2019, Stress-driven fluid flow controls long-term megathrust strength and deep accretionary dynamics: *Scientific Reports*, v. 9, 9714, <https://doi.org/10.1038/s41598-019-46191-y>.
- Menant, A., Angiboust, S., Gerya, T., Lacassin, R., Simoes, M., and Grandin, R., 2020, Transient stripping of subducting slabs controls periodic forearc uplift: *Nature Communications*, v. 11, 1823, <https://doi.org/10.1038/s41467-020-15580-7>.
- Meneghini, F., Marroni, M., Moore, J.C., Pandolfi, L., and Rowe, C.D., 2009, The processes of underthrusting and underplating in the geologic record: Structural diversity between the Franciscan Complex (California), the Kodiak Complex (Alaska) and the Internal Ligurian Units (Italy): *Geological Journal*, v. 44, p. 126–152, <https://doi.org/10.1002/gj.1144>.
- Miura, R., Nakamura, Y., Koda, K., Tokuyama, H., and Coffin, M.F., 2004, “Rootless” serpentinite seamount on the southern Izu-Bonin forearc: Implications for basal erosion at convergent plate margins: *Geology*, v. 32, p. 541–544, <https://doi.org/10.1130/G20319.1>.
- Moore, G.F., Park, J.-O., Bangs, N.L., Gulick, S.P., Tobin, H.J., Nakamura, Y., Sato, S., Tsuji, T., Yoro, T., Tanaka, H., Uraki, S., Kido, Y., Sanada, Y., Karamoto, S., and Taira, A., 2009, Structural and seismic stratigraphic framework of the NanTroSEIZE Stage 1 transect, in Kinoshita, M., Tobin, H., Ashi, J., Kimura, G., Lallemant, S., Scream, E.J., Curewitz, D., Masago, H., Moe, K.T., and the Expedition 314/315/316 Scientists, Proceedings of the Integrated Ocean Drilling Program, Volume 314/315/316: Washington, D.C., Integrated Ocean Drilling Program Management International, Inc., <https://doi.org/10.2204/iodp.proc.314315316.102.2009>.
- Moore, J.C., 1989, Tectonics and hydrogeology of accretionary prisms: Role of the décollement zone: *Journal of Structural Geology*, v. 11, p. 95–106, [https://doi.org/10.1016/0191-8141\(89\)90037-0](https://doi.org/10.1016/0191-8141(89)90037-0).
- Moore, J.C., Diebold, J., Fisher, M.A., Sample, J., Brocher, T., Talwani, M., Ewing, J., von Huene, R., Rowe, C., Stone, D., Stevens, C., and Sawyer, D., 1991, EDGE deep seismic reflection transect of the eastern Aleutian arc-trench layered lower crust reveals underplating and continental growth: *Geology*, v. 19, p. 420–424, [https://doi.org/10.1130/0091-7613\(1991\)019<0420:EDSRTO>2.3.CO;2](https://doi.org/10.1130/0091-7613(1991)019<0420:EDSRTO>2.3.CO;2).
- Moore, T.E., 1986, Petrology and tectonic implications of the blueschist-bearing Puerto Nuevo melange complex, Vizcaino Peninsula, Baja California Sur, Mexico, in Evans, B.W., and Brown, E.H., eds., *Blueschists and Eclogites*: Geological Society of America Memoir 164, p. 43–58, <https://doi.org/10.1130/MEM164-p43>.
- Moreno, M., Haberland, C., Oncken, O., Rietbrock, A., Angiboust, S., and Heibach, O., 2014, Locking of the Chile subduction zone controlled by fluid pressure before the 2010 earthquake: *Nature Geoscience*, v. 7, p. 292–296, <https://doi.org/10.1038/ngeo2102>.
- Moreno, M., Li, S., Melnick, D., Bedford, J.R., Baez, J.C., Motagh, M., Metzger, S., Vajedian, S., Sippl, C., Gutknecht, B.D., Contreras-Reyes, E., Deng, Z., Tassara, A., and Oncken, O., 2018, Chilean megathrust earthquake recurrence linked to frictional contrast at depth: *Nature Geoscience*, v. 11, p. 285–290, <https://doi.org/10.1038/s41561-018-0089-5>.
- Mountney, N.P., and Westbrook, G.K., 1997, Quantitative analysis of Miocene to Recent forearc basin evolution along the Colombian convergent margin: *Basin Research*, v. 9, p. 177–196, <https://doi.org/10.1046/j.1365-2117.1997.00040.x>.
- Mouslopoulou, V., Oncken, O., Hainzl, S., and Nicol, A., 2016, Uplift rate transients at subduction margins due to earthquake clustering: *Tectonics*, v. 35, p. 2370–2384, <https://doi.org/10.1002/2016TC004248>.
- Mulcahy, S.R., Starnes, J.K., Day, H.W., Coble, M.A., and Vervoort, J.D., 2018, Early onset of Franciscan subduction: *Tectonics*, v. 37, p. 1194–1209, <https://doi.org/10.1029/2017TC004753>.
- Muñoz-Montecinos, J., Angiboust, S., Cambeses, A., and García-Casco, A., 2020, Multiple veining in a paleo-accretionary wedge: The metamorphic rock record of prograde dehydration and transient high pore-fluid pressures along the subduction interface (Western Series, central Chile): *Geosphere*, v. 16, p. 765–786, <https://doi.org/10.1130/GES02227.1>.
- Nishimura, Y., 1998, Geotectonic subdivision and areal extent of the Sangun belt, Inner Zone of Southwest Japan: *Journal of Metamorphic Geology*, v. 16, p. 129–140, <https://doi.org/10.1111/j.1525-1314.1998.00059.x>.

- Nishiyama, T., Mori, Y., and Shigeno, M., 2017, Jadeitites and associated metasomatic rocks from serpentinite mélanges in the Nishisonogi unit, Nagasaki Metamorphic Complex, western Kyushu, Japan: A review: *Journal of Mineralogical and Petrological Sciences*, v. 112, p. 197–216, <https://doi.org/10.2465/jmps.170322>.
- Nishiyama, T., Ohfuji, H., Fukuba, K., Terauchi, M., Nishi, U., Harada, K., Unoki, K., Moribe, M., Yoshiasa, A., Ishimaru, S., Mori, Y., Shigeno, M., and Arai, S., 2020, Microdiamond in a low-grade metapelite from a Cretaceous subduction complex, western Kyushu, Japan: *Scientific Reports*, v. 10, 11645, <https://doi.org/10.1038/s41598-020-68599-7>.
- Noda, A., Saito, T., and Fukuyama, E., 2018, Slip-deficit rate distribution along the Nankai Trough, southwest Japan, with elastic lithosphere and viscoelastic asthenosphere: *Journal of Geophysical Research: Solid Earth*, v. 123, p. 8125–8142, <https://doi.org/10.1029/2018JB015515>.
- Noda, A., Koge, H., Yamada, Y., Miyakawa, A., and Ashi, J., 2020, Subduction of trench-fill sediments beneath an accretionary wedge: Insights from sandbox analogue experiments: *Geosphere*, v. 16, p. 953–968, <https://doi.org/10.1130/GES02212.1>.
- Obara, K., and Kato, A., 2016, Connecting slow earthquakes to huge earthquakes: *Science*, v. 353, p. 253–257, <https://doi.org/10.1126/science.aaf1512>.
- Oleskevich, D.A., Hyndman, R.D., and Wang, K., 1999, The updip and downdip limits to great subduction earthquakes: Thermal and structural models of Cascadia, south Alaska, SW Japan, and Chile: *Journal of Geophysical Research*, v. 104, p. 14,965–14,991, <https://doi.org/10.1029/1999JB900060>.
- Oncken, O., 1998, Evidence for precollisional subduction erosion in ancient collisional belts: The case of the Mid-European Variscides: *Geology*, v. 26, p. 1075–1078, [https://doi.org/10.1130/0091-7613\(1998\)026<1075:EFPSLE>2.3.CO;2](https://doi.org/10.1130/0091-7613(1998)026<1075:EFPSLE>2.3.CO;2).
- Oncken, O., Asch, G., Haberland, C., Metchie, J., Sobolev, S., Stiller, M., Yuan, X., Brasse, H., Buske, S., Giese, P., Görze, H.-J., Lueth, S., Scheuber, E., Shapiro, S., Wigger, P., Yoon, M.-K., Bravo, P., Vieytes, H., Chong, G., Gonzales, G., Wilke, H.-G., Lüschen, E., Martinez, E., Rössling, R., Ricaldi, E., and Rietbrock, A., 2003, Seismic imaging of a convergent continental margin and plateau in the central Andes (Andean Continental Research Project 1996 (ANCORP'96)): *Journal of Geophysical Research*, v. 108, 2328, <https://doi.org/10.1029/2002JB001771>.
- Oncken, O., Angiboust, S., and Dresen, G., 2021, Slow slip in subduction zones: Reconciling deformation fabrics with instrumental observations and laboratory results: *Geosphere*, v. 18, <https://doi.org/10.1130/GES02382.1>.
- Onishi, C.T., Kimura, G., Hashimoto, Y., Ikehara-Ohmori, K., and Watanabe, T., 2001, Deformation history of tectonic melange and its relationship to the underplating process and relative plate motion: An example from the deeply buried Shimanto Belt, SW Japan: *Tectonics*, v. 20, p. 376–393, <https://doi.org/10.1029/1999TC001154>.
- Palazzin, G., Raimbourg, H., Famin, V., Jolivet, L., Kusaba, Y., and Yamaguchi, A., 2016, Deformation processes at the down-dip limit of the seismogenic zone: The example of Shimanto accretionary complex: *Tectonophysics*, v. 687, p. 28–43, <https://doi.org/10.1016/j.tecto.2016.08.013>.
- Parada, M.A., Rivano, S., Sepúlveda, P., Hervé, M., Hervé, F., Puig, A., Munizaga, F., Brook, M., Pankhurst, R., and Snelling, N., 1988, Mesozoic and Cenozoic plutonic development in the Andes of central Chile (30° 30'–32° 30'S): *Journal of South American Earth Sciences*, v. 1, p. 249–260, [https://doi.org/10.1016/0895-9811\(88\)90003-X](https://doi.org/10.1016/0895-9811(88)90003-X).
- Park, J.-O., Tsuru, T., Takahashi, N., Hori, T., Kodaira, S., Nakanishi, A., Miura, S., and Kaneda, Y., 2002, A deep strong reflector in the Nankai accretionary wedge from multichannel seismic data: Implications for underplating and interseismic shear stress release: *Journal of Geophysical Research*, v. 107, no. B4, <https://doi.org/10.1029/2001JB000262>.
- Patzwahl, R., Mechie, J., Schulze, A., and Giese, P., 1999, Two-dimensional velocity models of the Nazca plate subduction zone between 19.5°S and 25°S from wide-angle seismic measurements during the CINCA95 project: *Journal of Geophysical Research*, v. 104, p. 7293–7317, <https://doi.org/10.1029/1999JB900008>.
- Pavlis, T.L., and Roeske, S.M., 2007, The Border Ranges fault system, southern Alaska, in Ridgway, K.D., Trop, J.M., Glen, J.M.G., and O'Neill, J.M., eds., *Tectonic Growth of a Collisional Continental Margin: Crustal Evolution of Southern Alaska*: Geological Society of America Special Paper 431, p. 95–127, [https://doi.org/10.1130/2007.2431\(05\)](https://doi.org/10.1130/2007.2431(05)).
- Pazzaglia, F.J., and Brandon, M.T., 2001, A fluvial record of long-term steady-state uplift and erosion across the Cascadia forearc high, western Washington State: *American Journal of Science*, v. 301, p. 385–431, <https://doi.org/10.2475/ajs.301.4-5.385>.
- Peacock, S.M., 1990, Fluid processes in subduction zones: *Science*, v. 248, p. 329–337, <https://doi.org/10.1126/science.248.4953.329>.
- Peacock, S.M., 2009, Thermal and metamorphic environment of subduction zone episodic tremor and slip: *Journal of Geophysical Research: Solid Earth*, v. 114, <https://doi.org/10.1029/2008JB005978>.
- Peacock, S.M., 2020, Advances in the thermal and petrologic modeling of subduction zones: *Geosphere*, v. 16, p. 936–952, <https://doi.org/10.1130/GES02213.1>.
- Peacock, S.M., and Hyndman, R.D., 1999, Hydrous minerals in the mantle wedge and the maximum depth of subduction thrust earthquakes: *Geophysical Research Letters*, v. 26, p. 2517–2520, <https://doi.org/10.1029/1999GL900558>.
- Peacock, S.M., and Wang, K., 1999, Seismic consequences of warm versus cool subduction metamorphism: Examples from southwest and northeast Japan: *Science*, v. 286, p. 937–939.
- Penniston-Dorland, S.C., Kohn, M.J., and Manning, C.E., 2015, The global range of subduction zone thermal structures from exhumed blueschists and eclogites: Rocks are hotter than models: *Earth and Planetary Science Letters*, v. 428, p. 243–254, <https://doi.org/10.1016/j.epsl.2015.07.031>.
- Petrini, C., Gerya, T., Yarushina, V., van Dinther, Y., Connolly, J., and Madonna, C., 2020, Seismo-hydro-mechanical modelling of the seismic cycle: Methodology and implications for subduction zone seismicity: *Tectonophysics*, v. 791, 228504, <https://doi.org/10.1016/j.tecto.2020.228504>.
- Plank, T., and Langmuir, C.H., 1993, Tracing trace elements from sediment input to volcanic output at subduction zones: *Nature*, v. 362, p. 739–743, <https://doi.org/10.1038/362739a0>.
- Platt, J.P., 1986, Dynamics of orogenic wedges and the uplift of high-pressure metamorphic rocks: *Geological Society of America Bulletin*, v. 97, p. 1037–1053, [https://doi.org/10.1130/0016-7606\(1986\)97<1037:DOOWAT>2.0.CO;2](https://doi.org/10.1130/0016-7606(1986)97<1037:DOOWAT>2.0.CO;2).
- Platt, J.P., 1987, The uplift of high-pressure-low-temperature metamorphic rocks: Philosophical Transactions of the Royal Society of London: Series A, Mathematical and Physical Sciences, v. 321, p. 87–103, <https://doi.org/10.1098/rsta.1987.0006>.
- Plunder, A., Agard, P., Chopin, C., Pourteau, A., and Okay, A.I., 2015, Accretion, underplating and exhumation along a subduction interface: From subduction initiation to continental subduction (Taşvanlı zone, W. Turkey): *Lithos*, v. 226, p. 233–254, <https://doi.org/10.1016/j.lithos.2015.01.007>.
- Polino, R., Dal Piaz, G.V., and Gosso, G., 1990, Tectonic erosion at the Adria margin and accretionary processes for the Cretaceous orogeny of the Alps: *Mémoires de la Société Géologique de France*, v. 156, p. 345–367.
- Raimbourg, H., Augier, R., Famin, V., Gadenne, L., Palazzin, G., Yamaguchi, A., and Kimura, G., 2014, Long-term evolution of an accretionary prism: The case study of the Shimanto Belt, Kyushu, Japan: *Tectonics*, v. 33, p. 936–959, <https://doi.org/10.1002/2013TC003412>.
- Raimbourg, H., Famin, V., Palazzin, G., Yamaguchi, A., Augier, R., Kitamura, Y., and Sakaguchi, A., 2019, Distributed deformation along the subduction plate interface: The role of tectonic mélanges: *Lithos*, v. 334, p. 69–87, <https://doi.org/10.1016/j.lithos.2019.01.033>.
- Ramos, C., Mechie, J., and Stiller, M., 2018, Reflection seismic images and amplitude ratio modelling of the Chilean subduction zone at 38.25°S: *Tectonophysics*, v. 747, p. 115–127, <https://doi.org/10.1016/j.tecto.2018.10.007>.
- Ranero, C.R., and von Huene, R., 2000, Subduction erosion along the Middle America convergent margin: *Nature*, v. 404, p. 748–752, <https://doi.org/10.1038/35008046>.
- Rapalini, A.E., Hervé, F., Ramos, V.A., and Singer, S.E., 2001, Paleomagnetic evidence for a very large counterclockwise rotation of the Madre de Dios Archipelago, southern Chile: *Earth and Planetary Science Letters*, v. 184, p. 471–487.
- Raymond, L.A., Ogawa, Y., and Maddock, M.E., 2020, Accretionary unit formats in subduction complexes: Examples from the Franciscan and Miura-Boso complexes: *International Geology Review*, v. 62, p. 1581–1609, <https://doi.org/10.1080/00206814.2019.1667881>.
- Rech, J.A., Currie, B.S., Jordan, T.E., Riquelme, R., Lehmann, S.B., Kirk-Lawlor, N.E., Li, S.Y., and Gooley, J.T., 2019, Massive middle Miocene gypsic paleosols in the Atacama Desert and the formation of the Central Andean rain-shadow: *Earth and Planetary Science Letters*, v. 506, p. 184–194, <https://doi.org/10.1016/j.epsl.2018.10.040>.
- Regalla, C.A., Rowe, C.D., Harrichhausen, N., Tarling, M.S., and Singh, J., 2018, Styles of underplating in the Marin Headlands terrane, Franciscan complex, California, in Byrne, T., Underwood, M.B., III, Fisher, D., McNeill, L., Saffer, D., Ujiie, K., and Yamaguchi, A., eds., *Geology and Tectonics of Subduction Zones: A Tribute to Gaku Kimura*: Geological Society of America Special Paper 534, p. 155–173, [https://doi.org/10.1130/2018.2534\(10\)](https://doi.org/10.1130/2018.2534(10)).
- Regard, V., Martinod, J., Saillard, M., Carretier, S., Leanni, L., Hérail, G., Audin, L., and Pedoja, K., 2021, Late Miocene–Quaternary forearc uplift in southern Peru: New insights from ¹⁰Be dates and rocky coastal sequences: *Journal of South American Earth Sciences*, v. 109, 103261, <https://doi.org/10.1016/j.jsames.2021.103261>.
- Richter, P.P., Ring, U., Willner, A.P., and Leiss, B., 2007, Structural contacts in subduction complexes and their tectonic significance: The Late Palaeozoic coastal accretionary wedge of central Chile: *Journal of the Geological Society*, v. 164, p. 203–214, <https://doi.org/10.1144/0016-76492005-181>.

- Ring, U., 2008, Deformation and Exhumation at Convergent Margins: The Franciscan Subduction Complex: Geological Society of America Special Paper 445, <https://doi.org/10.1130/SPE445>.
- Ring, U., and Brandon, M.T., 2008, Exhumation settings, Part I: Relatively simple cases: *International Geology Review*, v. 50, p. 97–120, <https://doi.org/10.2747/0020-6814.50.2.97>.
- Ring, U., Brandon, M.T., Willett, S.D., and Lister, G.S., 1999, Exhumation processes, in Ring, U., Brandon, M.T., Lister, G.S., and Willett, S.D., eds., *Exhumation Processes: Normal Faulting, Ductile Flow and Erosion*: Geological Society of London Special Publication 154, p. 1–27, <https://doi.org/10.1144/GSL.SP.1999.154.01.01>.
- Rios Reyes, C., Rios Escobar, V., Gómez Maya, C., and Castellanos Alarcón, O., 2008, Una contribución al estudio de la evolución tectono-metamórfica de las rocas de alta presión del Complejo Arquía, Cordillera Central, Andes Colombianos: *Geología Colombiana*, v. 33, p. 3–22.
- Roeske, S.M., Mattinson, J.M., and Armstrong, R.L., 1989, Isotopic ages of glaucophane schists on the Kodiak Islands, southern Alaska, and their implications for the Mesozoic tectonic history of the Border Ranges fault system: *Geological Society of America Bulletin*, v. 101, p. 1021–1037, [https://doi.org/10.1130/0016-7606\(1989\)101<1021:IAOGSO>2.3.CO;2](https://doi.org/10.1130/0016-7606(1989)101<1021:IAOGSO>2.3.CO;2).
- Rosenau, M., and Oncken, O., 2009, Fore-arc deformation controls frequency-size distribution of megathrust earthquakes in subduction zones: *Journal of Geophysical Research: Solid Earth*, v. 114, <https://doi.org/10.1029/2009JB006359>.
- Ruff, L.J., 1999, Dynamic stress drop of recent earthquakes: Variations within subduction zones, in Sauber, J., and Dmowska, R., eds., *Seismogenic and Tsunamigenic Processes in Shallow Subduction Zones*: Basel, Birkhäuser, p. 409–431, https://doi.org/10.1007/978-3-0348-8679-6_2.
- Ruh, J.B., 2020, Numerical modeling of tectonic underplating in accretionary wedge systems: *Geosphere*, v. 16, p. 1385–1407, <https://doi.org/10.1130/GES02273.1>.
- Ruh, J.B., Le Pourhiet, L., Agard, P., Burrov, E., and Gerya, T., 2015, Tectonic slicing of subducting oceanic crust along plate interfaces: Numerical modeling: *Geochemistry Geophysics Geosystems*, v. 16, p. 3505–3531, <https://doi.org/10.1002/2015GC005998>.
- Saffer, D.M., and Tobin, H.J., 2011, Hydrogeology and mechanics of subduction zone forearcs: Fluid flow and pore pressure: *Annual Review of Earth and Planetary Sciences*, v. 39, p. 157–186, <https://doi.org/10.1146/annurev-earth-040610-133408>.
- Sage, F., Collot, J.-Y., and Ranero, C.R., 2006, Interplate patchiness and subduction-erosion mechanisms: Evidence from depth-migrated seismic images at the central Ecuador convergent margin: *Geology*, v. 34, p. 997–1000, <https://doi.org/10.1130/G22790A.1>.
- Saillard, M., Hall, S.R., Audin, L., Farber, D.L., Hérail, G., Martinod, J., Regard, V., Finkel, R.C., and Bondoux, F., 2009, Non-steady long-term uplift rates and Pleistocene marine terrace development along the Andean margin of Chile (31°S) inferred from ¹⁰Be dating: *Earth and Planetary Science Letters*, v. 277, p. 50–63, <https://doi.org/10.1016/j.epsl.2008.09.039>.
- Saillard, M., Audin, L., Rousset, B., Avouac, J.-P., Chlieh, M., Hall, S.R., Husson, L., and Farber, D.L., 2017, From the seismic cycle to long-term deformation: Linking seismic coupling and Quaternary coastal geomorphology along the Andean megathrust: *Tectonics*, v. 36, p. 241–256, <https://doi.org/10.1002/2016TC004156>.
- Sakakibara, M., and Ota, T., 1994, Metamorphic evolution of the Kamuikotan high-pressure and low-temperature metamorphic rocks in central Hokkaido, Japan: *Journal of Geophysical Research*, v. 99, p. 22,221–22,235, <https://doi.org/10.1029/94JB00958>.
- Sakakibara, M., Ofuka, H., Kimura, C., Ishizuka, H., Miyashita, S., Okamura, M., and Melnikov, O.A., 1997, Metamorphic evolution of the Susunai metabasites in southern Sakhalin, Russian Republic: *Journal of Metamorphic Geology*, v. 15, p. 565–580, <https://doi.org/10.1111/j.1525-1314.1997.tb00636.x>.
- Sample, J.C., and Fisher, D.M., 1986, Duplex accretion and underplating in an ancient accretionary complex, Kodiak Islands, Alaska: *Geology*, v. 14, p. 160–163, [https://doi.org/10.1130/0091-7613\(1986\)14<160:DAAUIA>2.0.CO;2](https://doi.org/10.1130/0091-7613(1986)14<160:DAAUIA>2.0.CO;2).
- Sang, M., Xiao, W., and Windley, B.F., 2020, Unravelling a Devonian–Triassic seamount chain in the South Tianshan high-pressure/ultrahigh-pressure accretionary complex in the Atbashi area (Kyrgyzstan): *Geological Journal*, v. 55, p. 2300–2317, <https://doi.org/10.1002/gj.3776>.
- Savard, G., Bostock, M.G., and Christensen, N.I., 2018, Seismicity, metamorphism, and fluid evolution across the northern Cascadia fore arc: *Geochemistry Geophysics Geosystems*, v. 19, p. 1881–1897, <https://doi.org/10.1029/2017GC007417>.
- Scherwath, M., Kopp, H., Flueh, E.R., Henrys, S.A., Sutherland, R., Stagpoole, V.M., Barker, D.H.N., Reyners, M.E., Bassett, D.G., Planert, L., and Dannowski, A., 2010, Fore-arc deformation and underplating at the northern Hikurangi margin, New Zealand: *Journal of Geophysical Research*, v. 115, B06408, <https://doi.org/10.1029/2009JB006645>.
- Schmeling, H., Babeyko, A.Y., Enns, A., Faccenna, C., Fucicello, F., Gerya, T., Golabek, G.J., Grigull, S., Kaus, B.J.P., Morra, G., Schmalholz, S.M., and van Hunen, J., 2008, A benchmark comparison of spontaneous subduction models—Towards a free surface: *Physics of the Earth and Planetary Interiors*, v. 171, p. 198–223, <https://doi.org/10.1016/j.pepi.2008.06.028>.
- Schmidt, W.L., and Platt, J.P., 2018, Subduction, accretion, and exhumation of coherent Franciscan blueschist-facies rocks, northern Coast Ranges, California: *Lithosphere*, v. 10, p. 301–326, <https://doi.org/10.1130/L697.1>.
- Schmidt, W.L., and Platt, J.P., 2020, Metamorphic temperatures and pressures across the eastern Franciscan: Implications for underplating and exhumation: *Lithosphere*, v. 2020, 8853351, <https://doi.org/10.2113/2020/8853351>.
- Scholl, D.W., 2019, Seismic imaging evidence that forearc underplating built the accretionary rock record of coastal North and South America: *Geological Magazine*, v. 158, p. 104–117, <https://doi.org/10.1017/S0016756819000955>.
- Scholl, D.W., and von Huene, R., 2007, Crustal recycling at modern subduction zones applied to the past—Issues of growth and preservation of continental basement crust, mantle geochemistry, and supercontinent reconstruction, in Hatcher, R.D., Jr., Carlson, M.P., McBride, J.H., and Catalán, J.R.M., eds., *4-D Framework of Continental Crust*: Geological Society of America Memoir 200, p. 9–32, [https://doi.org/10.1130/2007.1200\(02\)](https://doi.org/10.1130/2007.1200(02)).
- Scholl, D.W., and von Huene, R., 2010, Subduction zone recycling processes and the rock record of crustal surface zones: *Canadian Journal of Earth Sciences*, v. 47, p. 633–654, <https://doi.org/10.1139/E09-061>.
- Scholl, D.W., von Huene, R., Vallier, T.L., and Howell, D.G., 1980, Sedimentary masses and concepts about tectonic processes at underthrust ocean margins: *Geology*, v. 8, p. 564–568, [https://doi.org/10.1130/0091-7613\(1980\)8<564:SMACAT>2.0.CO;2](https://doi.org/10.1130/0091-7613(1980)8<564:SMACAT>2.0.CO;2).
- Sedlock, R.L., 1988, Metamorphic petrology of a high-pressure, low-temperature subduction complex in west-central Baja California, Mexico: *Journal of Metamorphic Geology*, v. 6, p. 205–233, <https://doi.org/10.1111/j.1525-1314.1988.tb00416.x>.
- Sedlock, R.L., 1996, Syn-subduction forearc extension and blueschist exhumation in Baja California, México, in Bebout, G.E., Scholl, D.W., Kirby, S.H., and Platt, J.P., eds., *Subduction: Top to Bottom*: American Geophysical Union Geophysical Monograph 96, p. 155–162, <https://doi.org/10.1029/GM096p0155>.
- Seely, D.R., 1979, The evolution of structural highs bordering major forearc basins, in Watkins, J.S., Montadert, L., and Dickerson, P.W., eds., *Geological and Geophysical Investigations of Continental Margins*: American Association of Petroleum Geologists Memoir 29, p. 245–260, <https://doi.org/10.1306/M29405C17>.
- Selzer, C., Buitter, S.J., and Pfiffner, O.A., 2008, Numerical modeling of frontal and basal accretion at collisional margins: *Tectonics*, v. 27, TC3001, <https://doi.org/10.1029/2007TC002169>.
- Sepúlveda, F.A., Hervé, F., Calderón, M., and Lacassie, J.P., 2008, Petrological and geochemical characteristics of metamorphic and igneous units from the allochthonous Madre de Dios Terrane, Southern Chile: *Gondwana Research*, v. 13, p. 238–249, <https://doi.org/10.1016/j.gr.2007.06.004>.
- Shirzaei, M., Bürgmann, R., Oncken, O., Walter, T.R., Victor, P., and Ewiak, O., 2012, Response of forearc crustal faults to the megathrust earthquake cycle: InSAR evidence from Mejillones Peninsula, Northern Chile: *Earth and Planetary Science Letters*, v. 333, p. 157–164, <https://doi.org/10.1016/j.epsl.2012.04.001>.
- Sick, C., Yoon, M.-K., Rauch, K., Buske, S., Lüth, S., Araneda, M., Bataille, K., Chong, G., Giese, P., Krawczyk, C., Mechie, J., Meyer, H., Oncken, O., Reichert, C., Schmitz, M., Shapiro, S., Stiller, M., and Wigger, P., 2006, Seismic images of accretive and erosive subduction zones from the Chilean margin, in Oncken, O., Chong, G., Franz, G., Giese, P., Götz, H.-J., Ramos, V.A., Strecker, M.R., and Wigger, P., eds., *The Andes: Active Subduction Orogeny*: Berlin, Heidelberg, Springer, p. 147–169, https://doi.org/10.1007/978-3-540-48684-8_7.
- Sieh, K., Natawidjaja, D.H., Meltzner, A.J., Shen, C.-C., Cheng, H., Li, K.-S., Suwargadi, B.W., Galetzka, J., Philibosian, B., and Edwards, R.L., 2008, Earthquake supercycles inferred from sea-level changes recorded in the corals of west Sumatra: *Science*, v. 322, p. 1674–1678, <https://doi.org/10.1126/science.1163589>.
- Silver, E.A., Ellis, M.J., Breen, N.A., and Shipley, T.H., 1985, Comments on the growth of accretionary wedges: *Geology*, v. 13, p. 6–9, [https://doi.org/10.1130/0091-7613\(1985\)13<6:COTGOA>2.0.CO;2](https://doi.org/10.1130/0091-7613(1985)13<6:COTGOA>2.0.CO;2).
- Sisson, V.B., Pavlis, T.L., Roeske, S.M., and Thorkelson, D.J., 2003, Introduction: An overview of ridge-trench interactions in modern and ancient settings, in Sisson, V.B., Roeske, S.M., and Pavlis, T.L., eds., *Geology of a Transpressional Orogen Developed during Ridge-Trench Interaction along the North Pacific Margin*: Geological Society of America Special Paper 371, p. 1–18, <https://doi.org/10.1130/0-8137-2371-X.1>.
- Smith, C.A., Sisson, V.B., Avé Lallemant, H.G., and Copeland, P., 1999, Two contrasting pressure-temperature-time paths in the Villa de Cura blueschist belt, Venezuela: Possible evidence

- for Late Cretaceous initiation of subduction in the Caribbean: Geological Society of America Bulletin, v. 111, p. 831–848, [https://doi.org/10.1130/0016-7606\(1999\)111<0831:TCPTTP>2.3.CO;2](https://doi.org/10.1130/0016-7606(1999)111<0831:TCPTTP>2.3.CO;2).
- Snow, C.A., Wakabayashi, J., Ernst, W.G., and Wooden, J.L., 2010, Detrital zircon evidence for progressive underthrusting in Franciscan metagraywackes, west-central California: Geological Society of America Bulletin, v. 122, p. 282–291, <https://doi.org/10.1130/B26399.1>.
- St. Clair, J., Holbrook, W.S., Van Avendonk, H.J.A., and Lizarralde, D., 2016, Along-strike structure of the Costa Rican convergent margin from seismic a refraction/reflection survey: Evidence for underplating beneath the inner forearc: Geochemistry Geophysics Geosystems, v. 17, p. 501–520, <https://doi.org/10.1002/2015GC006029>.
- Stern, C.R., 2011, Subduction erosion: Rates, mechanisms, and its role in arc magmatism and the evolution of the continental crust and mantle: Gondwana Research, v. 20, p. 284–308, <https://doi.org/10.1016/j.gr.2011.03.006>.
- Strasser, M., Moore, G.F., Kimura, G., Kitamura, Y., Kopf, A.J., Lallemand, S., Park, J.-O., Scretton, E.J., Su, X., Underwood, M.B., and Zhao, X., 2009, Origin and evolution of a splay fault in the Nankai accretionary wedge: Nature Geoscience, v. 2, p. 648–652, <https://doi.org/10.1038/ngeo609>.
- Sutherland, R., Stagpoole, V., Uruski, C., Kennedy, C., Bassett, D., Henrys, S., Scherwath, M., Kopp, H., Field, B., Toulmin, S., Barker, D., Bannister, S., Davey, F., Stern, T., and Flueh, E.R., 2009, Reactivation of tectonics, crustal underplating, and uplift after 60 Myr of passive subsidence, Raukumara Basin, Hikurangi-Kermadec fore arc, New Zealand: Implications for global growth and recycling of continents: Tectonics, v. 28, TC5017, <https://doi.org/10.1029/2008TC002356>.
- Taetz, S., John, T., Bröcker, M., Spandler, C., and Stracke, A., 2018, Fast intraslab fluid-flow events linked to pulses of high pore fluid pressure at the subducted plate interface: Earth and Planetary Science Letters, v. 482, p. 33–43, <https://doi.org/10.1016/j.epsl.2017.10.044>.
- Tamblyn, R., Hand, M., Kelsey, D., Anczkiewicz, R., and Och, D., 2020, Subduction and accumulation of lawsonite eclogite and garnet blueschist in eastern Australia: Journal of Metamorphic Geology, v. 38, p. 157–182, <https://doi.org/10.1111/jmg.12516>.
- Tewksbury-Christie, C.M., Behr, W.M., and Helper, M.A., 2021, Tracking deep sediment underplating in a fossil subduction margin: Implications for interface rheology and mass and volatile recycling: Geochemistry Geophysics Geosystems, v. 22, e2020GC009463, <https://doi.org/10.1029/2020GC009463>.
- Thompson, S.N., and Hervé, F., 2002, New time constraints for the age of metamorphism at the ancestral Pacific Gondwana margin of southern Chile (42–52°S): Andean Geology, v. 29, p. 255–271, <https://doi.org/10.4067/S0716-02082002000200007>.
- Tonarini, S., Leeman, W.P., and Leat, P.T., 2011, Subduction erosion of forearc mantle wedge implicated in the genesis of the South Sandwich Island (SSI) arc: Evidence from boron isotope systematics: Earth and Planetary Science Letters, v. 301, p. 275–284, <https://doi.org/10.1016/j.epsl.2010.11.008>.
- Tranter, T.H., 1992, Underplating of an accretionary prism: An example from the LeMay Group of central Alexander Island, Antarctic Peninsula: Journal of South American Earth Sciences, v. 6, p. 1–20, [https://doi.org/10.1016/0895-9811\(92\)90013-O](https://doi.org/10.1016/0895-9811(92)90013-O).
- Trouw, R.A.J., Simões, L.S.A., and Valladares, C.S., 1998, Metamorphic evolution of a subduction complex, South Shetland Islands, Antarctica: Journal of Metamorphic Geology, v. 16, p. 475–490, <https://doi.org/10.1111/j.1525-1314.1998.00151.x>.
- Tsai, C.-H., Iizuka, Y., and Ernst, W.G., 2013, Diverse mineral compositions, textures, and metamorphic *P-T* conditions of the glaucophane-bearing rocks in the Tamayen mélange, Yuli belt, eastern Taiwan: Journal of Asian Earth Sciences, v. 63, p. 218–233, <https://doi.org/10.1016/j.jseaes.2012.09.019>.
- Tsuji, T., Minato, S., Kamei, R., Tsuru, T., and Kimura, G., 2017, 3D geometry of a plate boundary fault related to the 2016 Off-Mie earthquake in the Nankai subduction zone, Japan: Earth and Planetary Science Letters, v. 478, p. 234–244, <https://doi.org/10.1016/j.epsl.2017.08.041>.
- Tsujimori, T., Matsumoto, K., Wakabayashi, J., and Liou, J.G., 2006, Franciscan eclogite revisited: Reevaluation of the *P-T* evolution of tectonic blocks from Tiburon Peninsula, California, U.S.A.: Mineralogy and Petrology, v. 88, 243, <https://doi.org/10.1007/s00710-006-0157-1>.
- Uchida, N., Kirby, S.H., Okada, T., Hino, R., and Hasegawa, A., 2010, Supraslab earthquake clusters above the subduction plate boundary offshore Sanriku, northeastern Japan: Seismogenesis in a graveyard of detached seamounts?: Journal of Geophysical Research, v. 115, B09308, <https://doi.org/10.1029/2009JB006797>.
- Ueda, H., 2005, Accretion and exhumation structures formed by deeply subducted seamounts in the Kamuikotan high-pressure/temperature zone, Hokkaido, Japan: Tectonics, v. 24, TC2007, <https://doi.org/10.1029/2004TC001690>.
- Ujije, K., Saishu, H., Fagereng, Å., Nishiyama, N., Otsubo, M., Masuyama, H., and Kagi, H., 2018, An explanation of episodic tremor and slow slip constrained by crack-seal veins and viscous shear in subduction mélange: Geophysical Research Letters, v. 45, p. 5371–5379, <https://doi.org/10.1029/2018GL078374>.
- Ukar, E., and Cloos, M., 2014, Low-temperature blueschist-facies mafic blocks in the Franciscan mélange, San Simeon, California: Field relations, petrology, and counterclockwise *P-T* paths: Geological Society of America Bulletin, v. 126, p. 831–856, <https://doi.org/10.1130/B30876.1>.
- Underwood, M.B., and Laughland, M.M., 2001, Paleothermal structure of the Point San Luis slab of central California: Effects of Late Cretaceous underplating, out-of-sequence thrusting, and late Cenozoic dextral offset: Tectonics, v. 20, p. 97–111, <https://doi.org/10.1029/1999TC001153>.
- van Dinther, Y., Gerya, T.V., Dalguer, L.A., Mai, P.M., Morra, G., and Giardini, D., 2013, The seismic cycle at subduction thrusts: Insights from seismo-thermo-mechanical models: Journal of Geophysical Research: Solid Earth, v. 118, p. 6183–6202, <https://doi.org/10.1002/2013JB010380>.
- van Keken, P.E., Wada, I., Abers, G.A., Hacker, B.R., and Wang, K., 2018, Mafic high-pressure rocks are preferentially exhumed from warm subduction settings: Geochemistry Geophysics Geosystems, v. 19, p. 2934–2961, <https://doi.org/10.1029/2018GC007624>.
- Vannucchi, P., Galeotti, S., Clift, P.D., Ranero, C.R., and von Huene, R., 2004, Long-term subduction-erosion along the Guatemalan margin of the Middle America Trench: Geology, v. 32, p. 617–620, <https://doi.org/10.1130/G20422.1>.
- Victor, P., Sobiesiak, M., Glodny, J., Nielsen, S.N., and Oncken, O., 2011, Long-term persistence of subduction earthquake segment boundaries: Evidence from Mejillones Peninsula, northern Chile: Journal of Geophysical Research, v. 116, <https://doi.org/10.1029/2010JB007771>.
- Vinagre da Costa, R., de Moraes, R., Trouw, R.A.J., Simões, L.S.A., and Mendes, J.C., 2019, High-pressure medium-temperature metamorphism of semi-pelitic rocks in the Scotia Metamorphic Complex, Powell Island, South Orkney Islands, Antarctica: Journal of South American Earth Sciences, v. 91, p. 8–26, <https://doi.org/10.1016/j.jsames.2019.01.002>.
- Vitale-Brovarone, A., Beyssac, O., Malavieille, J., Molli, G., Beltrando, M., and Compagnoni, R., 2013, Stacking and metamorphism of continuous segments of subducted lithosphere in a high-pressure wedge: The example of Alpine Corsica (France): Earth-Science Reviews, v. 116, p. 35–56, <https://doi.org/10.1016/j.earsciev.2012.10.003>.
- Vithana, M.V.P., Xu, M., Zhao, X., Zhang, M., and Luo, Y., 2019, Geological and geophysical signatures of the East Pacific Rise 8°–10°N: Solid Earth Sciences, v. 4, p. 66–83, <https://doi.org/10.1016/j.sesci.2019.04.001>.
- Vogt, K., and Gerya, T., 2014a, Deep plate serpentinization triggers skinning of subducting slabs: Geology, v. 42, p. 723–726, <https://doi.org/10.1130/G35565.1>.
- Vogt, K., and Gerya, T.V., 2014b, From oceanic plateaus to allochthonous terranes: Numerical modelling: Gondwana Research, v. 25, p. 494–508, <https://doi.org/10.1016/j.gr.2012.11.002>.
- von Huene, R., and Lallemand, S., 1990, Tectonic erosion along the Japan and Peru convergent margins: Geological Society of America Bulletin, v. 102, p. 704–720, [https://doi.org/10.1130/0016-7606\(1990\)102<0704:TEATJA>2.3.CO;2](https://doi.org/10.1130/0016-7606(1990)102<0704:TEATJA>2.3.CO;2).
- von Huene, R., and Ranero, C.R., 2009, Neogene collision and deformation of convergent margins along the backbone of the Americas, in Kay, S.M., Ramos, V.A., and Dickinson, W.R., eds., Backbone of the Americas: Shallow Subduction, Plateau Uplift, and Ridge and Terrane Collision: Geological Society of America Memoir 204, p. 67–83, [https://doi.org/10.1130/2009.1204\(03\)](https://doi.org/10.1130/2009.1204(03)).
- von Huene, R., and Scholl, D.W., 1991, Observations at convergent margins concerning sediment subduction, subduction erosion, and the growth of continental crust: Reviews of Geophysics, v. 29, p. 279–316, <https://doi.org/10.1029/91RG00969>.
- von Huene, R., and Scholl, D.W., 1993, The return of sialic material to the mantle indicated by terrigenous material subducted at convergent margins: Tectonophysics, v. 219, p. 163–175, [https://doi.org/10.1016/0040-1951\(93\)90294-T](https://doi.org/10.1016/0040-1951(93)90294-T).
- von Huene, R., Langseth, M., Nasu, N., and Okada, H., 1982, A summary of Cenozoic tectonic history along the IPOD Japan Trench transect: Geological Society of America Bulletin, v. 93, p. 829–846, [https://doi.org/10.1130/0016-7606\(1982\)93<829:ASOCTH>2.0.CO;2](https://doi.org/10.1130/0016-7606(1982)93<829:ASOCTH>2.0.CO;2).
- von Huene, R., Ranero, C.R., and Vannucchi, P., 2004, Generic model of subduction erosion: Geology, v. 32, p. 913–916, <https://doi.org/10.1130/G20563.1>.
- von Huene, R., Miller, J.J., and Krabbenhoft, A., 2021, The Alaska convergent margin backstop splay fault zone, a potential large tsunami generator between the frontal prism and continental framework: Geochemistry, Geophysics, Geosystems, v. 22, e2019GC008901, <https://doi.org/10.1029/2019GC008901>.

- Wagreich, M., 1995, Subduction tectonic erosion and Late Cretaceous subsidence along the northern Austroalpine margin (Eastern Alps, Austria): *Tectonophysics*, v. 242, p. 63–78, [https://doi.org/10.1016/0040-1951\(94\)00151-X](https://doi.org/10.1016/0040-1951(94)00151-X).
- Wakabayashi, J., 1990, Counterclockwise P-T paths from amphibolites, Franciscan Complex, California: Relics from the early stages of subduction zone metamorphism: *The Journal of Geology*, v. 98, p. 657–680, <https://doi.org/10.1086/629432>.
- Wakabayashi, J., 1999, The Franciscan: California's classic subduction complex, in Moores, E.M., Sloan, D., and Stout, D.L., eds., *Classic Cordilleran Concepts: A View from California*: Geological Society of America Special Paper 338, p. 111–121, <https://doi.org/10.1130/0-8137-2338-8.111>.
- Wakabayashi, J., 2011, Mélanges of the Franciscan Complex, California: Diverse structural settings, evidence for sedimentary mixing, and their connection to subduction processes, in Wakabayashi, J., and Dilek, Y., eds., *Mélanges: Processes of Formation and Societal Significance*: Geological Society of America Special Paper 480, p. 117–141, [https://doi.org/10.1130/2011.2480\(05\)](https://doi.org/10.1130/2011.2480(05)).
- Wakabayashi, J., 2017, Serpentinities and serpentinites: Variety of origins and emplacement mechanisms of serpentinite bodies in the California Cordillera: *Island Arc*, v. 26, e12205, <https://doi.org/10.1111/iar.12205>.
- Wakabayashi, J., and Rowe, C.D., 2015, Whither the megathrust? Localization of large-scale subduction slip along the contact of a mélange: *International Geology Review*, v. 57, p. 854–870, <https://doi.org/10.1080/00206814.2015.1020453>.
- Wakita, K., 2013, Geology and tectonics of Japanese islands: A review—The key to understanding the geology of Asia: *Journal of Asian Earth Sciences*, v. 72, p. 75–87, <https://doi.org/10.1016/j.jseae.2012.04.014>.
- Wakita, K., 2019, Tectonic setting required for the preservation of sedimentary mélanges in Palaeozoic and Mesozoic accretionary complexes of southwest Japan: *Gondwana Research*, v. 74, p. 90–100, <https://doi.org/10.1016/j.gr.2019.03.006>.
- Walcott, R.L., 1987, Geodetic strain and the deformational history of the North Island of New Zealand during the late Cainozoic: *Philosophical Transactions of the Royal Society of London: Series A, Mathematical and Physical Sciences*, v. 321, p. 163–181, <https://doi.org/10.1098/rsta.1987.0009>.
- Wallace, L.M., Reyners, M., Cochran, U., Bannister, S., Barnes, P.M., Berryman, K., Downes, G., Eberhart-Phillips, D., Fagereng, A., Ellis, S., Nicol, A., McCaffrey, R., Beavan, R.J., Henrys, S., Sutherland, R., Barker, D.H.N., Litchfield, N., Townend, J., Robinson, R., Bell, R., Wilson, K., and Power, W., 2009, Characterizing the seismogenic zone of a major plate boundary subduction thrust: Hikurangi Margin, New Zealand: *Geochemistry, Geophysics, Geosystems*, v. 10, no. 10, <https://doi.org/10.1029/2009GC002610>.
- Wallis, S., 1998, Exhuming the Sanbagawa metamorphic belt: The importance of tectonic discontinuities: *Journal of Metamorphic Geology*, v. 16, p. 83–95, <https://doi.org/10.1111/j.1525-1314.1998.00072.x>.
- Wang, K., Hu, Y., von Huene, R., and Kukowski, N., 2010, Interplate earthquakes as a driver of shallow subduction erosion: *Geology*, v. 38, p. 431–434, <https://doi.org/10.1130/G30597.1>.
- Wells, R.E., Blakely, R.J., Sugiyama, Y., Scholl, D.W., and Dinterman, P.A., 2003, Basin-centered asperities in great subduction zone earthquakes: A link between slip, subsidence, and subduction erosion?: *Journal of Geophysical Research*, v. 108, 2507, <https://doi.org/10.1029/2002JB002072>.
- Willner, A.P., 2005, Pressure-temperature evolution of a Late Palaeozoic paired metamorphic belt in North-Central Chile (34°–35°30'S): *Journal of Petrology*, v. 46, p. 1805–1833, <https://doi.org/10.1093/petrology/egi035>.
- Willner, A.P., Hervé, F., and Massonne, H.-J., 2000, Mineral chemistry and pressure-temperature evolution of two contrasting high-pressure–low-temperature belts in the Chonos Archipelago, Southern Chile: *Journal of Petrology*, v. 41, p. 309–330, <https://doi.org/10.1093/petrology/41.3.309>.
- Willner, A.P., Glodny, J., Gerya, T.V., Godoy, E., and Massonne, H.-J., 2004a, A counterclockwise P-T path of high-pressure/low-temperature rocks from the Coastal Cordillera accretionary complex of south-central Chile: Constraints for the earliest stage of subduction mass flow: *Lithos*, v. 75, p. 283–310, <https://doi.org/10.1016/j.lithos.2004.03.002>.
- Willner, A.P., Hervé, F., Thomson, S.N., and Massonne, H.-J., 2004b, Converging P-T paths of Mesozoic HP-LT metamorphic units (Diego de Almagro Island, Southern Chile): Evidence for juxtaposition during late shortening of an active continental margin: *Mineralogy and Petrology*, v. 81, p. 43–84, <https://doi.org/10.1007/s00710-004-0033-9>.
- Willner, A.P., Massonne, H.-J., Ring, U., Sudo, M., and Thomson, S.N., 2012, P-T evolution and timing of a late Palaeozoic fore-arc system and its heterogeneous Mesozoic overprint in north-central Chile (latitudes 31–32°S): *Geological Magazine*, v. 149, p. 177–207, <https://doi.org/10.1017/S0016756811000641>.
- Wilson, T.J., Hanson, R.E., and Grunow, A.M., 1989, Multistage melange formation within an accretionary complex, Diego Ramirez Islands, southern Chile: *Geology*, v. 17, p. 11–14, [https://doi.org/10.1130/0091-7613\(1989\)017<0011:MMFWAA>2.3.CO;2](https://doi.org/10.1130/0091-7613(1989)017<0011:MMFWAA>2.3.CO;2).
- Xia, H., and Platt, J.P., 2017, Structural and rheological evolution of the Laramide subduction channel in southern California: *Solid Earth*, v. 8, p. 379–403, <https://doi.org/10.5194/se-8-379-2017>.
- Ye, S., Flueh, E.R., Klaeschen, D., and von Huene, R., 1997, Crustal structure along the EDGE transect beneath the Kodiak shelf off Alaska derived from OBH seismic refraction data: *Geophysical Journal International*, v. 130, p. 283–302, <https://doi.org/10.1111/j.1365-246X.1997.tb05648.x>.
- Yorath, C.J., Green, A.G., Clowes, R.M., Brown, A.S., Brandon, M.T., Kanasevich, E.R., Hyndman, R.D., and Spencer, C., 1985, Lithoprobe, southern Vancouver Island: Seismic reflection sees through Wrangellia to the Juan de Fuca plate: *Geology*, v. 13, p. 759–762, [https://doi.org/10.1130/0091-7613\(1985\)13<759:LSVISR>2.0.CO;2](https://doi.org/10.1130/0091-7613(1985)13<759:LSVISR>2.0.CO;2).
- Žák, J., Svojtka, M., Hajná, J., and Ackerman, L., 2020, Detrital zircon geochronology and processes in accretionary wedges: *Earth-Science Reviews*, v. 207, 103214, <https://doi.org/10.1016/j.earscirev.2020.103214>.